NATIONAL TECHNICAL UNIVERSITY OF ATHENS
SCHOOL OF NAVAL ARCHITECTURE AND
MARINE ENGINEERING

DIVISION OF SHIP DESIGN AND MARITIME
TRANSPORT

DIPLOMA THESIS
DEVELOPMENT OF A 3DOF MODEL FOR THE SIMULATION OF THE PARAMETRIC ROLLING MOTION OF A CONTAINERSHIP

STUDENT: NIKOLAOS A. GAVRIILIDIS
THESIS SUPERVISOR: PROF. K.J SPYROU

ATHENS
JUNE 2007

Acknowledgements

This thesis would not have been completed, if were not for the scientific guidance of Prof. K.J Spyrou. Special thanks to Phd candidates J. Tigkas and N. Themelis for their valuable help on the various problems arisen during the processing of the thesis.

1 Introduction

The transportation of cargo in containers first started in the 19th century, but it was not until the 1951 that the first containership was built. Due to lack of standardisation, containers had many different sizes and corner fittings from one country to another. In the 1970s the International Standardisation Organisation (ISO) caused the revolution in international intermodal transportation by launching the standardised TEU. Today containerised cargo represents about 90% of non-bulk cargo. Because of their relatively high speed and safety of cargo, containerships are chosen to transport many goods, from electronics to luxury yachts or even cars.

The increase in demand for products to be transported led to the growth of size of containerships. Although ten years ago the biggest carried about 6000 TEU the economic boom of the freight market led the shipowners to order much bigger ships creating the category of post panamax containerships. Many vessels can carry even 10000 TEU with the biggest one, Emma Maersk, being able to carry over 14500TEU. It is also said that the growth will only be restricted by the size of Malacca straits, a very busy shipping lane which links Indian with Pacific Ocean, creating a new category of ship size, the so-called Malaccamax. The dimensions of these ships may be about 470m length and 60m width.

Post panamax containerships were the first of that type of vessels to face the problem of parametric rolling. This term was used to describe the phenomenon of parametric resonance of a ship resulting in large roll angles. Because of the continuous resonance, severe roll motion causes large accelerations resulting in damage or even loss of cargo, machinery failure, structural damages and even capsizing.

Parametric rolling is not a new phenomenon for the scientific community. Back in 1955 J.E Kerwin published a paper indicating the danger of unstable roll motion in longitudinal waves. Until recently researchers considered only some small ships with marginal stability to be susceptible to parametric rolling. In October 1998 a post panamax containership heading from Taiwan to Seattle encountered a severe storm which lasted about 11 hours. During the most intense parts of the phenomenon, roll

angles of 35-40 degrees were reported combined with extreme pitching. The result of this incident was the loss of 400 containers and serious damage to another 400. The economic casualty was about $100 millions. Figures 1 and 2 depict some of the damaged containers indicating the severity of the phenomenon.

Figure1: Photo of the side of APL China.

Figure 2: Photo of the stern of APL China.

As it will be analytically described in the next chapter, the main cause of parametric rolling is the large fluctuation of stability occurring in longitudinal waves combined with the encounter frequency. The hullform, more specifically bow flare

and flat transom, is the cause of this fluctuation occurring when the ship is on wave crest and then on a wave trough. When on a wave crest the waterplane area is dramatically reduced causing loss of transverse stability. The opposite phenomenon happens when the ship is on a wave trough. If this fluctuation happens twice within a wave period, the ship may face parametric rolling.

Summarizing we could say that parametric roll happens when a combination of environmental, operational and design parameters occur. Concerning the environmental wavelength should be comparable to ship length and wave height should be rather large. Additionally the encounter frequency has to be twice the roll natural frequency. The operational parameters involve the sailing of the ship with a small heading angle to the wave direction and the loading of the ship which can result in marginal stability. As we will see in chapter 5 the design parameter that plays a very significant role is roll damping.

2 Critical review

2.1 Introduction

During past years several scientists suggested mathematical models in order to study and predict parametric rolling. Most of them focused on finding a precise model taking into account only roll motion with the majority of them using Mathieu equation. In later years several modeling improvements were introduced: the nonlinearity in restoring and/or damping were considered by a number of researchers. It has been known that if restoring and/or damping are nonlinear then stable oscillations may exist. The nonlinearity may in fact be beneficial, impeding capsize by 'arresting' the growing oscillation incurred at an instability point. Remarkably, this can happen although the nonlinear system may process less restoring at similar angles because the change in restoring causes de-tuning from resonance.

Fewer tried to couple two or more motions of the ship in order to simulate the behavior on seas which could cause parametric resonance. In the pages below most important of these works are presented so that the reader understands the positive and negative points of each and compare them with the one used in the current thesis.

2.2 A note on low cycle resonance of a ship in severe following waves (M. Hamamoto Osaka University)

This one degree of freedom model begins its study with the pendulum based equation:

$$\left(I_X + J_X\right)\ddot{\phi} + \mathrm{K}_{\dot{\phi}}\dot{\phi} + W \cdot GZ(\xi_G, \phi) = 0 \qquad (2.2.1)$$

with W being the weight of the ship and GZ(ξ,φ) righting arm of rolling angle φ and the relative position of ξ of ship to waves.

Much effort is made by the author to find a good approximation of the GZ which depends on not only ξ and φ but the hullform, metacentric height GM, wave length λ, and wave height H making it almost impossible to describe the complete expression of GZ with analytical function.

With some calculations in order to approximate GZ curve and some manipulations in order to linearize the equation, the author gets to the Mathieu equation:

$$\frac{d^2\Phi}{d\tau^2}+\left(\frac{T_e}{T}\right)^2\left[1-\left(\frac{a_e}{\pi}\right)^2+\left(\frac{\Delta GM}{GM}\right)\cos\tau\right]\Phi=0 \qquad (2.2.2)$$

by using the following relations:

$$\phi(t)=\Phi(t)\cdot e^{-a_e t} \quad \tau=\omega_e t \qquad (2.2.3)$$

where a_e is the effective extinction coefficient and T the natural period. This equation is a linear differential equation which has the presence of a time-dependent coefficient of the rolling motion variable Φ. The solutions to Mathieu's equation have a property of considerable importance in ship rolling problems in that for certain values of the period, the solution is unstable. This implies that if the rolling motion takes place in an unstable region, the amplitude will grow up.

The comparison of the results of the numerical solution of the linear model and a non-linear one (concerning the GZ curve) follows. The two of them are then compared to some experimental results where it is obvious that the non-linear model is much more precise than the non-linear one.

2.3 A mathematical model of ship motions leading to capsize in astern waves (Masami Hamamoto, Abdul Munif)

A mathematical model used in prediction of ships motions leading to capsize in astern waves was developed on the basis of a strip method. The authors suggest a model which on one hand couples heave and pitch motions while on the other hand couples sway, yaw and roll motions. Taking into account the variation of metacentric height in the roll motion the model becomes:

Combined motions of heave and pitch

$$(m+m_z)\ddot{\zeta}_G+Z_{\dot{\zeta}_G}\dot{\zeta}_G+Z_{\zeta_G}\zeta_G+Z_{\ddot{\theta}}\ddot{\theta}+Z_{\dot{\theta}}\dot{\theta}+Z_{\theta}\theta=\mathrm{Z}_C\cos\omega_e t+\mathrm{Z}_S\sin\omega_e t \qquad (2.3.1)$$

$$(I_{yy}+J_{yy})\ddot{\theta}+\mathrm{M}_{\dot{\theta}}\dot{\theta}+\mathrm{M}_{\theta}\theta+\mathrm{M}_{\ddot{\zeta}_G}\ddot{\zeta}_G+\mathrm{M}_{\dot{\zeta}_G}\dot{\zeta}_G+\mathrm{M}_{\zeta_G}\zeta_G=M_C\cos\omega_e t+M_S\sin\omega_e t \qquad (2.3.2)$$

Combined motions of sway, yaw and roll

$$(m+m_y)\ddot{\eta}_G + Y_{\dot{\eta}_G}\dot{\eta}_G + Y_{\ddot{\phi}}\ddot{\phi} + Y_{\dot{\phi}}\dot{\phi} + Y_{\ddot{\psi}}\ddot{\psi} + Y_{\dot{\psi}}\dot{\psi} + Y_{\psi}\psi = \mathrm{Y}_C \cos\omega_e t + \mathrm{Y}_S \sin\omega_e t \quad (2.3.3)$$

$$(I_{zz}+J_{zz})\ddot{\psi} + \mathrm{N}_{\dot{\psi}}\dot{\psi} + \mathrm{N}_{\psi}\psi + \mathrm{N}_{\ddot{\eta}_G}\ddot{\eta}_G + \mathrm{N}_{\dot{\eta}_G}\dot{\eta}_G + \mathrm{N}_{\ddot{\phi}}\ddot{\phi} + \mathrm{N}_{\dot{\phi}}\dot{\phi} = \mathrm{N}_C \cos\omega_e t + \mathrm{N}_S \sin\omega_e t \quad (2.3.4)$$

$$\left(\mathrm{I}_{xx}+J_{xx}\right)\ddot{\phi} + \mathrm{K}_{\dot{\phi}}\dot{\phi} + W\overline{GM}\left[1+\frac{\Delta\overline{GM}}{\overline{GM}}\cos(\omega_e t - k\xi_0)\right]\phi + K_{\ddot{\eta}_G}\ddot{\eta}_G + K_{\dot{\eta}_G}\dot{\eta}_G + K_{\ddot{\psi}}\ddot{\psi} +$$

$$K_{\dot{\psi}}\dot{\psi} + K_{\psi}\psi = K_C \cos\omega_e t + K_S \sin\omega_e t \quad (2.3.5)$$

where the hydrodynamic and hydrostatic coefficients are obtained from the ordinary strip method and the metacentric height taking into account the variation of righting moment in waves given by the equivalent linearization. It should be noted that the last equation regarding roll is a linear differential equation with respect to the roll angle φ although the unique feature of the equation is the presence of time dependent coefficient of the roll angle φ. Furthermore, this kind of equation has a property of considerable importance in ship rolling problem, for certain values of the encounter frequency ω_e, the solution is unstable. The unstable encounter frequency may be found from unstable solution of Mathieu's equation, in which unstable roll occurs when encounter frequency ω_e is equal to twice of the natural frequency ω_ϕ of roll.

Several numerical simulations follow having as parameters H/λ (wave steepness) and χ (encounter angle).

2.4 Theoritical and experimental study of the nonlinearly coupled heave, pitch and roll motions of a ship in longitudinal waves (I.Oh, A.Nayfeh, D.Mook)

In that paper, the authors describe the real situation more accurately than Blocki or Nayfeh and Sanchez. Specifically they lift the restriction of fore-and-aft symmetry, add a third degree of freedom (pitch), and consider head and following seas both theoretically and experimentally. The heave and pitch motions are assumed to be independent of the roll motion, an assumption that was verified experimentally. Due to the heave-pitch roll coupling, the amplitudes and frequencies of the heave and pitch motions play the role of an effective amplitude and frequency of the parametric excitation. The parametric term in the roll equation basically accounts for the time-dependent variation of the metacentric height. The authors investigate the principal

parametric resonance in which the excitation wave frequency is twice the natural frequency in roll.

The equations of motions suggested are:

$$\ddot{z} + 2\zeta_z \cdot \dot{z} + \omega_z^2 z = \overline{Z}(t) \qquad (2.4.1)$$

$$\ddot{\theta} + 2\zeta_\theta \cdot \dot{\theta} + \omega_\theta^2 \theta = \overline{\Theta}(t) \qquad (2.4.2)$$

$$\ddot{\phi} + \omega_\phi^2 \phi + 2\mu_1 \dot{\phi} + 2\mu_3 \dot{\phi}^3 - \alpha_3 \phi^3 -$$

$$\frac{1}{2}\left(\mathrm{K}_{\phi z}\phi z + \mathrm{K}_{\phi\theta}\phi\theta + \mathrm{K}_{\dot{\phi}\dot{z}}\dot{\phi}\dot{z} + \mathrm{K}_{\dot{\phi}\dot{\theta}}\dot{\phi}\dot{\theta}\right) = \overline{K}(t) \qquad (2.4.3)$$

where ζ_z and ζ_θ are damping coefficients; $\omega_z, \omega_\theta, \omega_\phi$ are the natural frequencies; μ_1, μ_3 are linear and cubic roll damping coefficients, a_3 is the constant cubic stiffness coefficient and $\mathrm{K}_{\phi z}, \mathrm{K}_{\phi\theta}, \mathrm{K}_{\dot{\phi}\dot{z}}, \mathrm{K}_{\dot{\phi}\dot{\theta}}$ are the constant coefficients of the quadratic coupling terms.

Assuming simple harmonic wave excitation, we write:

$$\overline{Z}(t) = \overline{Z}_0 \cos\Omega t \qquad (2.4.4)$$

$$\overline{\Theta}(t) = \overline{\Theta}_0 \cos(\Omega t + \tau_d) \qquad (2.4.5)$$

where Ω is the frequency of the exciting waves, τ_d is the phase delay of the pitch moment relative to the heave force, $\overline{Z}_0$ is a measure of the amplitude of heave excitation force, and $\overline{\Theta}_0$ is a measure of the amplitude of the pitch excitation moment. $\overline{Z}_0$ and $\overline{\Theta}_0$ are functions of the wave height as well as the position of the mass center in the wave. Since (2.4.1) and (2.4.2) are uncoupled linear equations, they are solved as

$$z = a_z \cos(\Omega t + \tau_z) \qquad (2.4.6)$$

$$\theta = a_\theta \cos(\Omega t + \tau_\theta) \qquad (2.4.7)$$

where a_z and a_θ are the amplitudes of heave and pitch respectively, τ_z *and* τ_θ are the phase lags of heave and pitch relative to excitation wave, and τ_θ is a function of ζ_θ and τ_d.

We consider the case in which the ship is in longitudinal waves so that $\overline{K}(t) = 0$ in equation (2.4.3)

Substituting (2.4.6) and (2.4.7) into (2.4.3) we obtain

$$\ddot{\phi} + \omega_{\phi}^2\phi + 2\mu_1\dot{\phi} + 2\mu_3\dot{\phi}^3 - \alpha_3\phi^3 + \left[f_1\cos(\Omega t + \tau_z) + f_3\cos(\Omega t + \tau_\theta)\right]\phi$$
$$+\left[f_2\sin(\Omega t + \tau_z) + f_4\sin(\Omega t + \tau_\theta)\right]\dot{\phi} = \overline{K}(t) \qquad (2.4.8)$$

where

$$f_1 = -\frac{1}{2}a_z K_{\phi z}, f_2 = \frac{1}{2}\Omega\alpha_z K_{\dot{\phi}\dot{z}}$$
$$f_3 = -\frac{1}{2}a_\theta K_{\phi\theta}, f_4 = \frac{1}{2}\Omega\alpha_\theta K_{\dot{\phi}\dot{\theta}}$$

2.5 Stability analysis of ships undergoing strong roll amplification in head seas (M.A.S Neves, C.Rodriguez)

The work presents a new mathematical model with nonlinearities defined up to the third order in terms of the heave, pitch, and roll couplings in order to simulate strong roll amplifications in head seas. The influence of non linear terms on the dynamics of roll parametric resonance appears to be relevant for low metacentric conditions and extreme waves.

The work of Prof. Neves intended to compare the stability of two fishing vessels with very similar characteristics but with different sterns. Uncoupled Mathieu and Mathieu Duffing equations and its variants are often used for parametric resonance investigations but tend to overpredict the resonant rolling motions. In order to overcome these deficiencies this third order mathematical model comprehensively couples the heave roll and pitch motions. Coupling coefficients were calculated analytically in terms of basic geometric hull characteristics. The results of the mathematical model were compared to some experimental results showing good agreement. The second order model failed to give finite response. Additionally, the dynamic behavior of two similar hulls were compared showing that the hull with flat transom was more susceptible in parametric rolling.

3 Objectives

The topic of this thesis stems from the recent accidents of post-panamax containerships resulting to serious economic losses. The objectives of the thesis were (sorted from the most general to the most specific):

- Study of the phenomenon of the parametric rolling affecting post panamax containerships. A problem which has emerged quite recently.
- Creation and programming of a 3 DOF mathematical model for the examination of ship's behavior in longitudinal waves under conditions stimulating the phenomenon of parametric rolling.
- Numerical solution of the above mentioned model for three different versions. The first version is a 1 DOF model taking into account only the roll motion. The second is a linear model with cross-coupling of roll, pitch and heave terms with the addition of a third order restoring term regarding the roll motion in order to get results with finite values. The previous also applies to the first model as well. Finally, a more complex version of the model was run in which there are up to third order terms with cross-coupling of roll, pitch and heave. The response of the three modes under parametric rolling conditions was derived in a graphical way while their comparison was an interesting part.
- Finding of parametric rolling boundaries for each of the three above mentioned model with numerical continuation. A plot that would present the critical wave height in function with the alpha parameter could very useful when designing such a ship.

4 Parametric resonance of pendulum

In the following chapter the correlation between a vertically driven pendulum and a ship undergoing parametric rolling is discussed.

4.1 The instability

The vertically driven pendulum is the only driven pendulum which has the same stationary solutions as the undriven pendulum, φ = 0 and φ = 180°. In the undriven case, these solutions are always stable and unstable, respectively. But vertical driving can change stability into instability and vice versa. Mainly the destabilization of the normally stable equilibrium of the pendulum will be described because is the ine having close relation with the thesis.

In order to investigate the stability of a fixed point, we have to linearize the equation of motion around a fixed point. For φ = 0 we get the damped Mathieu equation:

$$\frac{d^2\phi}{dt^2} + \gamma \frac{d\phi}{dt} + \left(\omega_0^2 + a\cos\omega_e t\right)\phi = 0 \qquad (4.1.1)$$

The same equation holds for φ = 180° except that ω_0^2 has a minus sign. Thus, one studies the Mathieu equation for positive as well as negative values of ω_0^2. Alpha parameter plays the role of destabilizing the restoring term as it happens with the fluctuation of GM for the ship. The vertical driving is similar to the stability fluctuation of the ship due to large longitudinal waves. γ obviously is the damping of the oscillation which has the same result as the linear damping of the ship which is introduced in the model used in this thesis and which is discussed analytically in Chapter "Application"

Even though the Mathieu equation is a linear differential equation, it cannot be solved analytically in terms of standard functions. The reason is that one of the

coefficients isn't constant but time-dependent just like the Mathieu equation used for parametric rolling prediction.

The final solutions have the following form:

$$\phi(t) = c(t) \cdot e^{\lambda t} \qquad (4.1.2)$$

where $c(t) = c(t + {}^{1}\!/\!_{f})$ (4.1.3) with f being defined in (4.1.4). The exponent λ is called Floquet exponent. It isn't uniquely defined because any factor exp(2πit/f) $e^{2\pi i t/f}$ can be either absorbed in c(t) or in $e^{\lambda t}$. We have a better view of the solutions in Figure 3

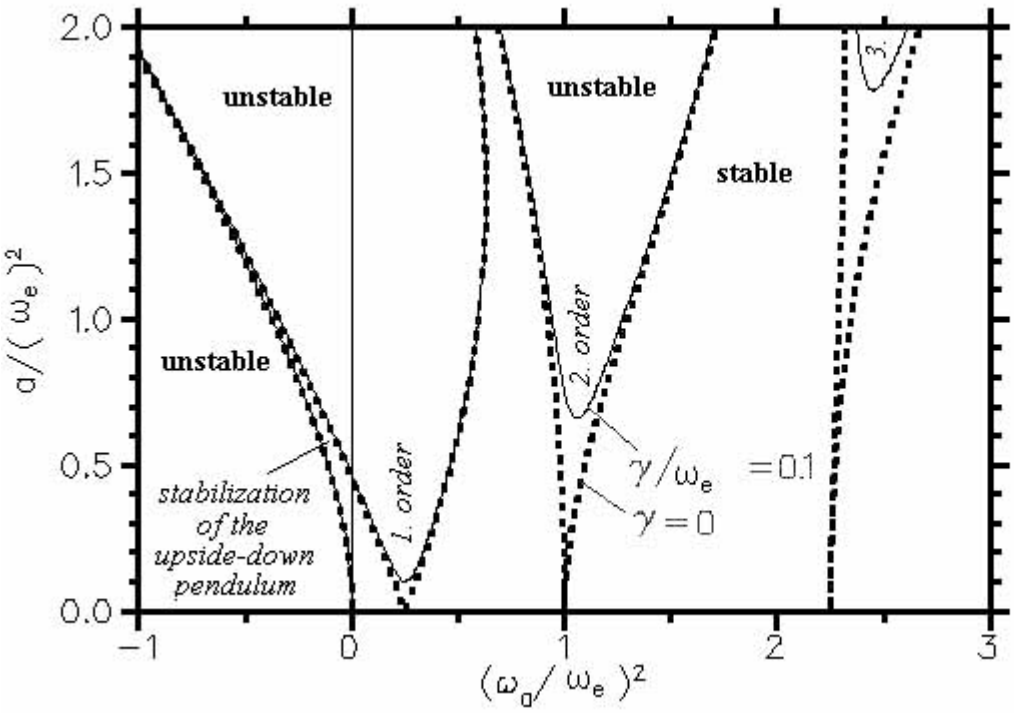

Figure 3: Plotting of solutions.

The solutions shown above are calculated numerically for a certain value of the damping constant. Note the small area of stability for negative values of ω_0^2. It denotes the possibility of stabilizing the upside-down pendulum. In the undamped case, the areas of stability form goes (dashed lines) down to zero. That is, an infinitesimal driving amplitude a destabilizes the down-hanging pendulum if the parametric resonance condition

$$f_0 \equiv \frac{\omega_0}{2\pi} = \frac{f}{2} n \qquad (4.1.4)$$

is fulfilled, where n is an integer defining the order of parametric resonance. In case of damping, a driving amplitude a exceeding a critical value $a_c \sim \gamma^{1/n}$ is necessary for destabilization.

4.2 Parametrically excited oscillations

In parametric resonance the amplitude of the unstable solution grows exponentially to infinity. Damping does not stop this growth contrary to normal resonance caused by an additive driving force. Thus, the nonlinearities in the parametrically driven pendulum are necessary for saturation. This saturation is caused by the fact that nonlinear oscillators have in general an amplitude-dependent eigenfrequency. The growth of the parametrically excited oscillation will shift the eigenfrequency out of resonance. For that reason it is essential to introduce some nonlinear terms in our model in order to get finite values of roll angles.

5 The phenomenon of parametric rolling

5.1 Ship's response in longitudinal waves

As mentioned above, parametric rolling is created by the fluctuation of the ship's stability when she is on a wave. When the mid of the ship is on a wave trough then the waterplane area is significantly greater than in calm water. In that case, the bow and stern have a greater draft than they have when being in still water while the midship has a smaller draft. Due to the above the GM has a greater value compared to the still water case. On the other hand when the midship is on a wave crest, the bow and stern have smaller drafts compared to the still water condition. Due to the fact that containerships have hull forms with pronounced bow flare and flat transom results to a dramatic change of ship's GM when facing longitudinal waves. The profile of the discussed above waterlines is presented in figure 4 for the former and in 5 for the latter case. In figure 6 we can see the waterplane area of the three cases.

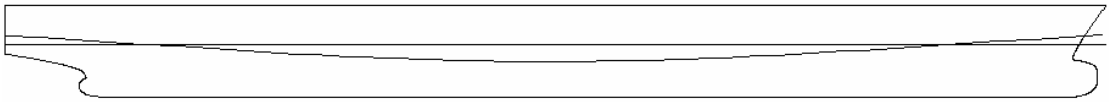

Figure 4: Form of waterline in wave trough vs in calm water.

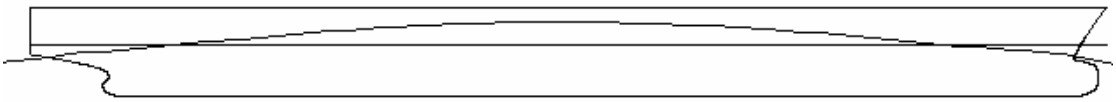

Figure 5: Form of waterline in wave crest vs in calm water.

.

Figure 6: Form of waterline in wave crest and wave trough vs. in calm water.

5.2 Ship's response in calm water

When an instantaneous force is applied on a ship laying in calm water an oscillatory damped motion is set up. The period of these oscillations, usually called natural roll period, is a function of ship's GM and inertia on the roll mode. The natural period of the ship tested and will be described in chapter 8 is shown in figure 7. We can observe that it is about 30 sec.

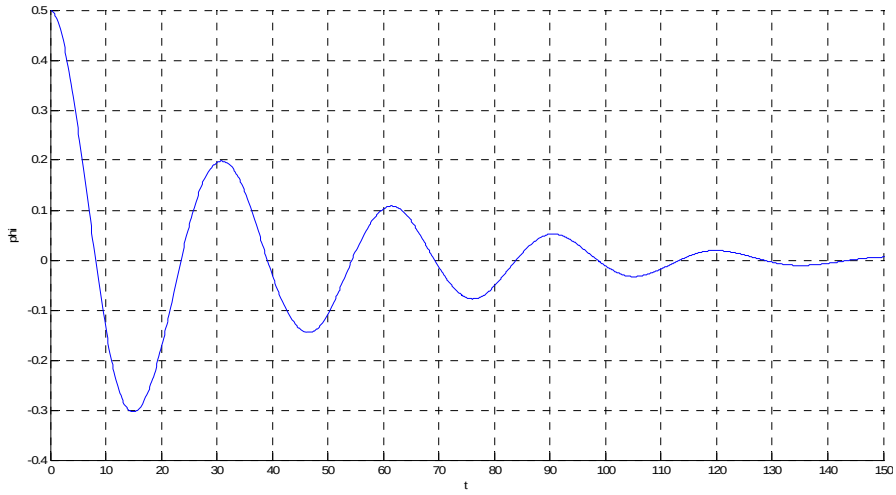

Figure 7: Sample of free roll motions.

When a ship encounters head or following waves there will be no wave excitation in the roll mode. The only excitation in this direction would be some wind gusts or some small waves not being exactly perpendicular to the ship's centerline. With the above conditions dominating when the roll equilibrium is disturbed e.g an instantaneous external force, our ship would roll with its natural frequency.

5.3 Physics of parametric resonance

As described in sub-paragraph 5.1 when a ship sails in head or following seas we have stability fluctuation. If this fluctuation occurs twice one natural period, roll angles may take significantly large values. There are two conditions that have to be satisfied in order to observe severe parametric roll. The first is that the ship's encounter frequency is double the natural frequency. The second is that the external excitation (wind gusts)have to be applied when the stability is increasing. With these conditions the restoring moment tend to return the ship to its equilibrium position

At the end of the first quarter of the period the ship returns to its equilibrium position and keeps rolling to the other side because of its inertia. In that critical point the midship is on the waves crest with reduced stability which causes a larger roll angle due to the smaller restoring moment. In the third quarter midship is on a wave trough while reaching equilibrium position creating a restoring moment greater than that of still water. To be simpler we could argue that the restoring moment is greater than the one needed. This phenomenon is similar to the one described for the first quarter. Respectively, in the fourth quarter the behavior is similar to that of the second quarter. While the above conditions are being satisfied the roll angle keeps growing until other factors start to take effect on the phenomenon. The differences in the roll angle development of parametric rolling in comparison with the free roll case are presented graphically in the plot of the ABS guide [13]. The fluctuation of GM is presented at this diagram as well.

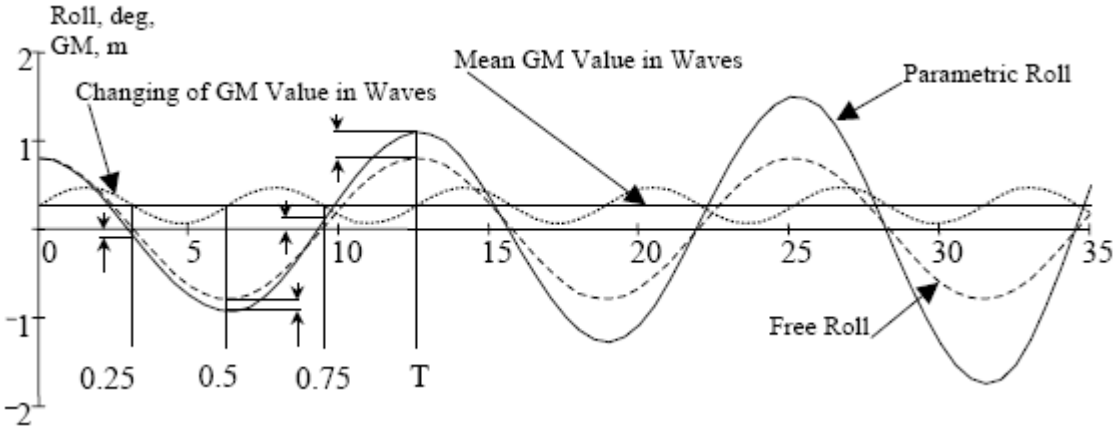

Figure 8: Development of parametric roll [13].

5.4 Influence of roll damping

As we will see below, roll damping plays a significant role on the development of parametric roll resonance. Roll damping is created due to the fact that a rolling ship generates waves and eddies and experiences viscous drag. The condition that indicates the parametric resonance development is the change on roll amplitude after one roll period. If the reduction of roll amplitude per period caused by damping is greater than the one caused by the changing of stability, then the roll angle will be reduced (damped). If the reverse phenomenon occurs then parametric resonance is taking

place. The above process is totally affected by the roll damping values. We can conclude that for given wave height there is a critical value of roll damping below which parametric resonance can occur.

5.5 Summary

As mentioned in a previous paragraph, GM value is the one of the most important parameters which determines the development of parametric rolling. GM is not only a parameter indicating the stability of a ship but also influences the natural period. The latter is directly connected to the encounter period which is also a function of the wave length. Taking into account all the above data, we can conclude that GM is the parameter affecting many aspects of parametric rolling.

6 Basics of ship motions

6.1 General

The response of a ship advancing in a seaway is a complicated phenomenon involving the interactions between the vessel dynamics and several distinct hydrodynamic forces. Therefore, in the following chapter we will concentrate on those aspects of theory and that were used by naval architects trying to predict ship motions in various conditions. Specifically a linear theory of ship motions will be presented in connection with the model used in the present thesis. All ship responses are nonlinear to some extent, but in many cases when nonlinearities are small a linear theory will yield good predictions. In our case, as we will find out later on our study, these nonlinearities play a significant role to the complicated phenomenon of parametric rolling. This mainly happens because of the large amplitude of the motions.

A ship sailing at a steady forward speed encountering a sequence of regular waves, will move in six degrees of freedom. That is, the ship's motion can be considered to be made up of three translational components, surge, sway and heave, and three rotational components, roll, pitch and yaw. Consequently for a randomly shaped vessel six nonlinear equations of motion, with six unknowns, must be set up and solved simultaneously. However, for slender vessels in low to moderate sea states it is possible to assume that the ship motions will be small so that a linear theory would give us a good approximation. For the usual case of an unrestrained ship with port/star board symmetry, the six nonlinear equations reduce to two sets of three linear equations. The vertical- plane or longitudinal motions (surge, heave, pitch) are uncoupled from the horizontal plane or transverse motions (sway, roll, yaw).

6.2 The head sea scenario

Parametric rolling occurs mainly in head seas which is the case taken in current thesis. As noted in the former subsection, the longitudinal motions of pitch, heave and surge of a symmetrical ship in regular waves can be considered separately from the transverse modes. Furthermore, it has been found that for most comparatively long and slender ships surge has a minor effect and can be neglected. The above assumes

that forward speed Uo is constant. The further simplification in this sub-paragraph is to consider only the case of head seas, or waves from directly ahead (μ=180 deg). It is assumed that both the wave excitation forces and the resultant oscillatory motions are linear and harmonic, acting at the frequency of wave encounter,

$$\omega_e = \omega + {\omega^2 g}/{U_0} \tag{6.2.1}$$

the equations of motion are based on Newton's second law [1] of motions which in one form states that for translational modes the forces acting on a body must equal the mass times the acceleration. For the rotational modes the moments acting on the body equal the mass moment of inertia times the angular acceleration. Thus, for heave, $\ddot{\eta}_3$, with the origin at the center of gravity (which must be located at the WL for this simple case),

$$m \cdot \ddot{n}_3 = F_3 \tag{6.2.2}$$

and for pitch, $\ddot{\eta}_5$

$$I_{55} \cdot \ddot{\eta}_5 = F_5 \tag{6.2.3}$$

where m is the mass (displacement), I_{55} mass moment of inertia about the y axis and F_3 and F_5 represent the total force and moment, respectively acting on the body as functions of time. For the simplified case, the total force and moment consist mainly of fluid forces both hydrostatic and hydrodynamic [1]. (The heave gravitational force is balanced by the static buoyancy force in calm water and this defines the $\eta_3 = 0$ position). In a linear theory the fluid forces (and moments) can be conveniently divided between the forces due to the waves acting on a restrained ship, i.e. , the forces that excite the motions, and the radiation forces due to the motions of the ship in an assumed calm sea. That is,

$$F_3(t) = F_{EX3}(t) + F_{H3}(t) \tag{6.2.4}$$

$$F_5(t) = F_{EX5}(t) + F_{H5}(t) \tag{6.2.5}$$

The excitations for sinusoidal waves are expressed as,

$$F_{EX3}(t) = \left|F_{EX3}\right| \cdot \cos(\omega_e t + \varepsilon_3) \tag{6.2.6}$$

$$F_{EX5}(t) = \left|F_{EX5}\right| \cdot \cos(\omega_e t + \varepsilon_5) \tag{6.2.7}$$

where $|F_{EX3}|$ refers to the amplitude of the heave force and $|F_{EX5}|$ to the amplitude of the pitch moment, and where ε_3 and ε_5 are the phase angles between the excitation and the waves.

6.3 Coupling of motions

The part of this chapter which has great interest for the thesis analyzes the coupling of motions. The accuracy of our calculations is relied on this coupling because of the energy transfer among the motions. In the linear theory the hydrodynamic radiation forces due to the coupled motions of the vessel in otherwise calm water can be expressed in terms that are directly proportional to the vertical displacements, velocities and accelerations. For sinusoidal motions, the hydrodynamic radiation force and moment can be written as [1],

$$F_{H3} = -\big[A_{33}(\omega)\ddot{\eta}_3 + B_{33}(\omega)\dot{\eta}_3 + C_{33}\eta_3 + A_{35}(\omega)\ddot{\eta}_5 + B_{35}(\omega)\dot{\eta}_5 + C_{35}\eta_5\big] \quad (6.3.1)$$

$$F_{H5} = -\big[A_{53}(\omega)\ddot{\eta}_3 + B_{53}(\omega)\dot{\eta}_3 + C_{53}\eta_3 + A_{55}(\omega)\ddot{\eta}_5 + B_{55}(\omega)\dot{\eta}_5 + C_{55}\eta_5\big] \quad (6.3.2)$$

where $A_{jk}(\omega)$ and $B_{jk}(\omega)$ are coefficients that are functions of frequency. The minus sign is introduced for convenience in the final equations of motion.

The double-subscript notation for the coefficients A_{jk}, B_{jk}, C_{jk} is adopted in anticipation of each necessary use for the complete 6 degree of freedom case to be discussed subsequently. Where the subscripts are the same (A_{33}, B_{33}) a simple uncoupled coefficient in the heave (3) or pitch (5) mode is intended. Where the subscripts are different (A_{35}, B_{35}) the meaning is that the k-mode is coupled into the j-mode (e.g., $A_{35} \cdot \ddot{\eta}_5$ represents the force in the heave mode due to a pitch acceleration).

The final coupled equations of motion for heave and pitch of a vessel in regular head seas are obtained by combining Equations (6.2.2), (6.2.3), (6.2.4) and (6.2.5). The radiation forces are moved to the left hand side of the equations because they are proportional to the unknown motions. Thus,

$$(A_{33} + m)\ddot{\eta}_3 + B_{33}\dot{\eta}_3 + C_{33}\eta_3 + A_{35}\ddot{\eta}_5 + B_{35}\dot{\eta}_5 + C_{35}\eta_5 = |F_{EX3}|\cos(\omega_e t + \varepsilon_3) \quad (6.3.3)$$

$$(A_{55}+I_{55})\ddot{\eta}_5+B_{55}\dot{\eta}_5+C_{55}\eta_5+A_{53}\ddot{\eta}_3+B_{53}\dot{\eta}_3+C_{53}\eta_3=\left|F_{EX5}\right|\cos(\omega_e t+\varepsilon_5) \quad (6.3.4)$$

The A_{jk}-terms correspond to added mass, in phase with vertical accelerations, the B_{jk}-terms to hydrodynamic damping in phase with vertical velocity. Terms involving the coefficient C_{jk} are called restoring forces and moments, representing the net hydrostatic buoyancy effects of the ship motions. It should be noted that the C_{jk} are related to the hydrostatic coefficients used in ships stability calculations, i.e., C_{33}, C_{35}, and C_{55} are related to tons per cm immersion, change in displacement per cm of trim and moment to trim 1 cm respectively.

The cross-coupling between heave and pitch results from the coefficients with subscripts 35 or 53. For a fore-and-aft symmetric, the cross coupling between heave and pitch is very important and must be retained in order to correctly predict the motions in head seas at forward speed.

The terms on the right-hand side of the equations represent the excitations, the forces or moments that would act on a restrained ship encountering wave at a forward speed Uo. $\left|F_{EX3}\right|$ and $\left|F_{EX5}\right|$ are the amplitudes of these harmonic forces and ε_3 and ε_5 the phase angles. In order to apply hydrodynamic theory to obtain expressions for the excitation amplitudes the exciting forces and moments are usually subdivided into the Froude-Krylov and diffraction excitations. The Froude-Krylov excitations represent the integration of the pressure over the body surface that would exist in the incident wave system if the body were not present. The diffraction exciting forces and moments are caused by the diffraction or modification of the incident waves due to the presence of the vessel. The Froude-Krylov forces and moments are sometimes used to approximate the total exciting forces. This is a good approximation if the wavelength is much longer that the vessel length. For shorter wavelengths the approximation is increasingly inaccurate because the diffraction force becomes significant. For short waves the diffraction force may become approximately one-half of the total exciting force.

The similarities of the above generic model with the one used in our calculations are made clear in the next chapter.

6.4 Theory of simple gravity waves

In the hydrodynamic theory of surface waves the following assumptions are made: the crests are straight, infinitely long, parallel and equally spaced, and wave heights are constant. The wave form advances in a direction perpendicular to the line of crests at a uniform velocity, Vc, usually referred to as celerity in order to underline that water particles don't move opposed to the wave form which is the one advancing. Such simple waves are usually referred to as two dimensional waves. It is assumed in wave theory that water has zero viscosity and is incompressible. It is convenient also to assume that, although waves are created by wind forces, atmospheric pressure on the water surface is constant after the wave train has been established.

With surface waves we can visualize the pressure changes and water-particle motions affecting the entire body of fluid- theoretically to its full depth. The motion of particles under the above ideal conditions can be sufficiently described by the velocity potential φ which is defined as a function whose negative derivative in any direction results to the velocity component of the fluid in the same direction. From its mathematical expression the necessary wave characteristics can be derived. Some manipulations in hydrodynamics can give the velocity potential for two dimensional wave in any depth of water and express the resulting wave form by a Fourier series. If the accuracy of our calculations can tolerate further simplifications the assumption of very small wave amplitudes is introduced resulting to the first-order theory which reduces the wave to the first harmonic alone. The simplified potential expression is shown below [1]:

$$\phi = -\overline{\zeta} \cdot V_C \cdot \frac{\cosh k(z+h)}{\sinh kh} \cdot \sin k(x - V_C t) \qquad (6.4.1)$$

The origin is taken at the still-water level directly over a hollow, x is the horizontal coordinate, positive in the direction of wave propagation, and z is the vertical coordinate, positive upward. This positive upward convention is adopted for consistency with the work on ship motions to follow, although it differs from some references.

Also

$\overline{\zeta}$ *is surface wave amplitude* (*half − height from crest to trough*)

L_W *is wave length*

h is depth of water

k is the wave number, $2\pi/L_W$

V_C *is the wave velocity or celerity*

t is time

For the case of deep water (roughly $h>L_W/2$) the ratio:

$\frac{\cosh k(z+h)}{\sinh kh}$ approaches e^{kz} and the expression for the velocity potential becomes:

$$\phi = -\overline{\zeta} \cdot V_C \cdot e^{kz} \cdot \sin k(x - V_C t) \tag{6.4.2}$$

Hence, the horizontal and vertical components of water velocity at any point in deep water are given by

$$u = -\frac{\partial \phi}{\partial x} = k \cdot \overline{\zeta} \cdot V_C \cdot e^{kz} \cdot \cos k(x - V_C t) \tag{6.4.3}$$

and

$$w = -\frac{\partial \phi}{\partial z} = k \cdot \overline{\zeta} \cdot V_C \cdot e^{kz} \cdot \sin k(x - V_C t) \tag{6.4.4}$$

If the path of a particular particle be traced through a complete cycle, it will be found that in deep water all particles describe circular paths having radii that are $\overline{\zeta}$ at the surface and decrease with depth in proportion to e^{kz}. Strictly, z should here be measured the center of the circular path described by the particle. In shallow water the particles move in ellipses with a constant horizontal distance between foci and with vertical semi-axes varying with depth. At the bottom, the vertical semi-axis is zero, and the particles oscillate back and forth on straight lines.

To determine the foregoing velocities in any particular case, it is necessary to derive an expression for wave velocity Vc. Books by Milne-Thompson and Korvin-Kroukovsky show that the conditions of velocity and pressure at the surface of the wave require that

$$\frac{\partial^2 \phi}{\partial x^2} + g \frac{\partial \phi}{\partial z} = 0 \tag{6.4.5}$$

Inserting equation (6.4.1) for the potential in (6.4.5) it can be shown that

$$V_C^2 = \frac{g}{k}\tanh kh \tag{6.4.6}$$

which defines the velocity of a wave in any depth of water. Then in very shallow water (roughly $h<L_W/25$)

$$V_C^2 = gh \tag{6.4.7}$$

and in deep water ($h> L_W/2$)

$$V_C^2 = \frac{g}{k} = \frac{gL_W}{2\pi} \tag{6.4.8}$$

For many problems the most important aspect of waves is the distribution of pressure below the surface. It is convenient to compute the pressure relative to horizontal lines of constant pressure in still water. The elevation ζ of lines of equal pressure in a wave relative to the still-water pressure lines is obtained from the expression:

$$\zeta = \frac{1}{g}\frac{\partial \phi}{\partial t} \tag{6.4.9}$$

which is derived in hydrodynamics texts (Lamb) by means of Bernoulli's theorem for a gravity force acting on a body of fluid under uniform atmospheric pressure, assuming that wave height is small. Then for water of any depth:

$$\zeta = \frac{k\overline{\zeta}V_C^2}{g}\frac{\cosh k(z+h)}{\sinh kh}\cos k(x - V_C t) \tag{6.4.10}$$

Since from equation (6.4.6) $\frac{kV_C^2}{g} = \tanh kh$ this can be simplified to:

$$\zeta = \overline{\zeta}\frac{\cosh(z+h)}{\cosh kh}\cos k(x - V_C t) \tag{6.4.11}$$

In deep water (large h) the ratio $\frac{\cosh(z+h)}{\cosh kh}$ approaches e^{kz}, and

$$\zeta = \overline{\zeta}\cos k(x - V_C t) \tag{6.4.12}$$

The last equation will be used in this exact form below to describe the wave profile which interacts with our ship. It is a function of the relative position of the wave to the ship and of time.

7 Mathematical Model Used

7.1 Generally

The model used in this thesis was based on the work of Prof. Neves, published in various scientific journals, titled as "Stability Analysis of Ships Undergoing Strong Roll Amplifications in Head Seas" [4].

Nomenclature

ρ *density of water*
ϕ *roll angular displacement*
θ *pitch angular displacement*
∇_0 *volume at average hull position*
A_0 *waterplane area at average hull position*
g *acceleration of gravity*
I_{xx0} *transversal 2nd moment of waterplane area*
I_{yy0} *longitudinal 2nd moment of waterplane area*
J_{xx} *transversal mass moment of inertia*
J_{yy} *longitudinal mass moment of inertia*
m *ship mass*
x_{f0} *longitudinal coordinate of centroid of waterplane*
z *heave displacement of the ship*
ζ *wave elevation*
ω_e *encounter frequency*

$\bar{x}$ *longitudinal position of a transversal station*

$\bar{y}$ *half – beam of a transversal station*

$\bar{z_G}$ *vertical position of the ship's centre of gravity*

$\bar{z_B}$ *vertical position of hull volume centroid*

7.2 System of equations

$$\left(m+Z_{\ddot{z}}\right)\cdot\ddot{z}+Z_{\dot{z}}\cdot\dot{z}+Z_{\ddot{\theta}}\cdot\ddot{\theta}+Z_{\dot{\theta}}\cdot\dot{\theta}+Z_{z}\cdot z+Z_{\theta}\cdot\theta+\frac{1}{2}Z_{zz}\cdot z^2+\frac{1}{2}Z_{\phi\phi}\cdot\phi^2+$$

$$+\frac{1}{2}Z_{\theta\theta}\cdot\theta^2+Z_{z\theta}\cdot z\theta+\frac{1}{6}Z_{zzz}\cdot z^3+\frac{1}{2}Z_{\phi\phi z}\cdot\phi^2\cdot z+\frac{1}{2}Z_{\phi\phi\theta}\cdot\phi^2\cdot\theta+\frac{1}{6}Z_{\theta\theta\theta}\cdot\theta^3+$$

$$+Z_{\zeta z}(t)\cdot z+Z_{\zeta\theta}(t)\cdot\theta+Z_{\zeta zz}(t)\cdot z^2+Z_{\zeta z\theta}(t)\cdot z\theta+Z_{\phi\phi\zeta}(t)\cdot\phi^2=Z_W(t)$$

$$\left(J_{xx}+K_{\ddot{\phi}}\right)\cdot\ddot{\phi}+K_{\dot{\phi}}\cdot\dot{\phi}+K_{\phi}\cdot\phi+K_{z\phi}\cdot z\phi+K_{\theta\phi}\cdot\theta\phi+\frac{1}{2}K_{zz\phi}\cdot z^2\phi+\frac{1}{2}K_{\theta\theta\phi}\cdot\theta^2\phi+$$

$$+\frac{1}{6}K_{\phi\phi\phi}\cdot\phi^3+K_{z\phi\theta}\cdot z\phi\theta+K_{\zeta\phi}(t)\cdot\phi+K_{\zeta\zeta\phi}(t)\cdot\phi+K_{\zeta z\phi}(t)\cdot z\phi+K_{\zeta\phi\theta}(t)\cdot z\phi\theta=\mathrm{K}_W(t)$$

$$\left(J_{yy}+M_{\ddot{\theta}}\right)\cdot\ddot{\theta}+M_{\dot{\theta}}\cdot\dot{\theta}+M_{\ddot{z}}\cdot\ddot{z}+M_{\dot{z}}\cdot\dot{z}+M_{z}\cdot z+M_{\theta}\cdot\theta+\frac{1}{2}M_{zz}\cdot z^2+\frac{1}{2}M_{\phi\phi}\cdot\phi^2+$$

$$+\frac{1}{2}M_{\theta\theta}\cdot\theta^2+M_{z\theta}\cdot z\theta+\frac{1}{2}M_{\phi\phi z}\cdot\phi^2\cdot z+\frac{1}{2}M_{\phi\phi\theta}\cdot\phi^2\cdot\theta+\frac{1}{2}M_{\theta\theta}\cdot\theta^2\cdot z+\frac{1}{6}M_{\theta\theta\theta}\cdot\theta^3+$$

$$M_{\zeta z}(t)\cdot z+M_{\zeta\theta}(t)\cdot\theta+M_{\zeta z\theta}(t)\cdot z\theta+M_{\phi\phi\zeta}(t)\cdot\phi^2=M_W(t)$$

On the right hand of the above equations, $Z_W(t)$, $K_W(t)$, $M_W(t)$, describe the wave external excitation in the heave, roll and pitch modes, respectively. On the left hand side of the equations, nonlinear restoring terms include dependence on all body modes (z, φ, θ) and wave profile (ζ). Dots refer to velocities, double dots to accelerations. In all modes, coefficients with dotted and double dotted subscripts are damping and added masses coefficients, respectively.

In the numerical implementation of this mathematical model added masses, vertical motions dampings and wave external excitations are assumed linear and are computed using the software “Seakeeper” of Maxsurf suite of applications.

At the next page, all the restoring coefficients are presented including the non linear coupling ones.

7.3 Coefficients

Hydrostatic restoring coefficients(Calm Water): Linear

$Z_z = \rho g A_0$	$K_z = 0$	$M_z = -\rho g A_0 x_{f0}$
$Z_\phi = 0$	$K_\phi = \rho g[\nabla_0(\bar{z}_{B0} - \bar{z}_{g0}) + I_{xx0}]$	$M_\phi = 0$
$Z_\theta = -\rho g A_0 x_{f0}$	$K_\theta = 0$	$M_\theta = \rho g[\nabla_0(\bar{z}_{B0} - \bar{z}_{g0}) + I_{yy0}]$

Hydrostatic restoring coefficients (calm water): Second order

$Z_{zz} = -2\rho g \int_L \bar{\frac{\partial \bar{y}}{\partial z}} dx$	$K_{zz} = 0$	$M_{zz} = 2\rho g \int_L \bar{x} \bar{\frac{\partial \bar{y}}{\partial z}} dx$
$Z_{z\phi} = 0$	$K_{z\phi} = -2\rho g \int_L \bar{y}^2 \bar{\frac{\partial \bar{y}}{\partial z}} dx$	$M_{z\phi} = 0$
$Z_{z\theta} = 2\rho g \int_L \bar{x} \bar{\frac{\partial \bar{y}}{\partial z}} dx$	$K_{z\theta} = 0$	$M_{z\theta} = -2\rho g \int_L \bar{x}^2 \bar{\frac{\partial \bar{y}}{\partial z}} dx$
$Z_{\phi\phi} = -2\rho g \int_L \bar{\frac{\partial \bar{y}}{\partial z}} dx$	$K_{\phi\phi} = 0$	$M_{\phi\phi} = 2\rho g \int_L \overline{xy}^2 \bar{\frac{\partial \bar{y}}{\partial z}} dx$
$Z_{\phi\theta} = 0$	$K_{\phi\theta} = 2\rho g \int_L \overline{xy}^2 \bar{\frac{\partial \bar{y}}{\partial z}} dx$	$M_{\phi\theta} = 0$
$Z_{\theta\theta} = -2\rho g \int_L \bar{x}^2 \bar{\frac{\partial \bar{y}}{\partial z}} dx$	$K_{\theta\theta} = 0$	$M_{\theta\theta} = 2\rho g \int_L \bar{x}^3 \bar{\frac{\partial \bar{y}}{\partial z}} dx$

Hydrostatic restoring coefficients (calm water): Third order

Heave

$Z_{zzz} = 0*$	$Z_{zz\phi} = 0$	$Z_{zz\theta} = 0*$
$Z_{\phi\phi z} = \rho g \left[4 \int_L \bar{y} \left(\bar{\frac{\partial \bar{y}}{\partial z}} \right)^2 dx + A_0 \right]$	$Z_{\phi\phi\phi} = 0$	$Z_{\phi\phi\theta} = -\rho g \left[4 \int_L \overline{xy} \left(\bar{\frac{\partial \bar{y}}{\partial z}} \right)^2 dx + A_0 x_{f0} \right]$
$Z_{\theta\theta z} = 0*$	$Z_{\theta\theta\phi} = 0$	$Z_{\theta\theta\theta} = 0*$

Roll

$K_{zzz}=0$	$K_{zz\phi}=\rho g\left[4\int_L \bar{y}\left(\frac{\partial \bar{y}}{\partial \bar{z}}\right)^2 dx + A_0\right]$	$K_{zz\theta}=0$
$K_{\phi\phi z}=0$	$K_{\phi\phi\phi}=\rho g\left[8\int_L \bar{y}^3\left(\frac{\partial \bar{y}}{\partial \bar{z}}\right)^2 dx + 2\mathrm{I}_{xx0} - \nabla_0 \bar{z}_{B0} + \nabla_0 \bar{z}_G\right]$*	$K_{\phi\phi\theta}=0$
$K_{\theta\theta z}=0$	$K_{\theta\theta\phi}=\rho g\left[4\int_L \bar{x}^2 \bar{y}\left(\frac{\partial \bar{y}}{\partial \bar{z}}\right)^2 dx + I_{yy0}\right]$	$K_{\theta\theta\theta}=0$

Pitch

$M_{zzz}=0$*	$M_{zz\phi}=0$	$M_{zz\theta}=0$*
$M_{\phi\phi z}=-\rho g\left[4\int_L \overline{xy}\left(\frac{\partial \bar{y}}{\partial \bar{z}}\right)^2 dx + A_0 x_{f0}\right]$	$M_{\phi\phi\phi}=0$	$M_{\phi\phi\theta}=\rho g\left[4\int_L \bar{x}^2 \bar{y}\left(\frac{\partial \bar{y}}{\partial \bar{z}}\right)^2 dx + I_{yy0}\right]$
$M_{\theta\theta z}=0$*	$M_{\theta\theta\phi}=0$	$M_{\theta\theta\theta}=\rho g\left[2I_{yy0} - \nabla_0 \bar{z}_{B0} + \nabla_0 \bar{z}_G\right]$*

Heave-roll-pitch coupling

$Z_{z\phi\theta}=0$	$K_{z\phi\theta}=-\rho g\left[4\int_L \overline{x\bar{y}}\left(\frac{\partial \bar{y}}{\partial \bar{z}}\right)^2 dx + A_0 x_{f0}\right]$	$M_{z\phi\theta}=0$

*Obtained analytically for a wedge-sided ship. It is a good approximation for ships of conventional forms, small displacements and smooth transversal curvatures $\frac{\partial^2 \bar{y}}{\partial \bar{z}^2}$ at the considered water-line.

Derivatives due to wave passage: Second order

$Z_{\zeta z}(t) = 2\rho g \int_L \frac{\partial \bar{y}}{\partial z} \zeta \, dx$	$K_{\zeta z}(t) = 0$	$M_{\zeta z}(t) = -2\rho g \int_L \bar{x} \frac{\partial \bar{y}}{\partial z} \zeta \, dx$
$Z_{\zeta\phi}(t) = 0$	$K_{\zeta\phi}(t) = 2\rho g \int_L \bar{y}^2 \frac{\partial \bar{y}}{\partial z} \zeta \, dx$	$M_{\zeta\phi}(t) = 0$
$Z_{\zeta\theta}(t) = -2\rho g \int_L \bar{x} \frac{\partial \bar{y}}{\partial z} \zeta \, dx$	$K_{\zeta\theta}(t) = 0$	$M_{\zeta\theta}(t) = 2\rho g \int_L \bar{x}^2 \frac{\partial \bar{y}}{\partial z} \zeta \, dx$

Derivatives due to wave passage: Third order

Heave

$Z_{\zeta\zeta z}(t) = 0^*$	$Z_{\zeta\zeta z}(t) = 0$	$Z_{\zeta\zeta\theta}(t) = 0^*$
$Z_{\zeta zz}(t) = 0^*$	$Z_{\zeta z\phi}(t) = 0$	$Z_{\zeta z\theta}(t) = 0^*$
$Z_{\phi\phi\zeta}(t) = -\rho g \int_L \left[2\bar{y} \left(\frac{\partial \bar{y}}{\partial z} \right)^2 + \bar{y} \right] \zeta \, dx$	$Z_{\theta\theta\zeta}(t) = 0^*$	$Z_{\zeta\phi\theta}(t) = 0$

Roll

$K_{\zeta\zeta z}(t) = 0$	$K_{\zeta\zeta\phi}(t) = \rho g \int_L \left[2\bar{y} \left(\frac{\partial \bar{y}}{\partial z} \right)^2 + \bar{y} \right] \zeta^2 \, dx$	$K_{\zeta\zeta\theta}(t) = 0$
$K_{\zeta zz}(t) = 0$	$K_{\zeta z\phi}(t) = -\rho g \int_L \left[4\bar{y} \left(\frac{\partial \bar{y}}{\partial z} \right)^2 + 2\bar{y} \right] \zeta \, dx$	$K_{\zeta z\theta}(t) = 0$
$K_{\phi\phi\zeta}(t) = 0$	$K_{\theta\theta\zeta}(t) = 0$	$K_{\zeta\phi\theta}(t) = \rho g \int_L \left[4\overline{xy} \left(\frac{\partial \bar{y}}{\partial z} \right)^2 + 2\overline{xy} \right] \zeta \, dx$

Pitch

$M_{\zeta\zeta z}(t) = 0^*$	$M_{\zeta\zeta\phi}(t) = 0$	$M_{\zeta\zeta\theta}(t) = 0^*$
$M_{\zeta zz}(t) = 0^*$	$M_{\zeta z\phi}(t) = 0^*$	$M_{\zeta z\theta}(t) = 0^*$
$M_{\phi\phi\zeta}(t) = \rho g \int_L \left[2\overline{xy} \left(\frac{\partial \bar{y}}{\partial z} \right)^2 + \overline{xy} \right] \zeta \, dx$	$M_{\theta\theta\zeta}(t) = 0^*$	$M_{\zeta\phi\theta}(t) = 0$

7.4 System of co-ordinates

Oxyz is a right handed co-ordinate system with axis Oz passing through the centre of mass G (also through buoyancy center), Ox pointing forward and plane Oxy coinciding with the calm water surface as it is seen in figure 9. Heave motion is referenced to point O. A positive heave motion implies in a lower immersed volume. The centre of gravity is defined by z_G, coordinate of point **g**. The vertical coordinate of the centre of buoyancy z_B necessarily will negative.

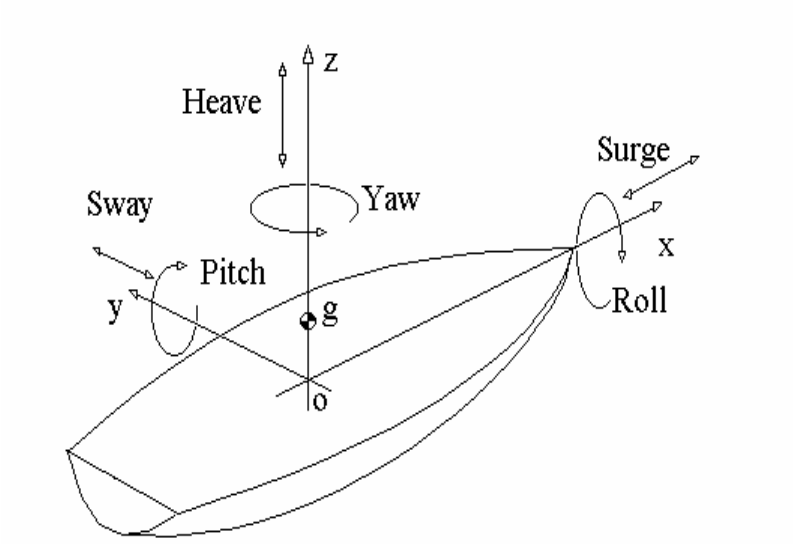

Figure 9: The system of co-ordinates used.

8 Application

In order to run the model we had to compute all the necessary coefficients presented in the chapter “Mathematical model used”

All the calculations were made with Excel while added masses and dampings for heave and pitch, as well as their coupled coefficients, were derived with Maxsurf Seakeeper. Hydrostatic data like Immersed Volume, Displacement, GM, BM, BM_L, Waterplane Area, Waterplane Area Centroid, Transversal and Longitudinal 2^{nd} moment of Waterplane Area. All necessary geometric data were obtained by the body-plan of the ship using AutoCAD.

8.1 The ship

The Ship that was used in the calculations of this thesis was a 6600TEU Post-Panamax Containership tested in the towing tank of the National Maritime Research Institute of Japan.

Through the Body Plan we can notice the bow and stern flare which is typical for that kind of ships and which is the major reason which creates the parametric instability.

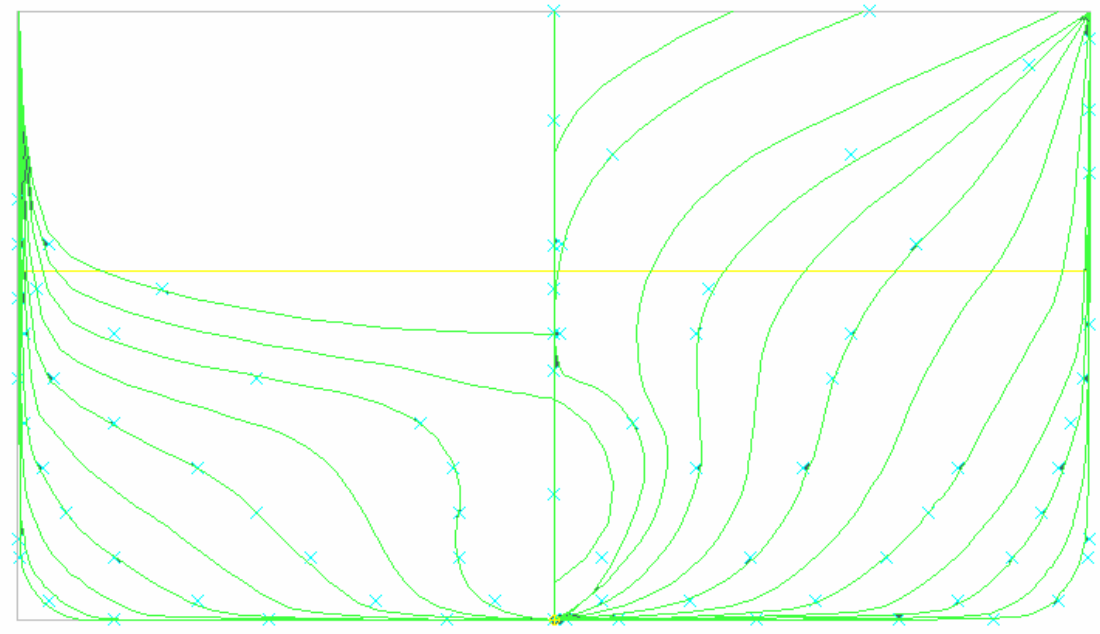

Figure 11: Body plan of the ship.

At this point we have to highlight once again the significance of the hull form since that is the most important parameter which creates the variation of GM when the ship travels in head or following seas. In the next chapter we can see the role of the form of the sections to the model used in this thesis.

The Main Particulars of the ship can be found at the Tab below:

L (m)	*286.87*
B (m)	*42.8*
D (m)	*24*
T (m)	*14*
Δ (t)	*113,956*
C_B	*0.647*
GM (m)	*1.08*
KG (m)	*18.827*
LCG (m) from amid.+ve for	*-9.323*
Waterplane area (m^2)	*10114*
T_0 (natural roll period) (s)	*30.26*
ω_o (natural roll frequency) (rad/s)	*0.2076*

Some other interesting characteristics of the ship are presented in the next sub-paragraphs here they are analytically computed in order to be inserted into the algorithm

8.2 Added masses and dampings

The added masses and dampings were derived with Maxsurf Seakeeper. In order to make the necessary hydrodynamic calculations the Hull geometry was inserted. Additional input was the ship's forward speed which was 4 kn and the wave heading which was fixed at 180 deg. The following results were obtained:

mass+added mass 33 $m + Z_{\ddot{z}}$	149.647.024 kg
Inertia+added inertia 55 $J_{yy} + M_{\ddot{\theta}}$	752.763.959.062 $kg \cdot m^2$
Damping 33 $Z_{\dot{z}}$	72.870.518 kg/s
Added mass 35 $Z_{\ddot{\theta}}$	1.810.274.280 $kg \cdot m$
Damping 35 $Z_{\dot{\theta}}$	1767114533 $kg \cdot m/s$
Damping 55 $M_{\dot{\theta}}$	380795280003 $kg \cdot m^2/s$
Added inertia 53 $M_{\ddot{z}}$	3706664872 $kg \cdot m$
Damping 53 $M_{\dot{z}}$	1074248812 $kg \cdot m/s$

The added mass of the ship concerning the roll mode can be calculated from the following formula:

$$\omega_0^2 = \left(\frac{2\pi}{T_0}\right)^2 = \frac{mgGM}{\left(J_{XX} + K_{\ddot{\phi}}\right)} \Rightarrow J_{XX} + K_{\ddot{\phi}} = \frac{mgGM}{\left(\frac{2\pi}{T_0}\right)^2} = 27999662000 kg \cdot m$$

The damping used to the calculations is the linear term. It was computed using Vought's diagram figure 12. The method[1] used to calculate the damping $K_{\dot{\phi}}$ gives the undimensional sectional damping coefficient. The procedure for the final value

[1] Principles of Naval Architecture Volume III

included the calculation of the damping for each section and then integration of these values along the ship.

The final value was $K_{\dot{\phi}} = 1.6 \cdot 10^9 \frac{N \cdot m}{(rad/s)^2}$

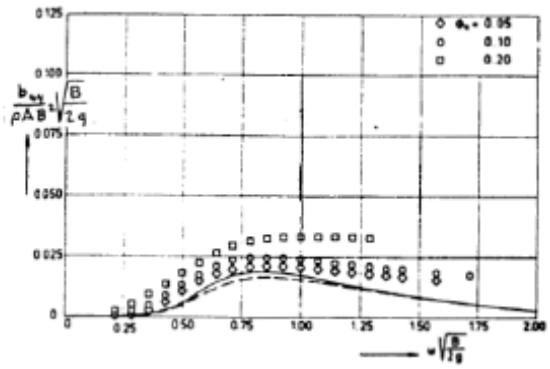

Figure12: Vought's diagram.

8.3 Definition of $\left(\frac{\partial \bar{y}}{\partial \bar{z}}\right)$

The quantity $\left(\frac{\partial \bar{y}}{\partial \bar{z}}\right)$ is the cotangent of the angle presented below in figure 10 and it is considered always greater than zero in case of a conventional hull form. It represents how fast the beam of the ship changes in relation with the draught. It plays a significant role on the variation of the stability caused by a long wave passing along the ship resulting in a smaller waterplane area. The smaller the waterplane area is the smaller the righting arm becomes.

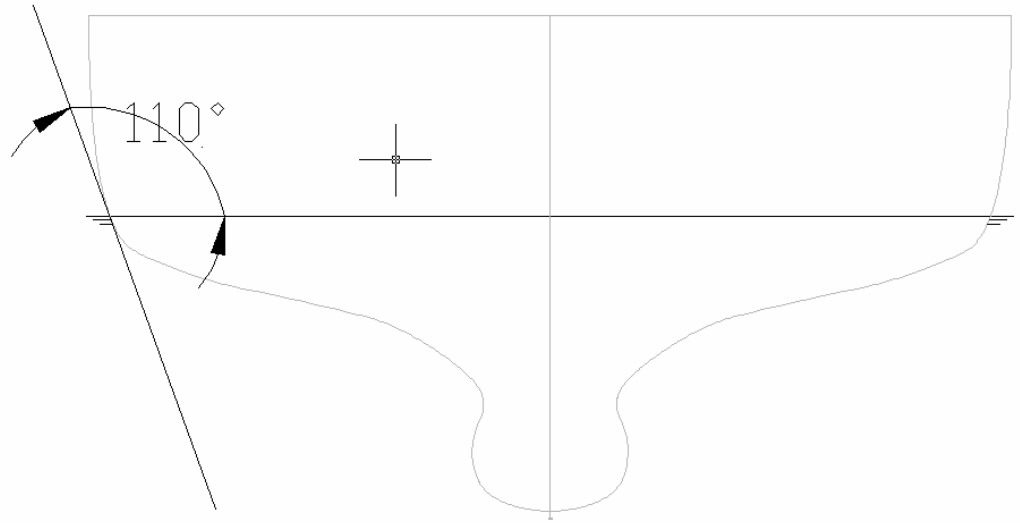

Figure 10: Definition and measurement of $\left(\frac{\partial \bar{y}}{\partial \bar{z}}\right)$.

The ship was divided to 21 sections which were given from the National Maritime Research Institute of Japan. Each section has its $\bar{x}$ which stands for its longitudinal co-ordinate and $\bar{y}$ is the half-beam of the section. So, in the integrals which are used in the restoring coefficients $\bar{x}$ and $\bar{y}$ are measured for each section and then numerically integrated in order to get the final result.

8.4 Hydrostatic restoring coefficients

In order to calculate the hydrostatic restoring coefficients (linear, 2nd order and 3rd order) some geometric characteristics of the vessel were necessary. They are presented at the table in the next page:

ρ	1025 kg/m^3
g	9,81 m/s^2
A_0	10.114 m^2
∇	111.176 m^3
Δ	113.956.000 t
z_g	4,827 m
z_B	-6.32 m
x_{f0}	-13.38m

Another important characteristic of the ship which was imported into the model via the restoring coefficients is the hull's shape at the calm waterline. This plays a significant role on the parametric rolling phenomenon keeping in mind that its main cause is the variation of the stability due to the flare of stern. Calculating and using the derivative $\left(\frac{\partial \bar{y}}{\partial \bar{z}}\right)$, the model can "feel" this variation of the waterline area which results in the variation of the stability. In ships with vertical wall sided hull this derivative equals to zero, but on the parts of the ship where the flare becomes significant this quantity cannot be neglected. The former quantity is always greater

than zero so that that the new waterline area for a positive heave is smaller than the original. $\Rightarrow \left.\frac{\partial A}{\partial z}\right|_0 = -2\int_L \frac{\partial \overline{y}}{\partial \overline{z}} dx$

$\left(\frac{\partial \overline{y}}{\partial \overline{z}}\right)$ was calculated separately for each section and then it was multiplied, depending on the coefficient calculated, with the half-beam of its section or its x-coordinate or their powers.

The values for each section are presented on the next page:

Section	dy/dz
0	2.6051
1	0.8391
2	0.2493
3	0.1944
4	0.0699
5	0.0349
6	0.0175
7	0.0000
8	0.0000
9	0.0000
10	0.0000
11	0.0000
12	0.0087
13	0.0175
14	0.1584
15	0.7813
16	0.7536
17	0.8098
18	0.7536
19	0.4452
20	0.1405

Having calculated all the above necessary quantities we can now proceed to the presentation of the hydrostatic coefficients described at the chapter “Mathematical Model Used”

Hydrostatic restoring coefficients(Calm Water): Linear

$Z_z = 101.698.799$	$K_z = 0$	$M_z = 1.360.729.924$
$Z_\phi = 0$	$K_\phi = 1.200.633.579$	$M_\phi = 0$
$Z_\theta = 1.360.729.924$	$K_\theta = 0$	$M_\theta = 501.777.639.019$

Hydrostatic restoring coefficients (calm water): Second order

$Z_{zz} =$ -2.248.333	$K_{zz} = 0$	$M_{zz} =$ -28.198.195
$Z_{z\phi} = 0$	$K_{z\phi} =$ -572.683.808	$M_{z\phi} = 0$
$Z_{z\theta} =$ -28.198.195	$K_{z\theta} = 0$	$M_{z\theta} =$ -30.727.106.142
$Z_{\phi\phi} =$ -572.683.809	$K_{\phi\phi} = 0$	$M_{\phi\phi} =$ -35.978.008.003
$Z_{\phi\theta} = 0$	$K_{\phi\theta} =$ -35.978.008.003	$M_{\phi\theta} = 0$
$Z_{\theta\theta} =$ -30.727.106.143	$K_{\theta\theta} = 0$	$M_{\theta\theta} =$ -916.776.984.097

Hydrostatic restoring coefficients (calm water): Third order

Heave

$Z_{zzz} = 0*$	$Z_{zz\phi} = 0$	$Z_{zz\theta} = 0*$
$Z_{\phi\phi z} = 198.242.332$	$Z_{\phi\phi\phi} = 0$	$Z_{\phi\phi\theta} = 10.191.624.112$
$Z_{\theta\theta z} = 0*$	$Z_{\theta\theta\phi} = 0$	$Z_{\theta\theta\theta} = 0*$

Roll

$K_{zzz}=0$	$K_{zz\phi}=198.242.332$	$K_{zz\theta}=0$
$K_{\phi\phi z}=0$	$K_{\phi\phi\phi}=7.233.976.949**$	$K_{\phi\phi\theta}=0$
$K_{\theta\theta z}=0$	$K_{\theta\theta\phi}=2.060.120.263.668$	$K_{\theta\theta\theta}=0$

Pitch

$M_{zzz}=0*$	$M_{zz\phi}=0$	$M_{zz\theta}=0*$
$M_{\phi\phi z}=10.191.624.112$	$M_{\phi\phi\phi}=0$	$M_{\phi\phi\theta}=2.060.120.263.668$
$M_{\theta\theta z}=0*$	$M_{\theta\theta\phi}=0$	$M_{\theta\theta\theta}=1.040.935.897.781*$

Heave-roll-pitch coupling

$Z_{z\phi\theta}=0$	$K_{z\phi\theta}=10.191.624.111$	$M_{z\phi\theta}=0$

*Obtained analytically for a wedge-sided ship. It is a good approximation for ships of conventional forms, small displacements and smooth transversal curvatures $\frac{\partial^2 \overline{y}}{\partial \overline{z}^2}$ at the considered water-line.

8.5 Derivatives due to wave passage

Concerning the derivatives due to wave passage, their calculation is made inside the algorithm of the model because of the fact that they are time dependant. Analyzing the integral inside the coefficient e.g. $Z_{\zeta z}(t)=2\rho g\int_L \frac{\partial \overline{y}}{\partial \overline{z}}\zeta\, dx$ we make the following steps:

1. We calculate the wave profile $\zeta=\overline{\zeta}\cos k(x-V_C t)$ at each section. ζ is different at each section because of the variable x which is the coordinate of the wave related to the ship. t remains as a variable

2. We multiply the result of the above calculation with $\left(\frac{\partial \bar{y}}{\partial \bar{z}}\right)$ of each section.
3. Inside the algorithm's equations we integrate numerically the results for each section along the ship's length.

8.6 Types of calculations

Three types of calculations were made:

One model, whose mass and added mass for the heave motion and inertia and added inertia for the pitch mode were artificially set in very big values, would calculate the roll angle by taking into account only one degree of freedom. To be called in the results as "roll only"

One model with three degrees of freedom which takes into account only the linear coupling coefficients and the respective derivatives due to wave passage. To be called in the results as "Linear Coupled"

One model with all the coefficients mentioned above taken into account. To be called in the results as "Full Coupled"

Important note: On both "Roll only" and "Linear Coupled" models a third order restoring term in the roll mode was inserted in order to keep the response of the system in finite values.

8.7 Numerical calculations

8.7.1 State space transformation

The complete algorithm which was used to solve the system is presented in Appendix I. In order to solve numerically our system of non linear second order differential equations with Runge Kutta Method we have to make some manipulations. We can reduce the order of the equations by inserting more equations. System of equations

$$\left(m+Z_{\ddot{z}}\right)\cdot\ddot{z}+Z_{\dot{z}}\cdot\dot{z}+Z_{\ddot{\theta}}\cdot\ddot{\theta}+Z_{\dot{\theta}}\cdot\dot{\theta}+Z_{z}\cdot z+Z_{\theta}\cdot\theta+\frac{1}{2}Z_{zz}\cdot z^2+\frac{1}{2}Z_{\phi\phi}\cdot\phi^2+$$

$$+\frac{1}{2}Z_{\theta\theta}\cdot\theta^2+Z_{z\theta}\cdot z\theta+\frac{1}{6}Z_{zzz}\cdot z^3+\frac{1}{2}Z_{\phi\phi z}\cdot\phi^2\cdot z+\frac{1}{2}Z_{\phi\phi\theta}\cdot\phi^2\cdot\theta+\frac{1}{6}Z_{\theta\theta\theta}\cdot\theta^3+$$

$$+Z_{\zeta z}(t)\cdot z+Z_{\zeta\theta}(t)\cdot\theta+Z_{\zeta zz}(t)\cdot z^2+Z_{\zeta z\theta}(t)\cdot z\theta+Z_{\phi\phi\zeta}(t)\cdot\phi^2=Z_W(t)$$

$$\left(J_{xx}+K_{\ddot{\phi}}\right)\cdot\ddot{\phi}+K_{\dot{\phi}}\cdot\dot{\phi}+K_{\phi}\cdot\phi+K_{z\phi}\cdot z\phi+K_{\theta\phi}\cdot\theta\phi+\frac{1}{2}K_{zz\phi}\cdot z^2\phi+\frac{1}{2}K_{\theta\theta\phi}\cdot\theta^2\phi+-$$

$$+\frac{1}{6}K_{\phi\phi\phi}\cdot\phi^3+K_{z\phi\theta}\cdot z\phi\theta+K_{\zeta\phi}(t)\cdot\phi+K_{\zeta\zeta\phi}(t)\cdot\phi+K_{\zeta z\phi}(t)\cdot z\phi+K_{\zeta\phi\theta}(t)\cdot z\phi\theta=\mathrm{K}_W(t)$$

$$\left(J_{yy}+M_{\ddot{\theta}}\right)\cdot\ddot{\theta}+M_{\dot{\theta}}\cdot\dot{\theta}+M_{\ddot{z}}\cdot\ddot{z}+M_{\dot{z}}\cdot\dot{z}+M_{z}\cdot z+M_{\theta}\cdot\theta+\frac{1}{2}M_{zz}\cdot z^2+\frac{1}{2}M_{\phi\phi}\cdot\phi^2+$$

$$+\frac{1}{2}M_{\theta\theta}\cdot\theta^2+M_{z\theta}\cdot z\theta+\frac{1}{2}M_{\phi\phi z}\cdot\phi^2\cdot z+\frac{1}{2}M_{\phi\phi\theta}\cdot\phi^2\cdot\theta+\frac{1}{2}M_{\theta\theta}\cdot\theta^2\cdot z+\frac{1}{6}M_{\theta\theta\theta}\cdot\theta^3+$$

$$M_{\zeta z}(t)\cdot z+M_{\zeta\theta}(t)\cdot\theta+M_{\zeta z\theta}(t)\cdot z\theta+M_{\phi\phi\zeta}(t)\cdot\phi^2=M_W(t)$$

In our case we have three unknown variables in three second order differential equations. We can introduce three new variables:

$$p=\dot{\phi}$$
$$q=\dot{\theta}$$
$$w=\dot{z}$$

With these new variables our system is transformed to:

$$\left(m+Z_{\ddot{z}}\right)\cdot\dot{w}+Z_{\dot{z}}\cdot w+Z_{\ddot{\theta}}\cdot\dot{q}+Z_{\dot{\theta}}\cdot q+Z_{z}\cdot z+Z_{\theta}\cdot\theta+\frac{1}{2}Z_{zz}\cdot z^2+\frac{1}{2}Z_{\phi\phi}\cdot\phi^2+$$

$$+\frac{1}{2}Z_{\theta\theta}\cdot\theta^2+Z_{z\theta}\cdot z\theta+\frac{1}{6}Z_{zzz}\cdot z^3+\frac{1}{2}Z_{\phi\phi z}\cdot\phi^2\cdot z+\frac{1}{2}Z_{\phi\phi\theta}\cdot\phi^2\cdot\theta+\frac{1}{6}Z_{\theta\theta\theta}\cdot\theta^3+$$

$$+Z_{\zeta z}(t)\cdot z+Z_{\zeta\theta}(t)\cdot\theta+Z_{\zeta zz}(t)\cdot z^2+Z_{\zeta z\theta}(t)\cdot z\theta+Z_{\phi\phi\zeta}(t)\cdot\phi^2=Z_{W}(t)$$

$$\left(J_{yy}+M_{\ddot{\theta}}\right)\cdot\dot{q}+M_{\dot{\theta}}\cdot q+M_{\ddot{z}}\cdot\dot{w}+M_{\dot{z}}\cdot w+M_{z}\cdot z+M_{\theta}\cdot\theta+\frac{1}{2}M_{zz}\cdot z^2+\frac{1}{2}M_{\phi\phi}\cdot\phi^2+$$

$$+\frac{1}{2}M_{\theta\theta}\cdot\theta^2+M_{z\theta}\cdot z\theta+\frac{1}{2}M_{\phi\phi z}\cdot\phi^2\cdot z+\frac{1}{2}M_{\phi\phi\theta}\cdot\phi^2\cdot\theta+\frac{1}{2}M_{\theta\theta}\cdot\theta^2\cdot z+\frac{1}{6}M_{\theta\theta\theta}\cdot\theta^3+$$

$$M_{\zeta z}(t)\cdot z+M_{\zeta\theta}(t)\cdot\theta+M_{\zeta z\theta}(t)\cdot z\theta+M_{\phi\phi\zeta}(t)\cdot\phi^2=M_{W}(t)$$

which is a non linear first order system of differential equations which can be easily solved numerically using Runge Kutta method. With the form of equations presented above we may do all the necessary calculations related to the simulation of motions of the ship under study.

8.7.2 Numerical continuation

To take the next step and run numerical continuation on our system, in order to find the boundaries of parametric roll in dependence to the wave height or α, we have to make some more changes on the form of our equations. Numerical continuation requires the elimination of time in the model. That can be done by inserting two more equations known as Fitzhugh-Nagumo:

$$x'=x+\beta y-x\left(x^2+y^2\right)$$

$$y'=-\beta x+y-y\left(x^2+y^2\right)$$

which have the asymptotic solution $x=\sin(\beta t)$, $y=\cos(\beta t)$

In our case β is substituted by encounter frequency ω_e . The above conversion of the system of equations was made because of the algorithm which is used to continuation and requires that time "t" does not exist as a parameter in the system. It is obvious that simulation can also be done when inserting Fitzhugh-Nagumo equations but there is no reason to do so due to the complexity of the system.

8.8 Results of time simulation

Most of the results of time simulation presented in figures 12 to 51 were almost presumable. Figures presented at this part of the thesis are for a fix wave height of 8 meters except these of "Full coupled" which are for wave height of 6 meters. Figures 13 to 17 of "Roll only" model are shown to be compared with the Figures of Linear and Full Coupled plotting roll response. Concerning the models with cross-coupling terms, diagrams of pitch and heave are shown as well. As it is stated in "Head-Sea Parametric Rolling and Its Influence on Container Lashing Systems (W.N. France)" concerning a true accident, during parametric rolling extreme pitching occurs indicating that pitch response is also important to know. This also occurs to our model as it is made clear in figures 19,22,25,28,31,34,37,40,43,46. Pitch angles 0.02 rad or higher are developed during the resonance. These values are quite big significant for a ship of that size. With a fast calculation we can see that θ=0.02 rad creates trim:

$$t = \frac{L}{2} \cdot \tan\theta = 2.9m$$

Heave diagrams 20,23,26,29,32,35,38,41,44,47 are presented to indicate the energy transfer between the motions which cannot be neglected as we can observe that heave takes relatively high values too. All the figures derived with numerical simulation are presented in Appendix II.

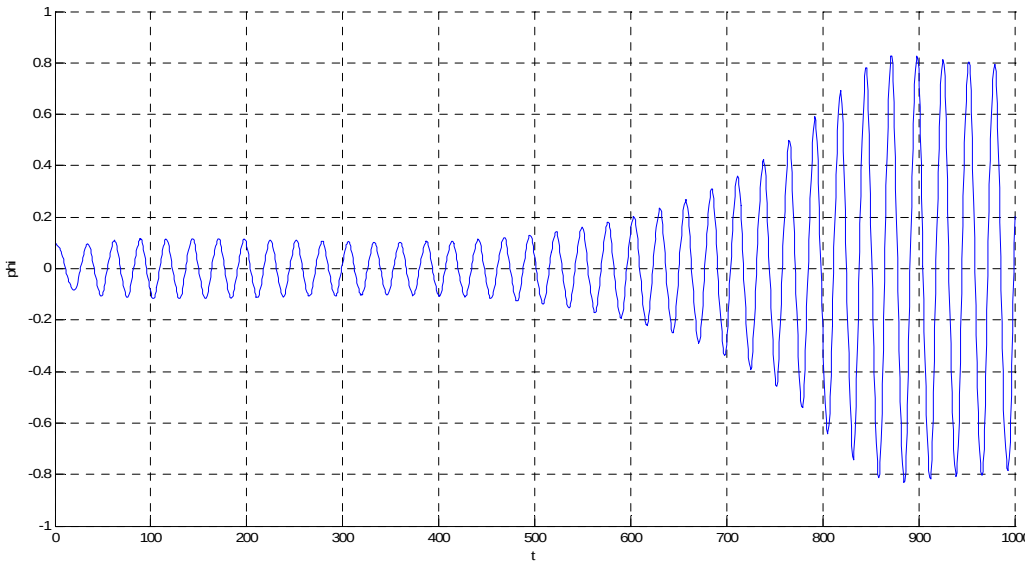

Figure 13: Roll only a=0.8 H=8.2m.

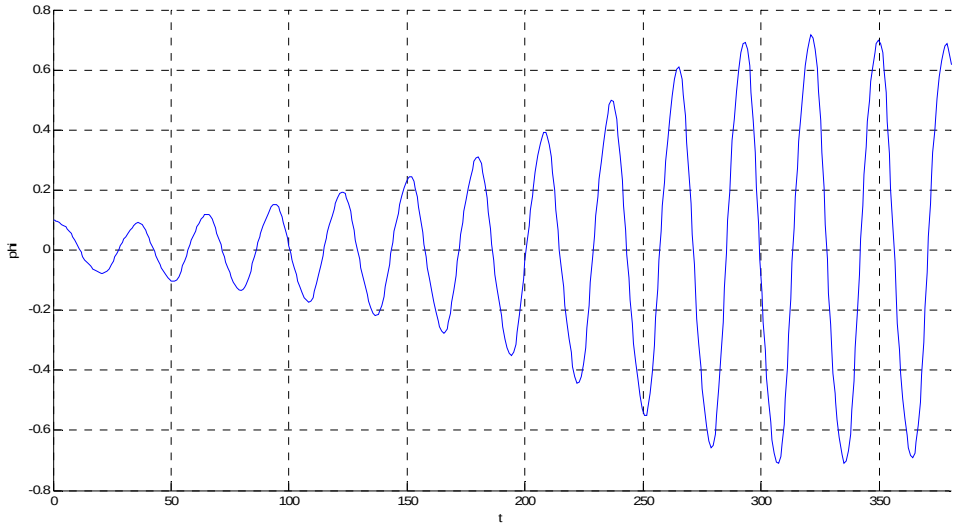

Figure 14: Roll only a=0.9 H=8m.

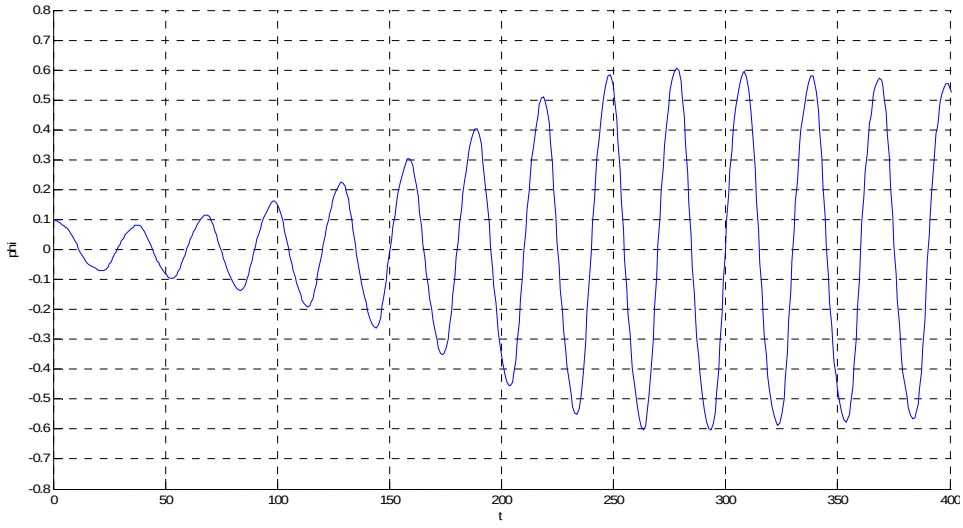

Figure 15: Roll only a=1 H=8m.

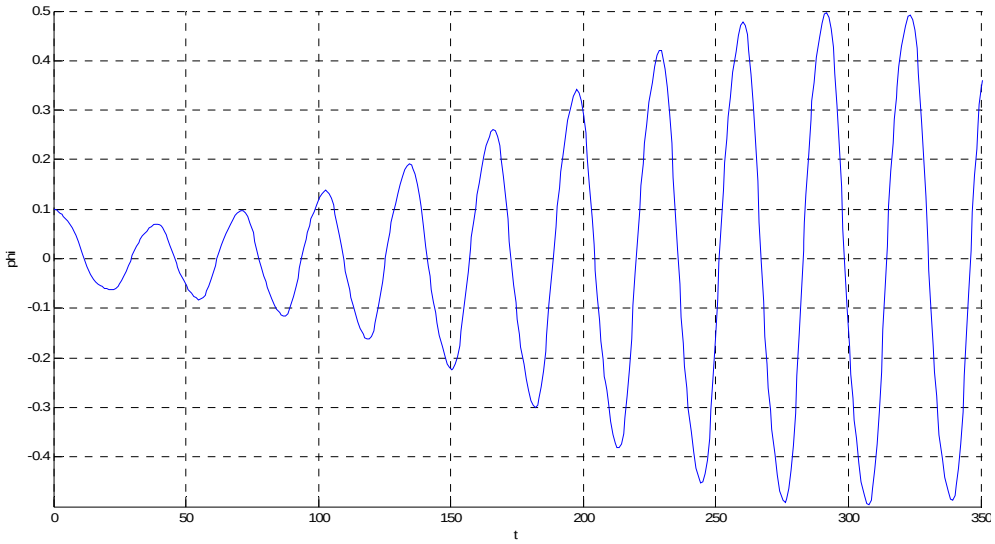

Figure 16: Roll only a=1.1 H=8m.

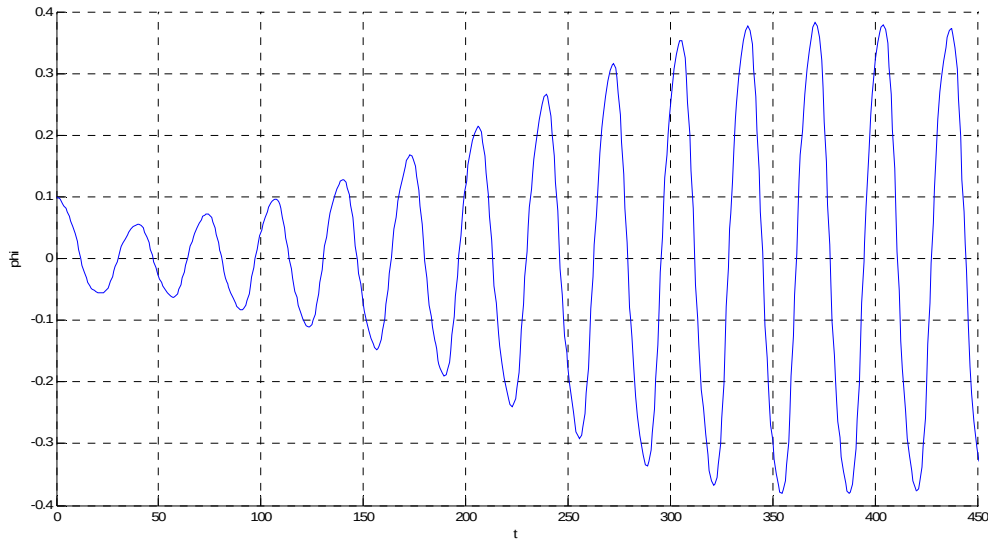

Figure 17: Roll only a=1.2 H=8m.

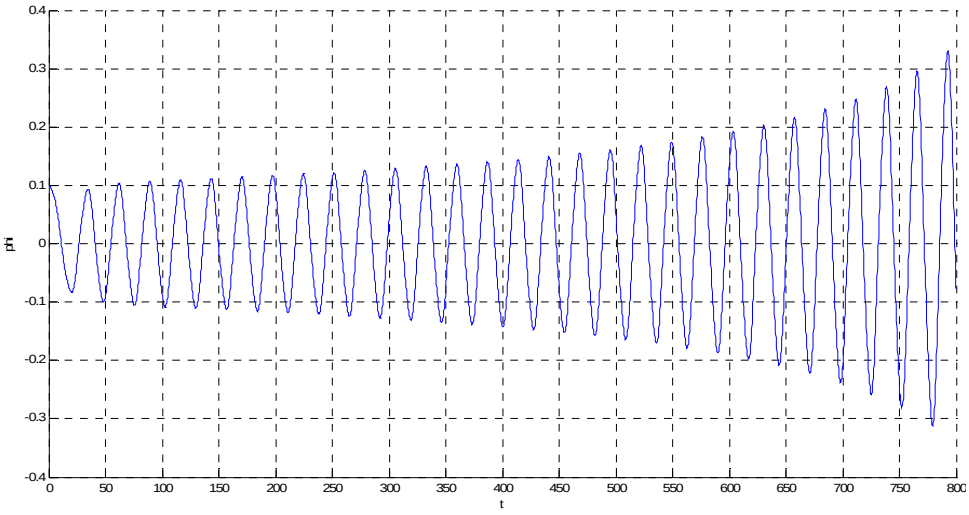

Figure 18: Linear Coupled a=0.8 H=8m Roll.

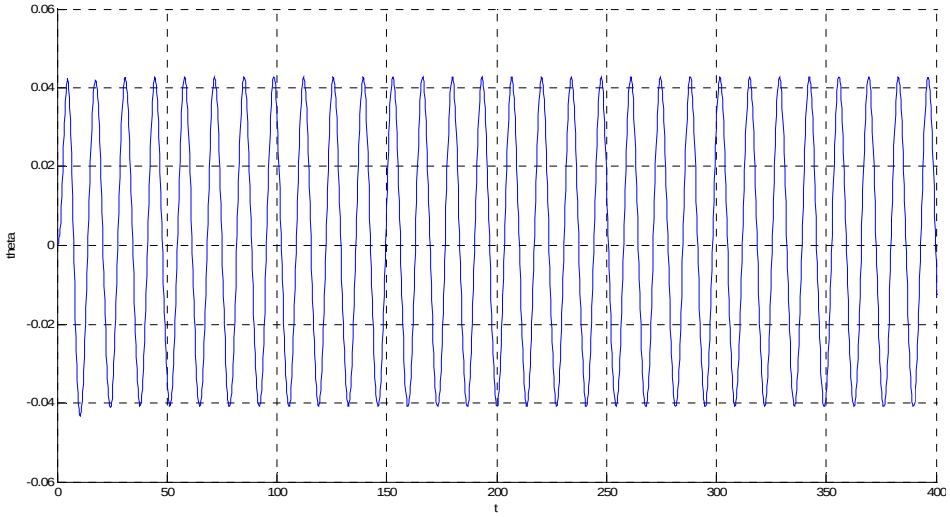

Figure 19: Linear Coupled a=0.8 H=8m Pitch.

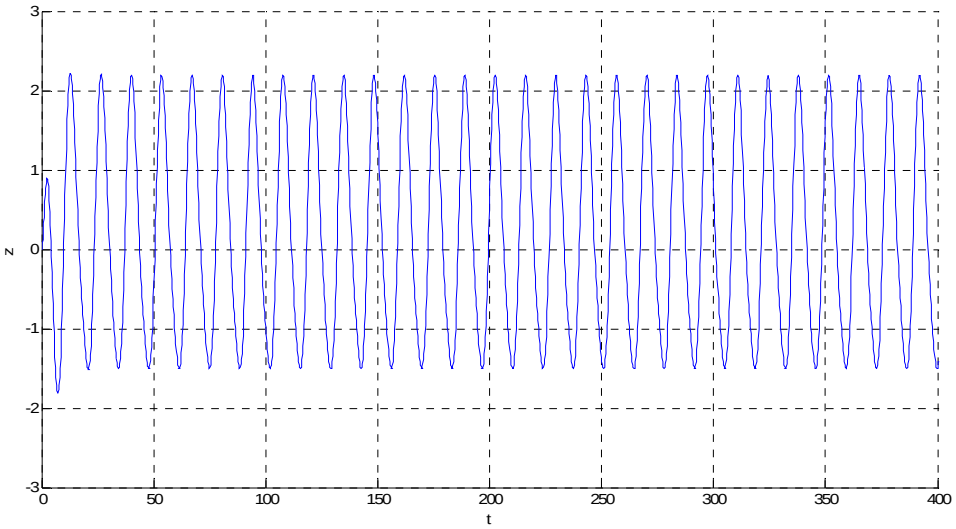

Figure 20: Linear Coupled a=0.8 H=8m Heave.

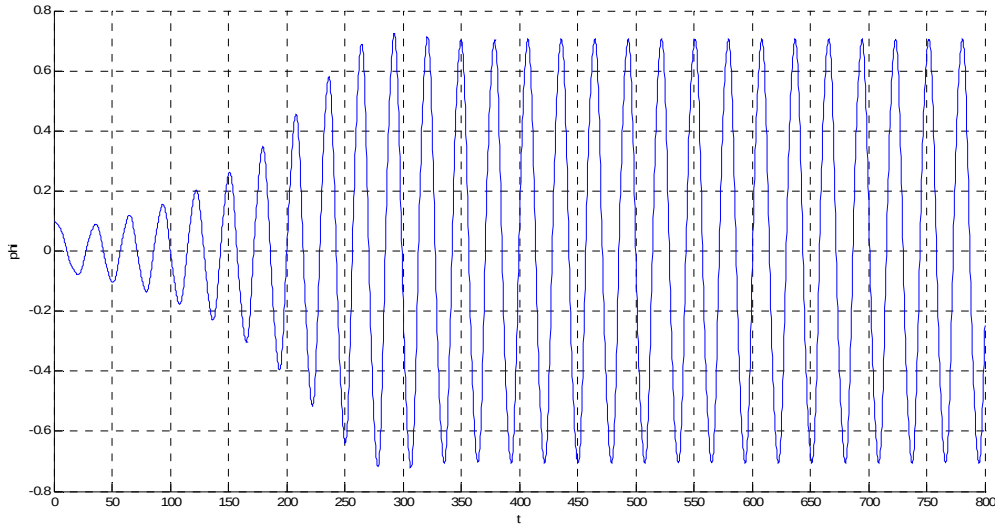

Figure 21: Linear Coupled a=0.9 H=8m Roll.

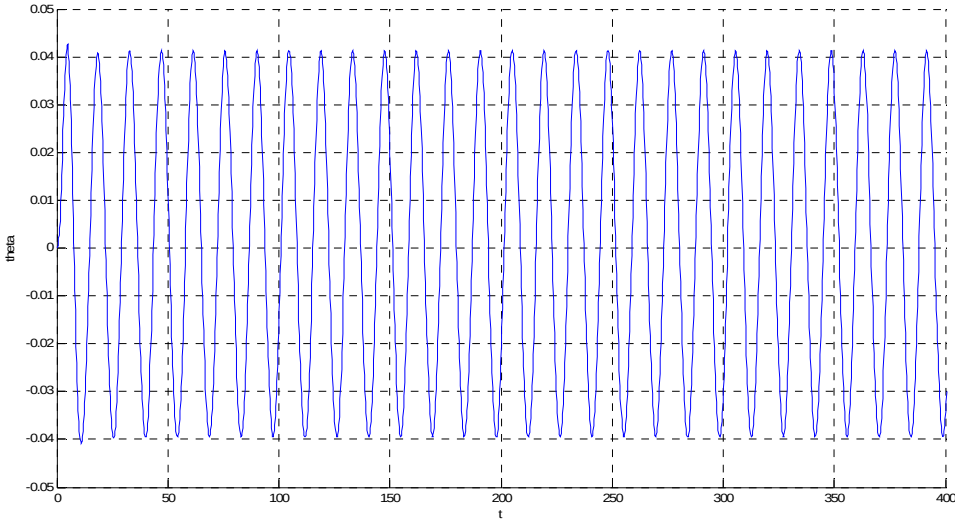

Figure 22: Linear Coupled a=0.9 H=8m Pitch.

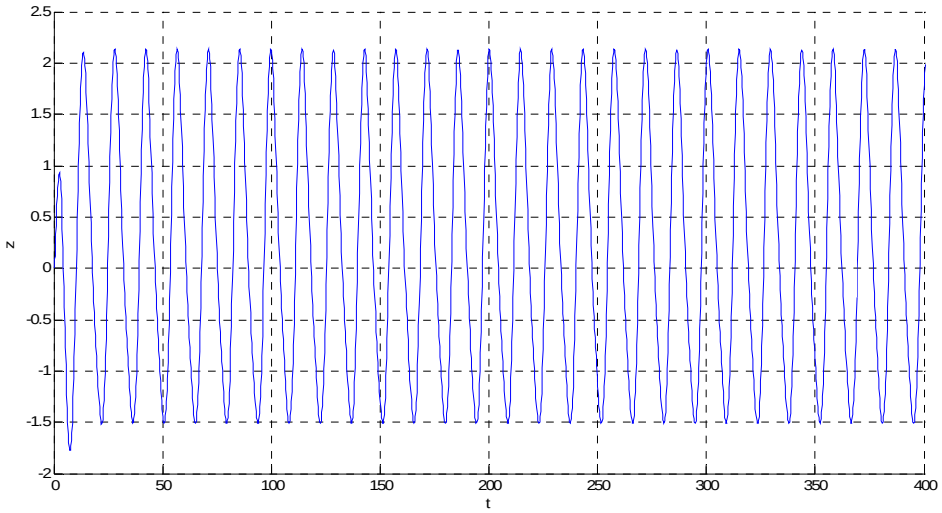

Figure 23: Linear Coupled a=0.9 H=8m Heave.

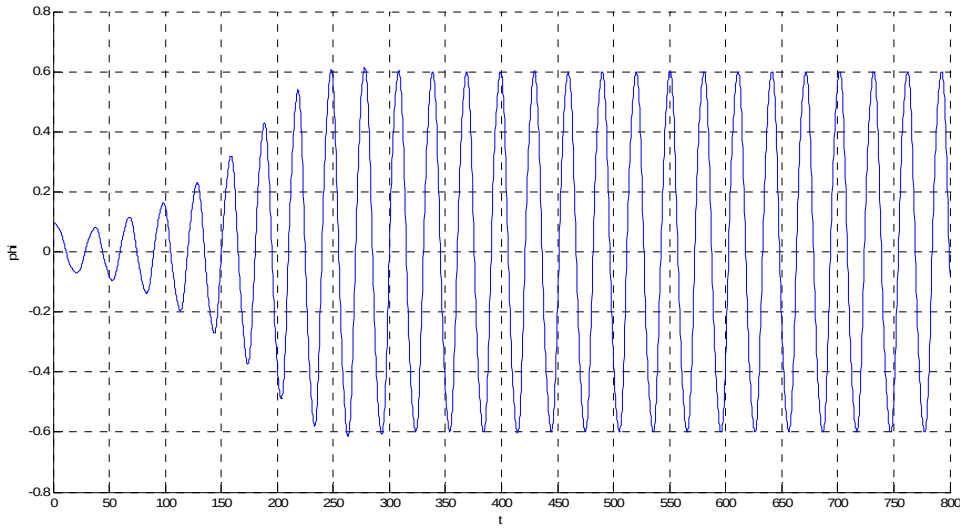

Figure 24: Linear Coupled a=1 H=8m Roll.

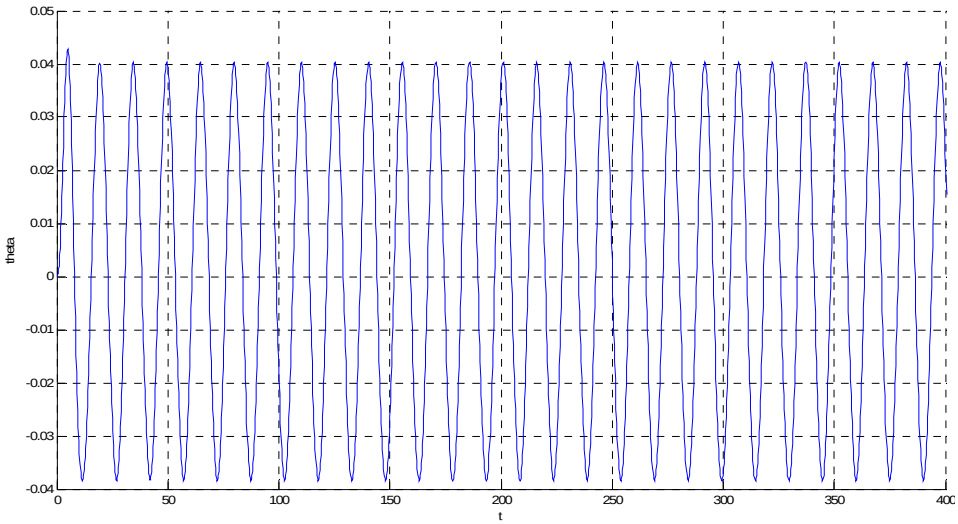

Figure 25: Linear Coupled a=1 H=8m Pitch.

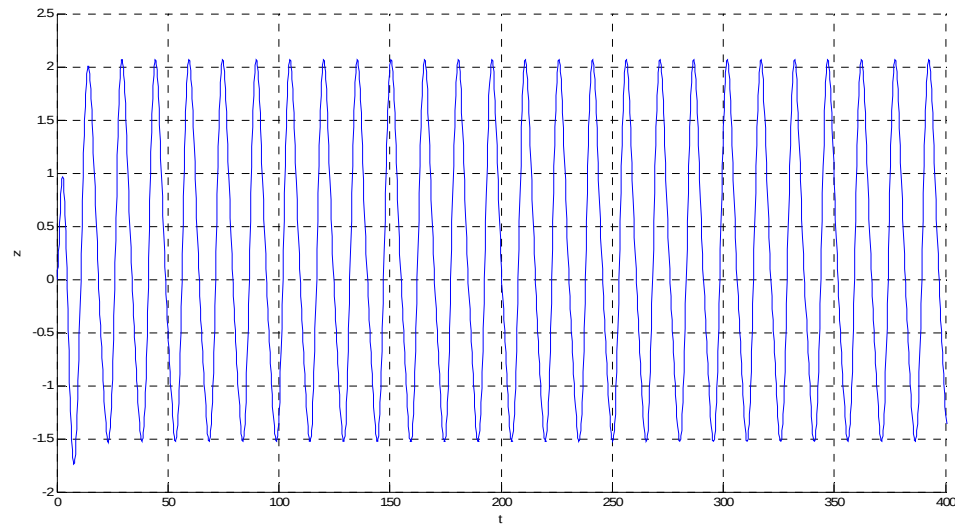

Figure 26: Linear Coupled a=1 H=8m Heave.

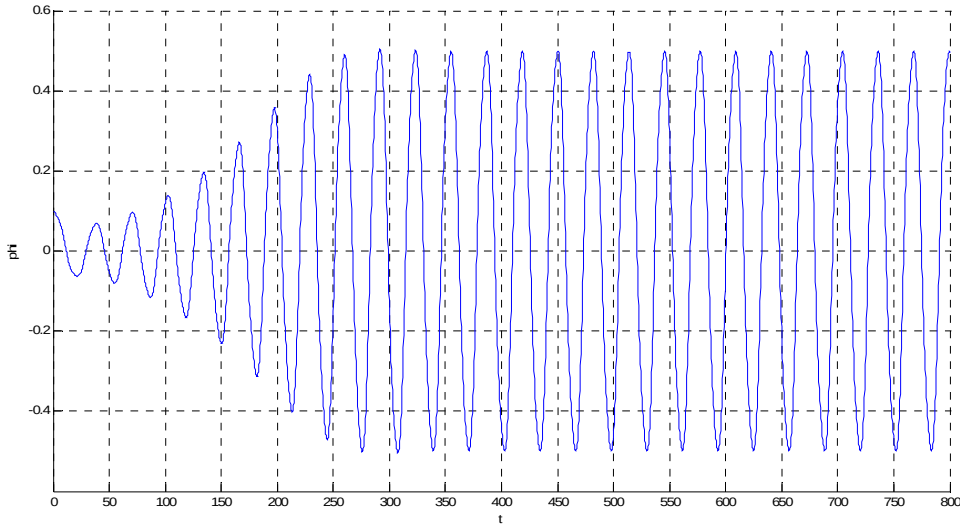

Figure 27: Linear Coupled a=1.1 H=8m Roll.

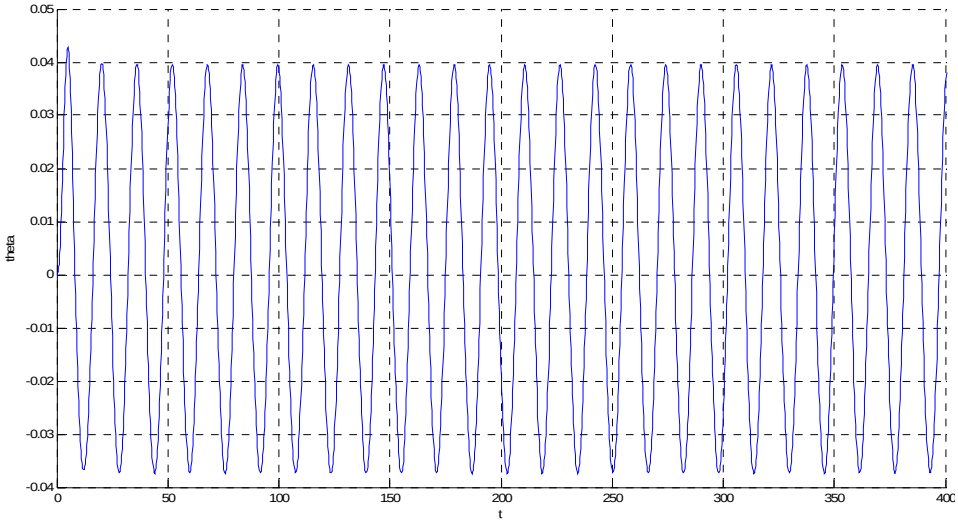

Figure 28: Linear Coupled a=1.1 H=8m Pitch.

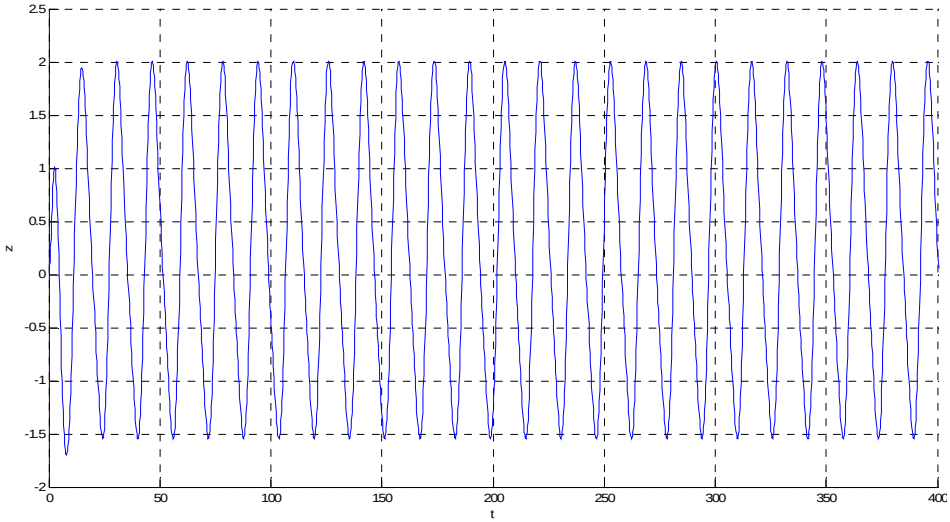

Figure 29: Linear Coupled a=1.1 H=8m Heave.

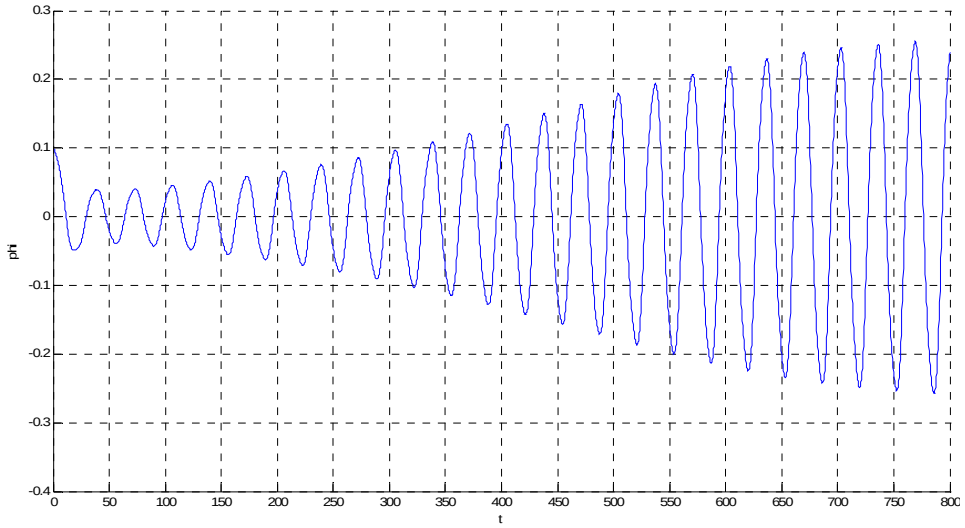

Figure 30: Linear Coupled a=1.2 H=8m Roll.

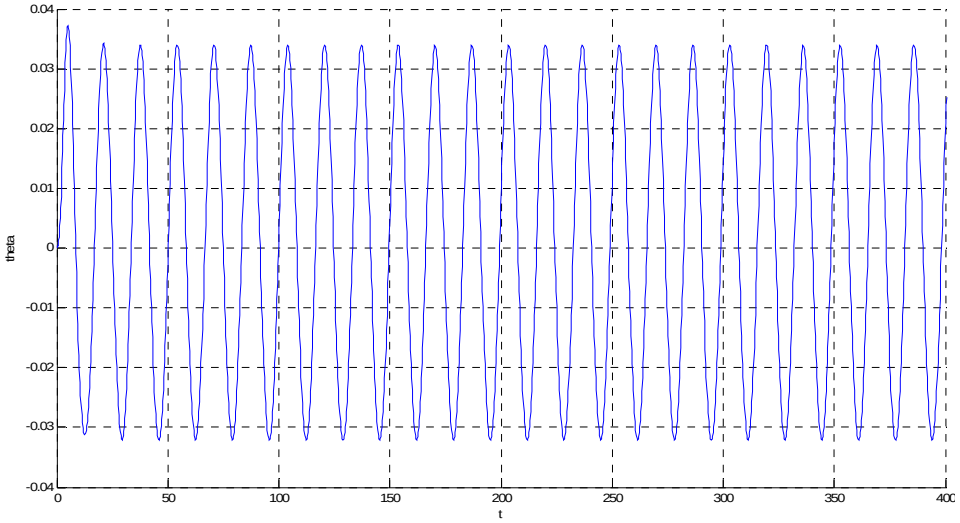

Figure 31: Linear Coupled a=1.2 H=8m Pitch.

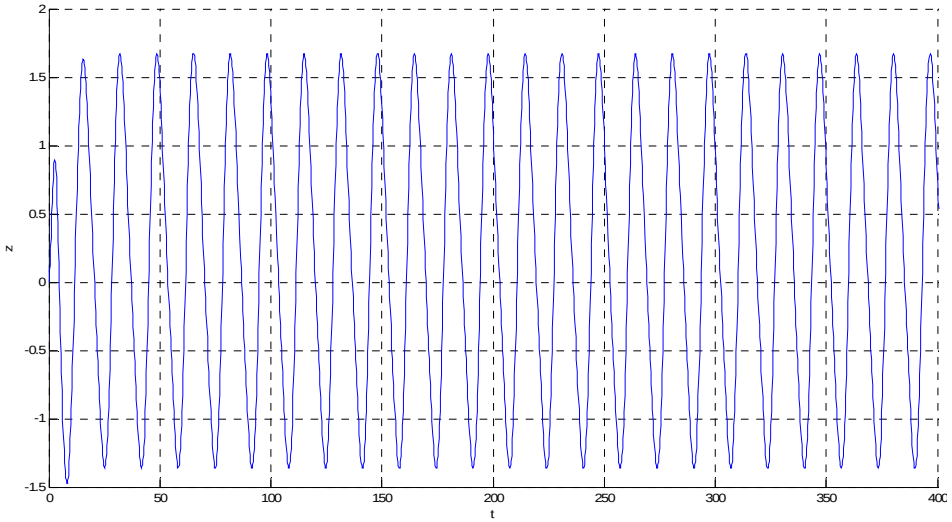

Figure 32: Linear Coupled a=1.2 H=8m Heave.

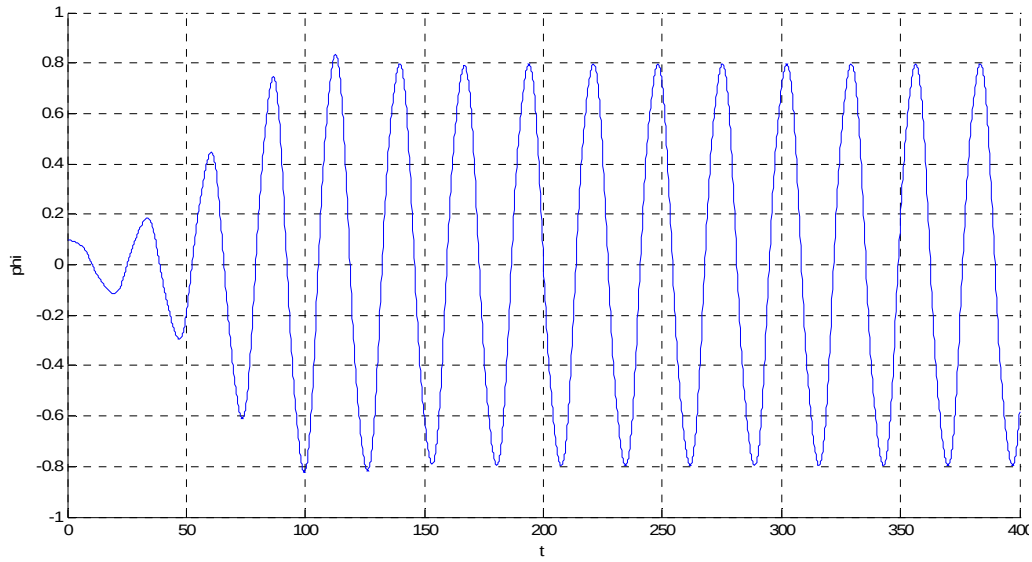

Figure 33: Full Coupled a=0.8 H=6m Roll.

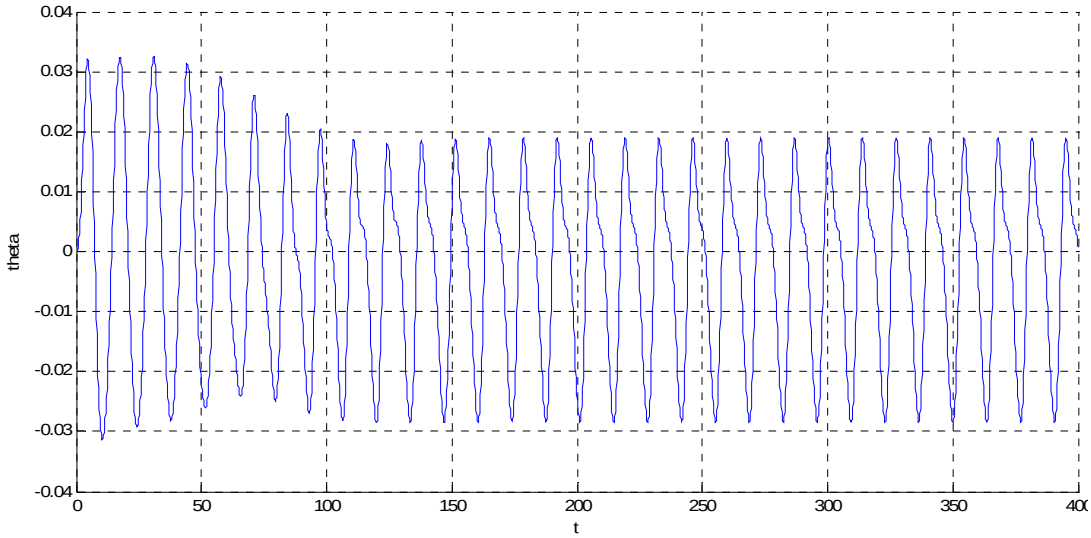

Figure 34: Full Coupled a=0.8 H=6m Pitch..

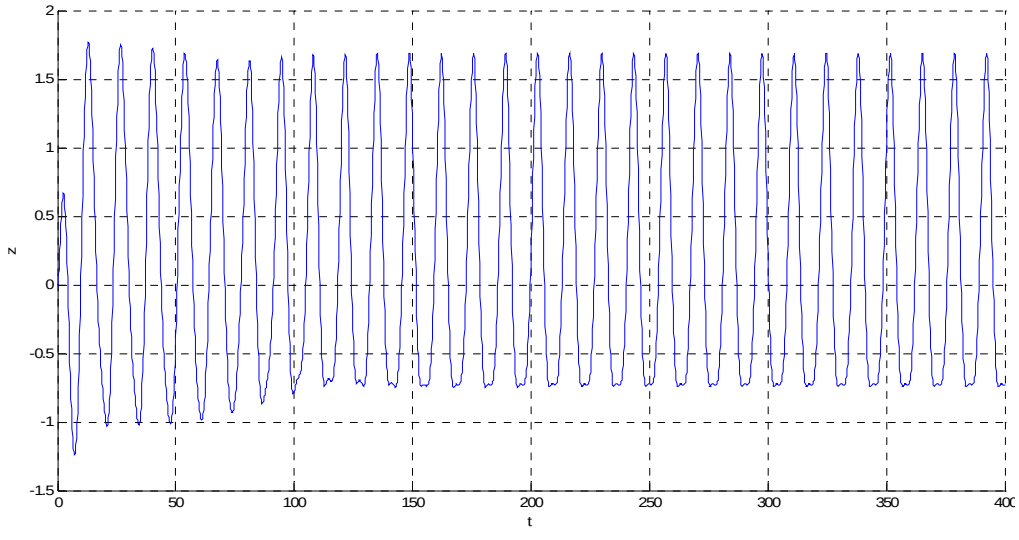

Figure 35: Full Coupled a=0.8 H=6m Heave.

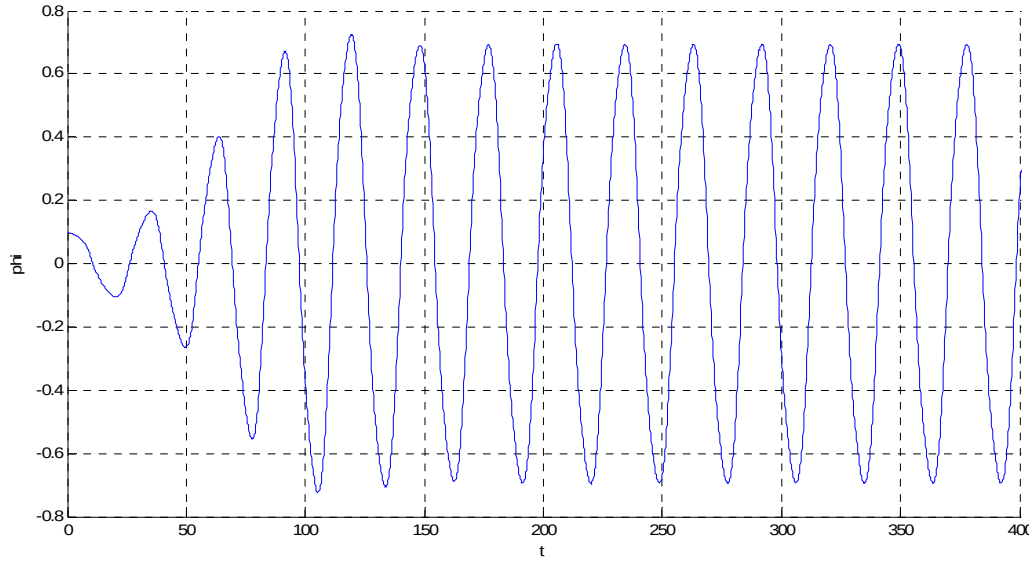

Figure 36: Full Coupled a=0.9 H=6m Roll.

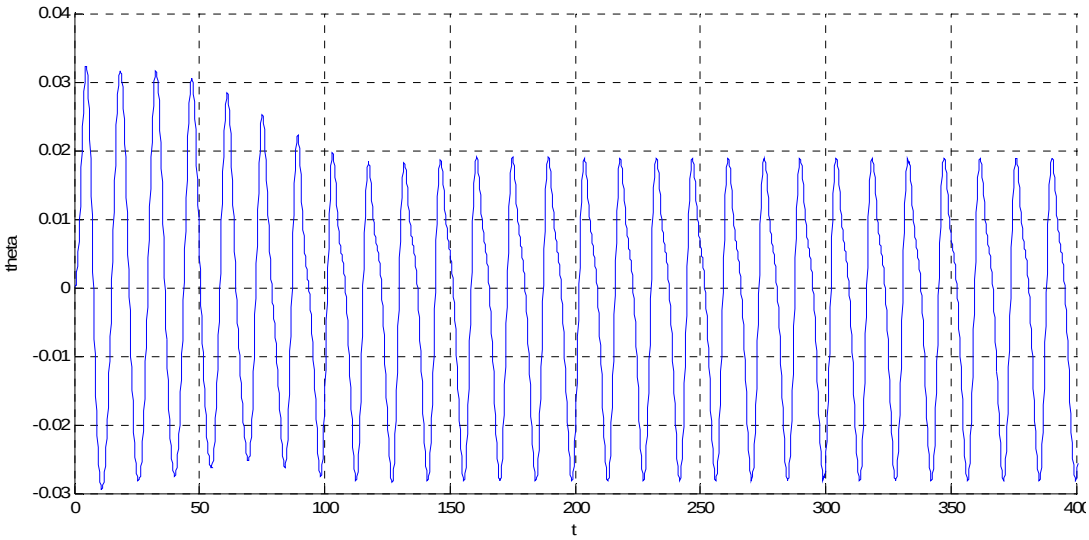

Figure 37: Full Coupled a=0.9 H=6m Pitch.

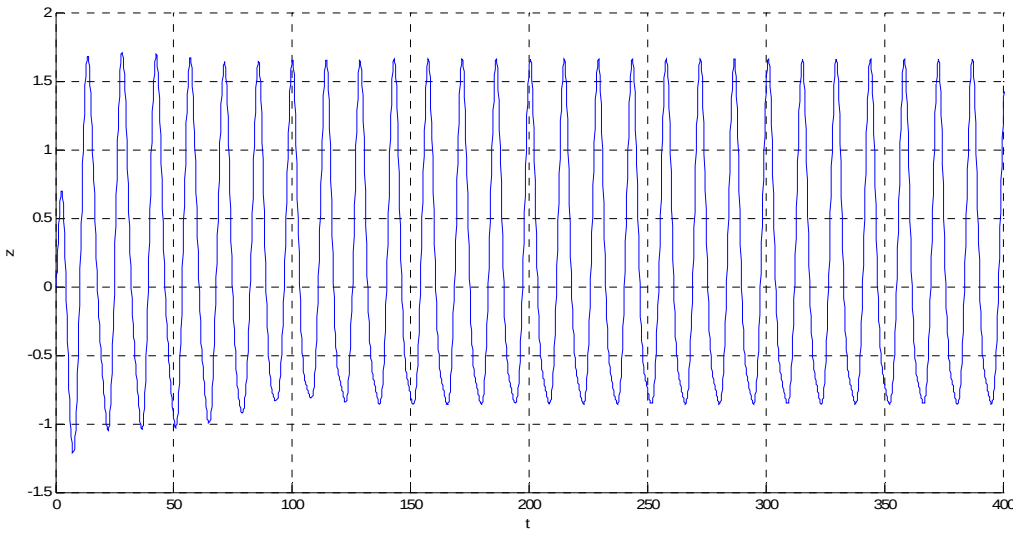

Figure 38: Full Coupled a=0.9 H=6m Heave.

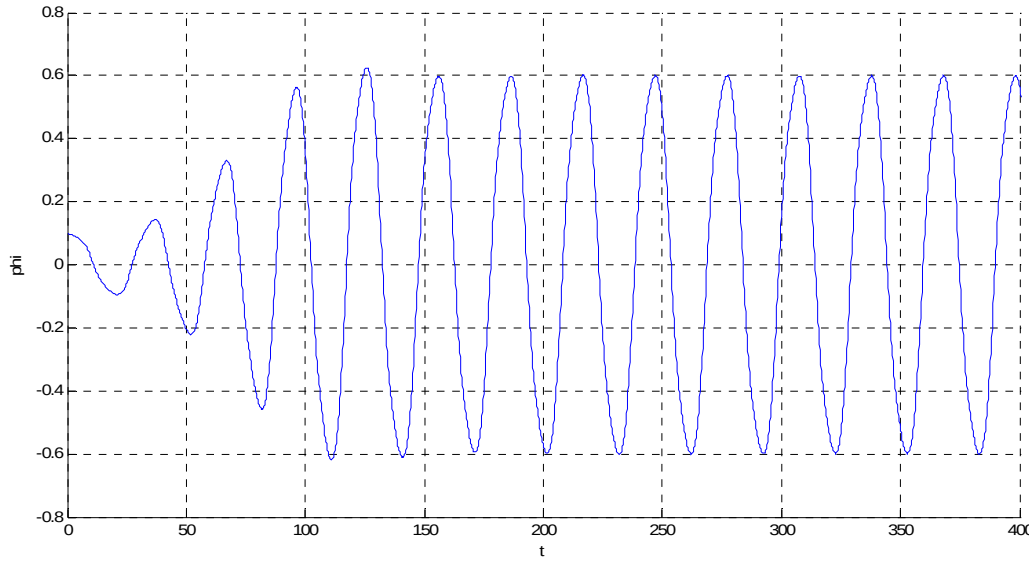

Figure 39: Full Coupled a=1 H=6m Roll.

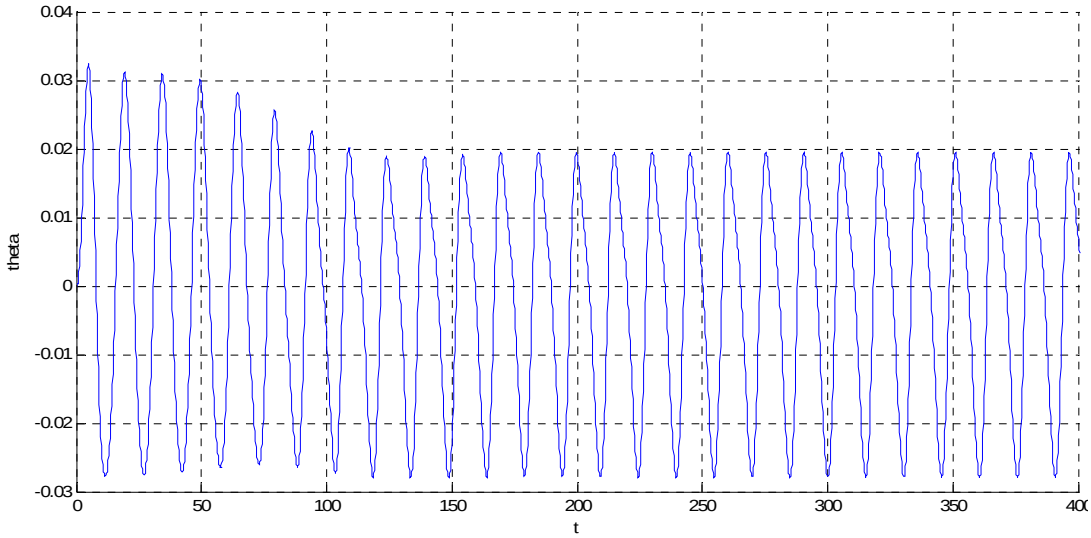

Figure 40: Full Coupled a=1 H=6m Pitch.

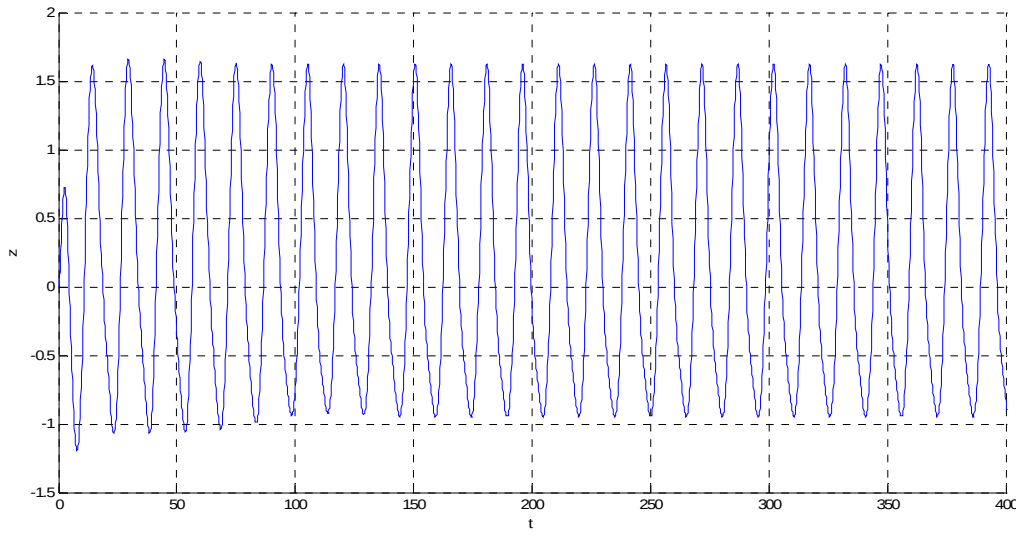

Figure 41: Full Coupled a=1 H=6m Heave.

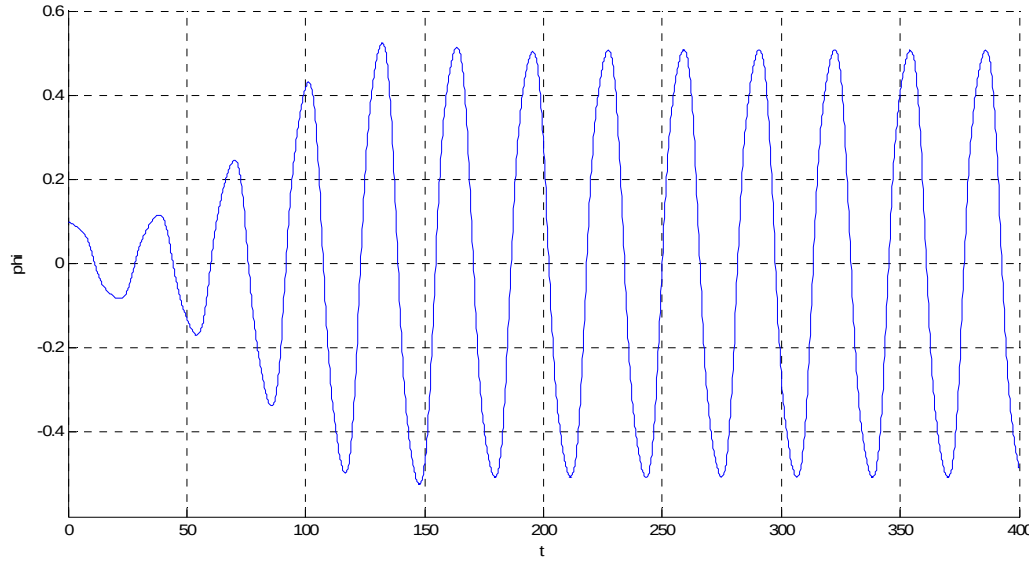

Figure 42: Full Coupled a=1.1 H=6m Roll.

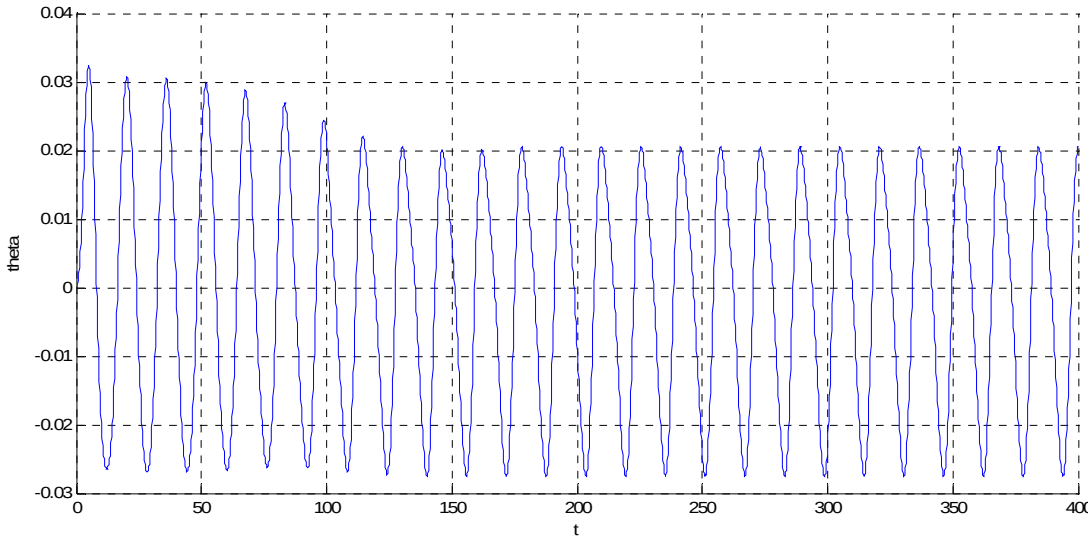

Figure 43: Full Coupled a=1.1 H=6m Pitch.

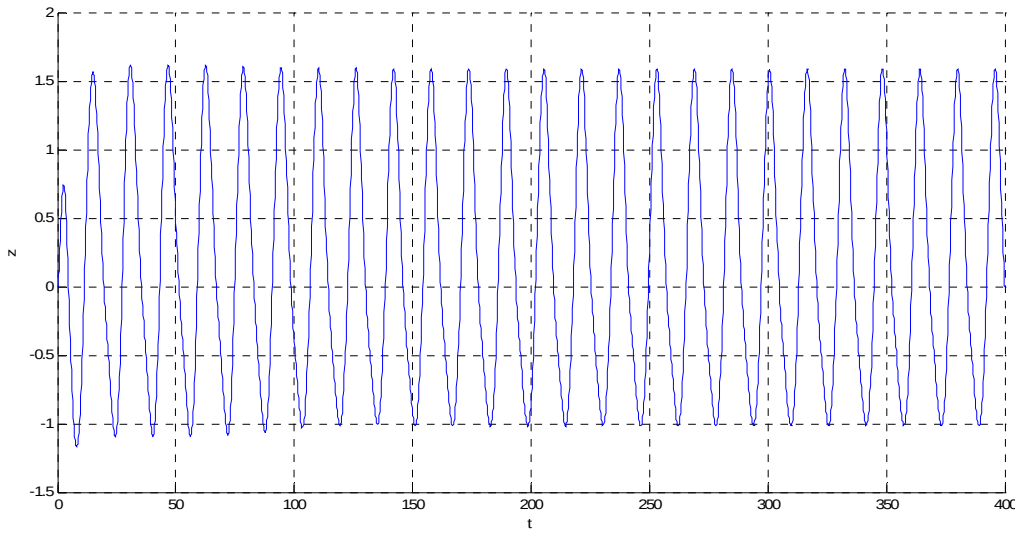

Figure 44: Full Coupled a=1.1 H=6m Heave.

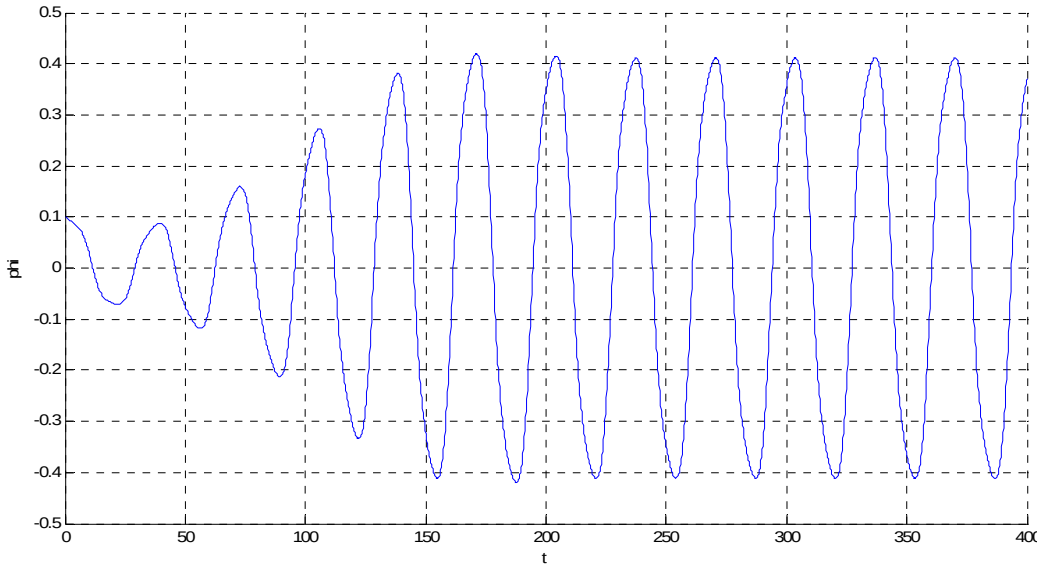

Figure 45: Full Coupled a=1.2 H=6m Roll.

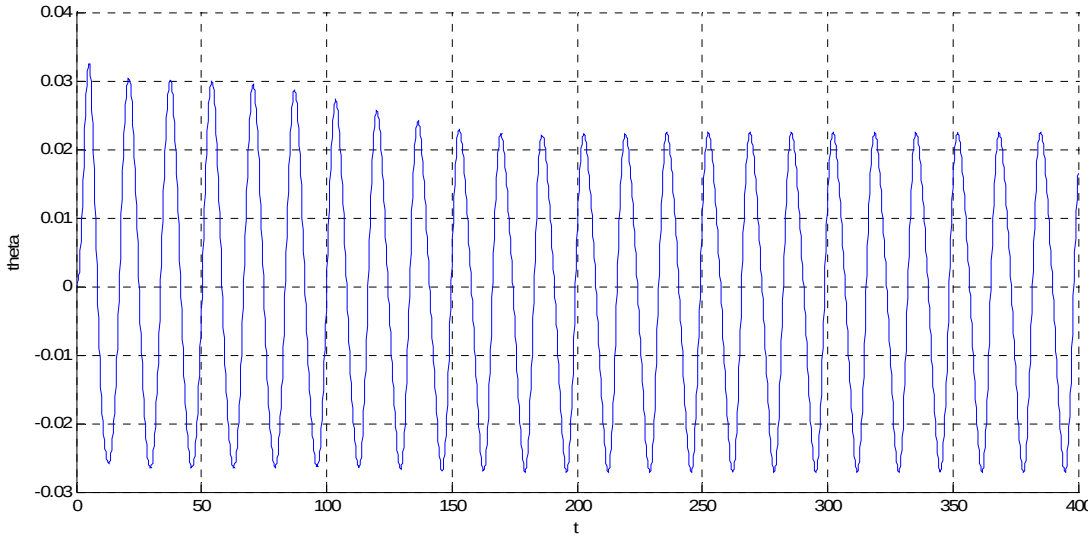

Figure 46: Full Coupled a=1.2 H=6m Pitch.

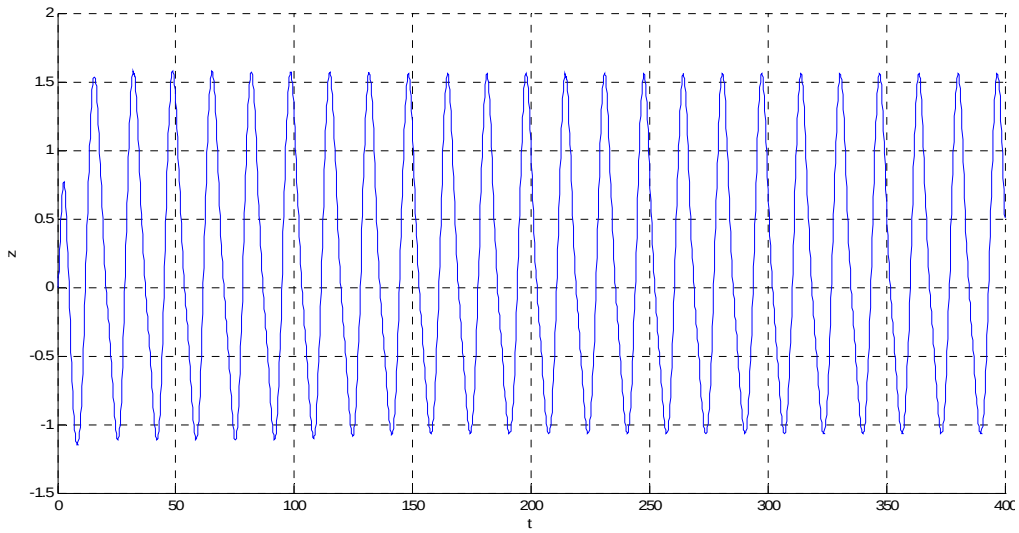

Figure 47: Full Coupled a=1.2 H=6m Heave.

8.9 Results of numerical continuation

The following diagrams were derived with numerical continuation to our models showing the response of each version for particular wave amplitude. In figure 48 and 49 we can see the response of "Roll only" and "Linear coupled" model for five different values of alpha parameter. We can notice the subcritical region for a=0.8 and a=0.9 for both of them. In figure 50 the same type of figure is presented for the "Full Coupled" model. In the last case the subcritical region does not appear at the figure probably because of some minor defects that may have risen due to the complexity of the model. Figure 51 presents the boundaries of parametric rolling for the three models. We can use this model to find the wave height which "ignites" parametric rolling for a given alpha. All the figures derived with numerical continuation are presented in Appendix II.

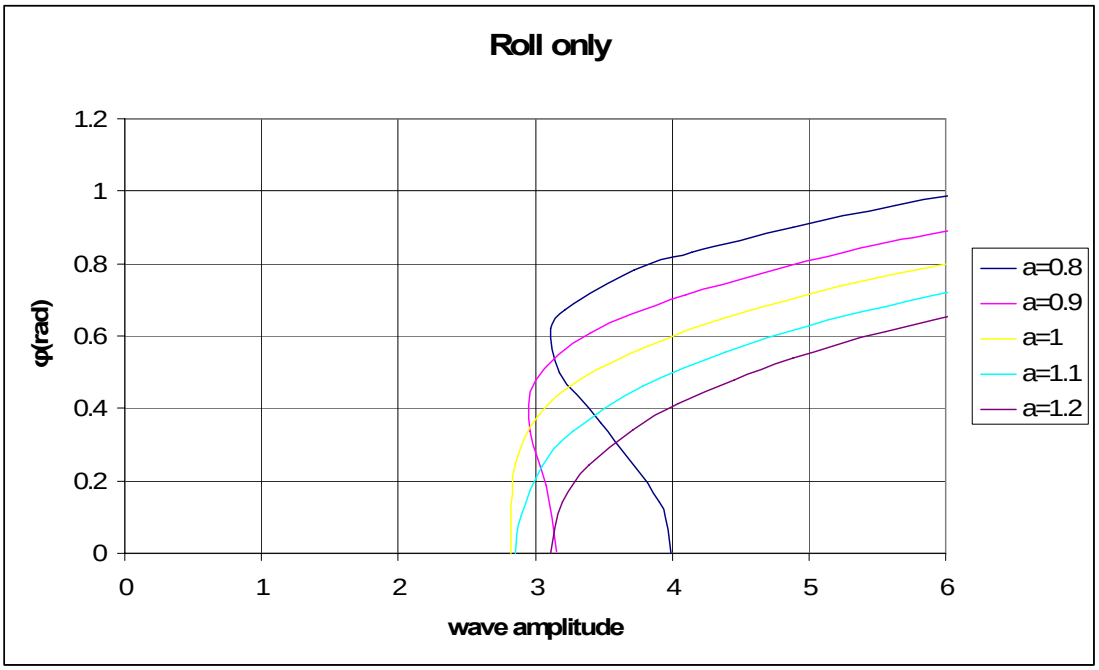

Figure 48: Amplitude of response for the "Roll only" model.

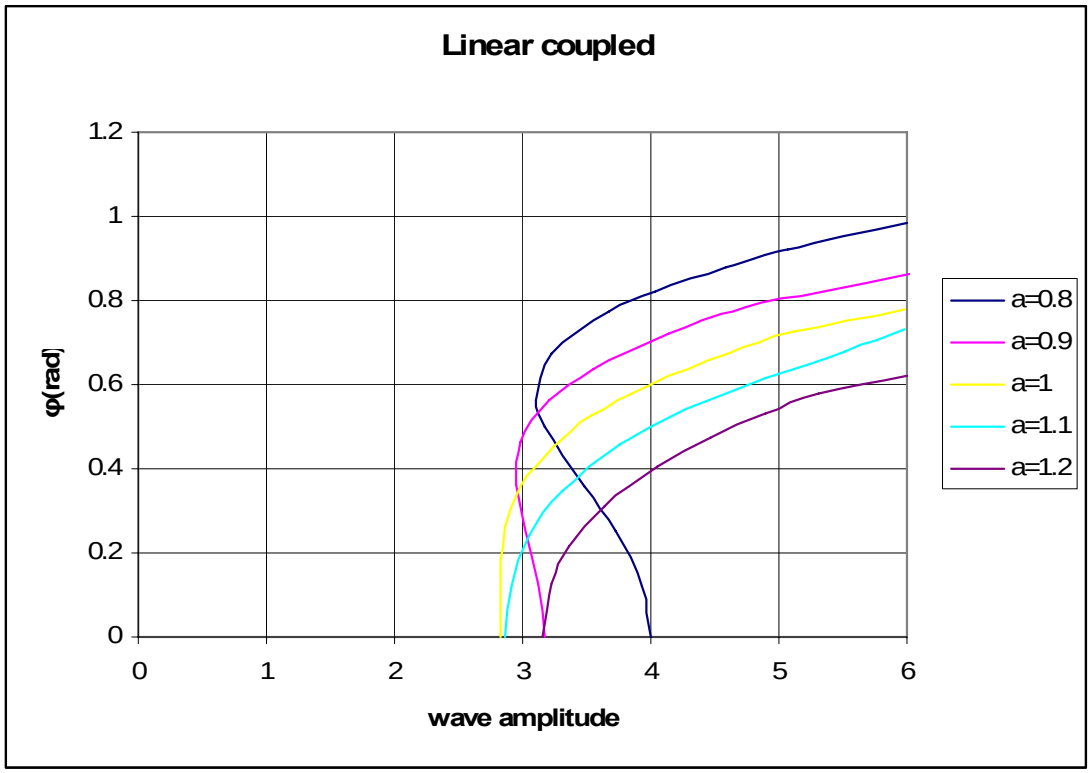

Figure 49: Amplitude of response for the "Linear coupled" model.

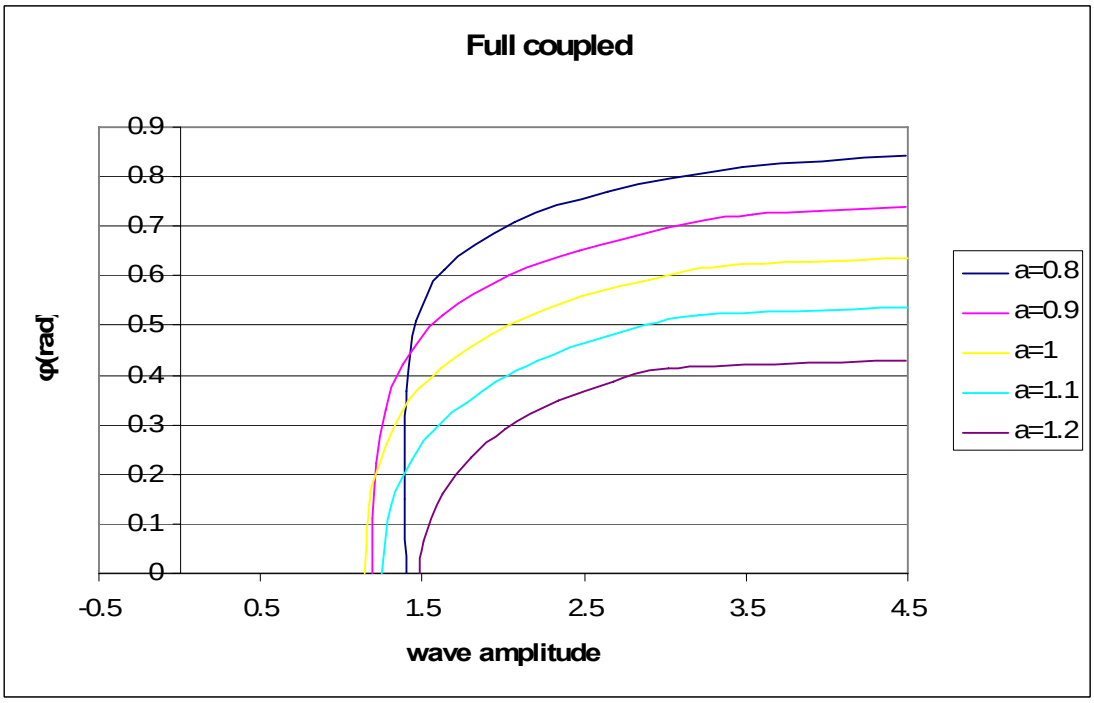

Figure 50: Amplitude of response for the "Full coupled" model.

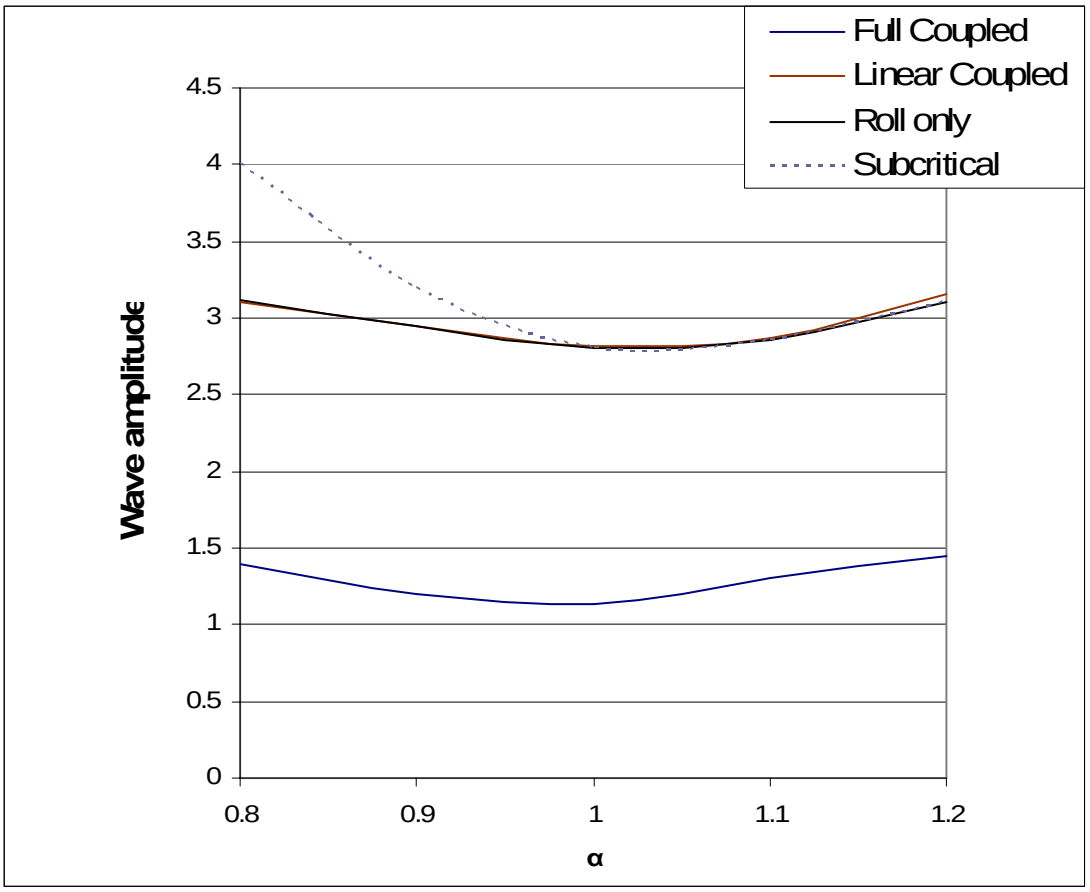

Figure 51: Boundaries of parametric rolling for the three models.

9 Further study

9.1 The problem

As it is discussed in the next chapter, one of the main weaknesses of the model consists of the lack of an analytical expression of GZ curve that could be introduced into the model. The author of this thesis made a hard effort to find an accurate fitting of the GZ curve which would be used in the above model but the results were not the ones expected. Unlike other models with 1DOF, the model used in this thesis needs a GZ expression that calculates the value of the restoring arm in function with φ, θ, z, wave height, position of the ship in relevance with the wave and finally wave length.

Obviously an accurate fitting of all these variables into one analytical expression is very difficult, if not impossible, to be done. In order to simplify the problem, a researcher should isolate one or more variables to make the problem easier to manipulate. It goes without saying that φ, θ, z cannot be omitted due to the fact that they are core variables of the model. Additionally the position of the wave in relevance with the ship cannot be omitted either since it is used in the calculations of the derivatives due to wave passage.

On the other hand, wave length is a parameter that can be decided before running the algorithm. All the calculations of the GZ curve can be done presuming that the ship is on a wave with specific length. If the researcher wants to test the ship for a different wave length should run his calculations again calculating GZ with the new wave length. The previous procedure results to a fitting which has one less variable. Actually this is quite practical keeping in mind that someone would like to test a ship for quite a few different wave lengths.

The big dilemma arises when it comes to wave height. Unfortunately a five variable (φ, θ, z, wave position, wave height) fitting is very difficult too. High order polynomials could not even predict the trend of the curve, let alone have an accurate value. Several other functions (some of them quite complex) did not give the expected results either.

9.2 A preliminary solution

In order to make a first approach to the solution of the above problem the decision of reducing the range of φ was taken. During many unsuccessful trials of different functions that could not approximate accurately the GZ curve, the author finally "invented" a function that could approximate the GZ curve with very good accuracy. The defect of the above function is that gives accurate results by restraining the range of φ to 20 degrees. The function consists of a third order polynomial plus a sum of seven sinusoidal expressions that inside their arguments have third order polynomials of the variables. Its mathematical formula is:

$$GZ(x_1,x_2,x_3,x_4,x_5)=\sum_{j=1}^{3}\sum_{i=1}^{5}a_{ij}x_i^j+\sum_{1}^{7}b_k\cdot\sin\left(\sum_{l=1}^{3}\sum_{i=1}^{5}c_{li}\cdot x_i^l+p_k\right)$$

Some samples of the results of this fitting are presented below:

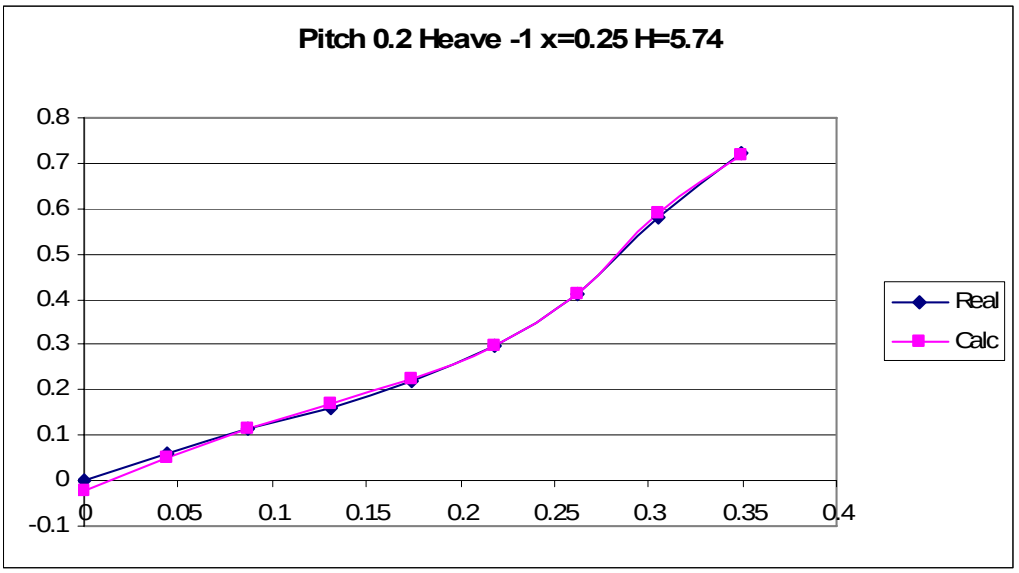

Figure 52: GZ(φ) fitting for pitch 0.2 deg, Heave -1m, wave phase offset 0.25, wave height 5.74m.

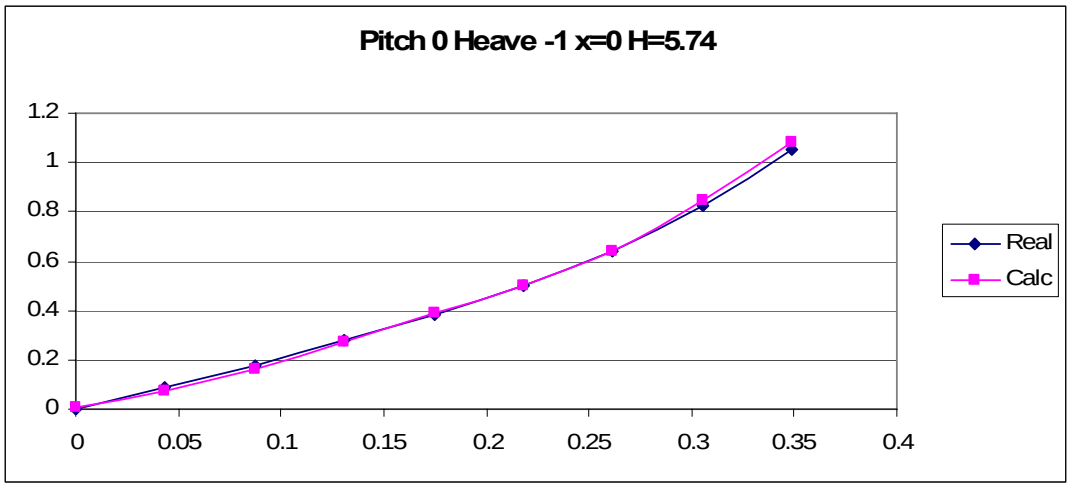

Figure 53: GZ(φ) fitting for pitch 0 deg, Heave -1m, wave phase offset 0, wave height 5.74m.

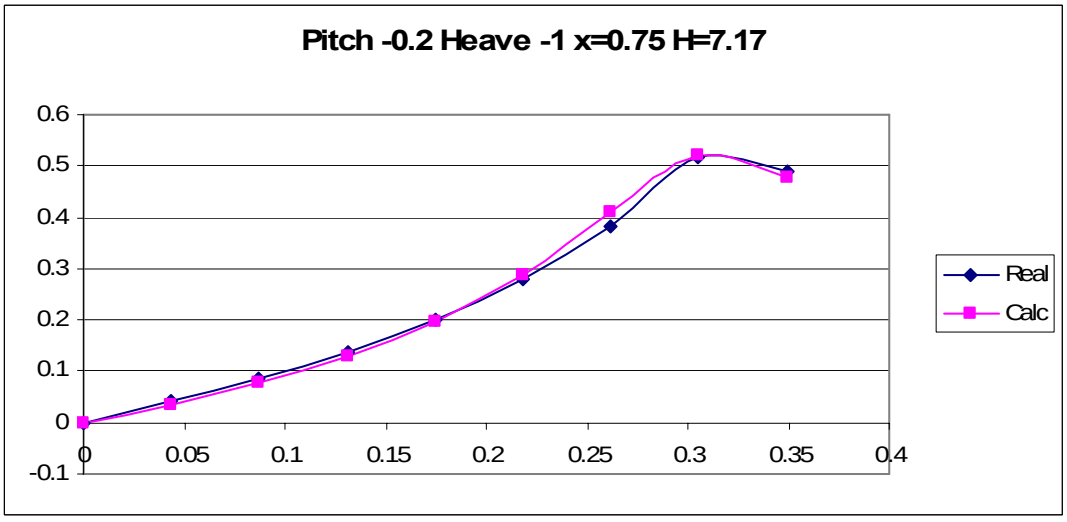

Figure 54: GZ(φ) fitting for pitch -0.2 deg, Heave -1m, wave phase offset 0.75, wave height 7.17m.

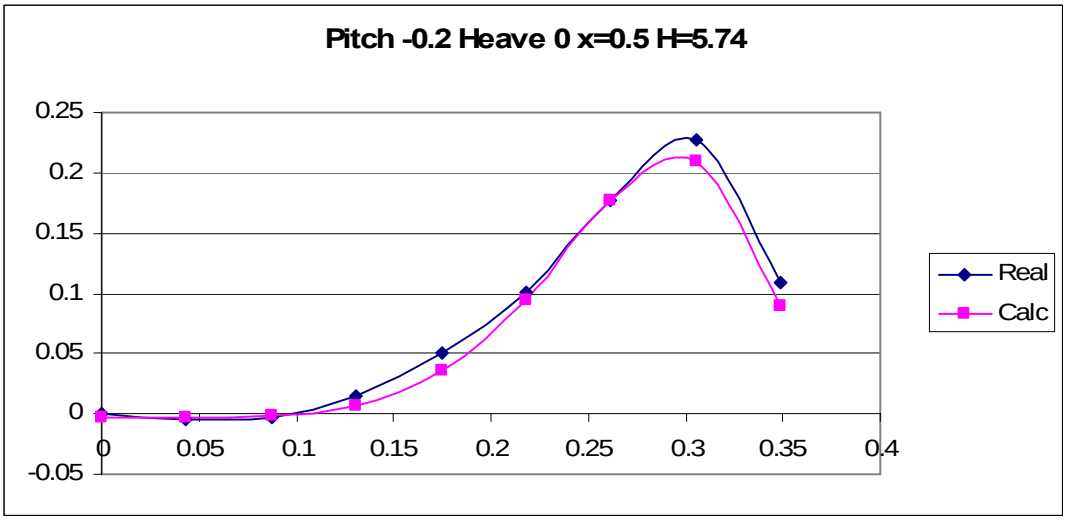

Figure 55: GZ(φ) fitting for pitch -0.2 deg, Heave 0m, wave phase offset 0.5, wave height 5.74m.

We observe that in figures 52,53 where the curvature does not change, the accuracy is almost perfect, while on the other hand in figures 54,55 where the curve reaches a peak and starts falling, the accuracy is not ideal.

9.3 Summary

A researcher willing to take things one or more steps further has take into account that a quite complex function is needed. Fitting a curve with so many parameters is not easy but the final results may worth it. If we find an accurate expression which works for many different wave heights and with no restriction to the φ angle, then we will do an important step for more accurate prediction of parametric rolling.

10 Discussion and conclusions

A 3DOF model was assessed in predicting the response of a ship during the parametric rolling phenomenon. A post-panamax containership was used for the calculations, which is a category of ships which suffers more from this severe phenomenon. All the necessary coefficients were calculated from scratch for the specific vessel. The "Roll only" model discussed above resembles an uncoupled Mathieu type model. For that reason, results are also comparable with such a model.

Our model has some strengths and some weaknesses either compared to the mentioned above models or in an absolute way. Compared to the first model, our model examines the phenomenon of parametric rolling taking into account three degrees of freedom while the quoted one takes only one. Concerning the second model, it couples heave and pitch motions but not roll. This is coupled with sway and yaw, something that our model is not able to do. On the other hand our model couples roll, pitch and heave with each other. Compared to the third model we have to notice that ours has simpler numeric manipulations and couples three motions with each other while the quoted one assumes that roll does not interact with heave and pitch.

Making a closer examination to our model we have to notice a couple of weaknesses. The first notification that has to be done is that the model "feels" the hull of the ship only at the calm waterline. No matter how much the heave has changed, the model assumes that the cotangent of the waterline is the same. Examining a ship with considerable flare, we get in some misleading results. The other point of interest that should be noted is the real values of GZ curve. In our model the first order restoring term, concerning roll, is function of GM at calm water. Introducing second and third order terms, we obtain a better accuracy of the restoring of the ship which is still not very accurate. When the ship changes its roll and pitch angle or its heave displacement, it has a variant GZ value. This could be partially solved with a high order fitting of GZ curve which takes into account φ, θ, z, wave height and its position related to the ship.

The main conclusions are the following:

- The model which takes into account only the roll motion did not have much difference at its response compared to the linear coupled model. For a=1.1 and a=1.2 the response for the coupled model was a little lower. This is explained by the fact that energy transfer occurs among the motions "consuming" energy from the roll mode and giving to the two remaining. On the other hand, something relevant was expected for a=0.8, 0,9, 1 but for some reasons did not happen.

- The "Full coupled" model gave a much lower response which is quite reasonable taking into account that terms up to third order helped for more accurate calculations of ship motions. Due to the fact that during parametric rolling we have large amplitudes of the motions of the ship, third order terms play a rather significant role contributing to the accuracy of the model. The fact that the results are much lower than in previous models agrees to the statement of Prof. Neves (Stability analysis of ships undergoing strong roll amplifications in head seas) "It is not uncommon for these models (referring to Mathieu type models) to overpredict the resonant rolling motions observed in experiments".

- Interesting results came up also with the numerical continuation which showed that the boundaries of the "Linear" models are almost the same. On the other hand the curve indicating the boundaries of "Full" model was much lower.

11 References

1. E.V Lewis, 1989 *"Principles of Naval Architecture Volume III" SNAME*
2. K.J Spyrou, 2005 *"Design Criteria for Parametric Rolling" Oceanic Engineering International, Vol.9 No.1 pp.11-27*
3. I.Oh, A.Nayfeh, D.Mook *"Theoretical and experimental study of the nonlinearly coupled Heave, Pitch and roll motions of a ship in longitudinall waves"*
4. M.A.S Neves, C.A Rodriguez, 2005*"Stability analysis of ships undergoing strong roll amplifications in head seas" Proceedings of 8th International Stability Workshop, Istanbul*
5. K.J Spyrou, 2000 *"Designing against parametric instability in following seas" Ocean Engineering 27*
6. M.Hamamoto, A. Munif, 2000 *"A mathematical model of ship motions leading to capsize in astern waves" Contemporary Ideas on Ship Stability*
7. W.Blocki *"Ship safety in connection with parametric resonance of the roll"*
8. N.Umeda, H.Hashimoto, D.Vassalos,2003 *"Nonlinear dynamics of parametric roll resonance with realistic numerical modeling" 8th International Conference on the Stability of Ships and Ocean Vehicles*
9. J.R Paulling, R.M Rosenberg, 1959*"On unstable ship motions resulting from nonlinear coupling" Journal of ship research*
10. J.E Kerwin, 1955 *"Notes on rolling in longitudinal waves" I.S.P Vol.2, No16*
11. M.Hamamoto "*A note on low cycle resonance of a ship in severe following waves"*
12. J.R Paulling, 1961 "*The transverse stability if a ship in a longitudinal seaway" Journal of ship research*
13. ABS "*Criteria for Parametric Roll of Large Containerships in Longitudinal Seas"*
14. http://monet.unibas.ch/~elmer/
15. http://www.cargolaw.com

16. http://www.wikipedia.com
17. T.M Egyedi Delft University "*The standardized container: Gateway Technologies in cargo transportation*" *Delft University of Technology*
18. Lloyd's Register, 2003 "*Head sea parametric rolling of containerships"*

Appendix I

The algorithm was programmed in the toolbox of MATLAB Matcont developed in Ghent University. The program allows the user to run simulations of his mathematical model having as main parameter the time and can then run numerical continuation in order to find the boundaries of a specific behavior by isolating time. The algorithm consists of the definition of the six variables and the 3 parameters that are used. Then all the necessary coefficients, as they were calculated in Chapter 8, are introduced in order to be "read" by the system. Finally the system of equations is set in its manipulated form described in chapter 8.

w,q,p,z,theta,phi
omega,wavep,lamda

m=113956000
Zzdot2=35691024
msinZzdot2= 149647024
JxxsinKphidot2=27999662000
JpsipsisinMthetadot2=752763959062
Kphidot=1600000000
Zzdot=72870518
Mtheta=501776521111
Zthetadot=1767114533
Zthetadot2=1810274280
Mthetadot=375660764600
Mzdot2=3706664872
Mzdot=1074248812
Zz=101698798
Kphi=1200552461
Ztheta=1360729924
Mz=1360729924
Kzzphi=198242332
Kphiphiphi=7233976949
Kthetathetaphi=2060120263668
Zzz=-2248333
Zztheta=-28198195
Zphiphi=-572683800
Zthetatheta=-30727106143
Kzphi=-572683809
Kphitheta=-35978008004
Mzz=-28198195
Mztheta=-30727106143

Mphiphi=-35978008004
Mthetatheta=-916776984098
Mphiphiz=10191624112
Mphiphitheta=2060120263668
Mthetathetatheta=1040940369414
Zphiphiz=198242332
Zphiphitheta=10191624112
Zthetathetatheta=2721459848
Kzphitheta=10191624112

Zzetaz0=52389.64364*wavep*cos(-841.6/lamda-omega*t)
Zzetaz1=16874.71313*wavep*cos(-752.4/lamda-omega*t)
Zzetaz2=5014.110801*wavep*cos(-663.3/lamda-omega*t)
Zzetaz3=3909.085207*wavep*cos(-574.11/lamda-omega*t)
Zzetaz4=1406.263152*wavep*cos(-484.96/lamda-omega*t)
Zzetaz5=702.2741349*wavep*cos(-395.80/lamda-omega*t)
Zzetaz6=351.0300832*wavep*cos(-306.64/lamda-omega*t)
Zzetaz7=0*wavep*cos(-217.48/lamda-omega*t)
Zzetaz8=0*wavep*cos(-128.32/lamda-omega*t)
Zzetaz9=0
Zzetaz10=0
Zzetaz11=0
Zzetaz12=175.5016747*wavep*cos(228.31/lamda-omega*t)
Zzetaz13=351.0300832*wavep*cos(317.47/lamda-omega*t)
Zzetaz14=3185.190287*wavep*cos(406.63/lamda-omega*t)
Zzetaz15=15712.04459*wavep*cos(495.79/lamda-omega*t)
Zzetaz16=15154.34872*wavep*cos(584.95/lamda-omega*t)
Zzetaz17=16285.1618*wavep*cos(674.1/lamda-omega*t)
Zzetaz18=15154.34872*wavep*cos(763.27/lamda-omega*t)
Zzetaz19=8953.771476*wavep*cos(852.42/lamda-omega*t)
Zzetaz20=2826.346456*wavep*cos(941.58/lamda-omega*t)

Zzetatheta0=7017226.037*wavep*cos(-841.6/lamda-omega*t)
Zzetatheta1=2020797.522*wavep*cos(-752.4/lamda-omega*t)
Zzetatheta2=529304.5785*wavep*cos(-663.3/lamda-omega*t)
Zzetatheta3=357184.8426*wavep*cos(-574.11/lamda-omega*t)
Zzetatheta4=108539.6088*wavep*cos(-484.96/lamda-omega*t)
Zzetatheta5=44238.35458*wavep*cos(-395.80/lamda-omega*t)
Zzetatheta6=17131.32115*wavep*cos(-306.64/lamda-omega*t)
Zzetatheta7=0*wavep*cos(-217.48/lamda-omega*t)
Zzetatheta8=0*wavep*cos(-128.32/lamda-omega*t)
Zzetatheta9=0
Zzetatheta10=0
Zzetatheta11=0
Zzetatheta12=-6377.204354*wavep*cos(228.31/lamda-omega*t)
Zzetatheta13=-17736.49702*wavep*cos(317.47/lamda-omega*t)
Zzetatheta14=-206135.9598*wavep*cos(406.63/lamda-omega*t)
Zzetatheta15=-1239790.303*wavep*cos(495.79/lamda-omega*t)
Zzetatheta16=-1410824.403*wavep*cos(584.95/lamda-omega*t)
Zzetatheta17=-1747186.154*wavep*cos(674.1/lamda-omega*t)

Zzetatheta18=-1840904.82*wavep*cos(763.27/lamda-omega*t)
Zzetatheta19=-1214731.31*wavep*cos(852.42/lamda-omega*t)
Zzetatheta20=-423547.8009*wavep*cos(941.58/lamda-omega*t)

Mzetaz0=7017226.037*wavep*cos(-841.6/lamda-omega*t)
Mzetaz1=2020797.522*wavep*cos(-752.4/lamda-omega*t)
Mzetaz2=529304.5785*wavep*cos(-663.3/lamda-omega*t)
Mzetaz3=357184.8426*wavep*cos(-574.11/lamda-omega*t)
Mzetaz4=108539.6088*wavep*cos(-484.96/lamda-omega*t)
Mzetaz5=44238.35458*wavep*cos(-395.80/lamda-omega*t)
Mzetaz6=17131.32115*wavep*cos(-306.64/lamda-omega*t)
Mzetaz7=0*wavep*cos(-217.48/lamda-omega*t)
Mzetaz8=0*wavep*cos(-128.32/lamda-omega*t)
Mzetaz9=0
Mzetaz10=0
Mzetaz11=0
Mzetaz12=6377.204354*wavep*cos(228.31/lamda-omega*t)
Mzetaz13=17736.49702*wavep*cos(317.47/lamda-omega*t)
Mzetaz14=206135.9598*wavep*cos(406.63/lamda-omega*t)
Mzetaz15=1239790.303*wavep*cos(495.79/lamda-omega*t)
Mzetaz16=1410824.403*wavep*cos(584.95/lamda-omega*t)
Mzetaz17=1747186.154*wavep*cos(674.1/lamda-omega*t)
Mzetaz18=1840904.82*wavep*cos(763.27/lamda-omega*t)
Mzetaz19=1214731.31*wavep*cos(852.42/lamda-omega*t)
Mzetaz20=423547.8009*wavep*cos(941.58/lamda-omega*t)

Kzetaphi0=17163371.15*wavep*cos(-841.6/lamda-omega*t)
Kzetaphi1=6682555.148*wavep*cos(-752.4/lamda-omega*t)
Kzetaphi2=2090765.871*wavep*cos(-663.3/lamda-omega*t)
Kzetaphi3=1691226.624*wavep*cos(-574.11/lamda-omega*t)
Kzetaphi4=626082.4177*wavep*cos(-484.96/lamda-omega*t)
Kzetaphi5=315630.0872*wavep*cos(-395.80/lamda-omega*t)
Kzetaphi6=159258.8385*wavep*cos(-306.64/lamda-omega*t)
Kzetaphi7=0*wavep*cos(-217.48/lamda-omega*t)
Kzetaphi8=0*wavep*cos(-128.32/lamda-omega*t)
Kzetaphi9=0
Kzetaphi10=0
Kzetaphi11=0
Kzetaphi12=79847.80389*wavep*cos(228.31/lamda-omega*t)
Kzetaphi13=157766.9606*wavep*cos(317.47/lamda-omega*t)
Kzetaphi14=1319058.965*wavep*cos(406.63/lamda-omega*t)
Kzetaphi15=4784356.858*wavep*cos(495.79/lamda-omega*t)
Kzetaphi16=2819460.518*wavep*cos(584.95/lamda-omega*t)
Kzetaphi17=1628516.18*wavep*cos(674.1/lamda-omega*t)
Kzetaphi18=706933.6982*wavep*cos(763.27/lamda-omega*t)
Kzetaphi19=133407.6135*wavep*cos(852.42/lamda-omega*t)
Kzetaphi20=28.26346456*wavep*cos(941.58/lamda-omega*t)

Mzetatheta0=939908307.1*wavep*cos(-841.6/lamda-omega*t)

Mzetatheta1=241996565.6*wavep*cos(-752.4/lamda-omega*t)
Mzetatheta2=55874979.22*wavep*cos(-663.3/lamda-omega*t)
Mzetatheta3=32637050.62*wavep*cos(-574.11/lamda-omega*t)
Mzetatheta4=8377412.628*wavep*cos(-484.96/lamda-omega*t)
Mzetatheta5=2786706.67*wavep*cos(-395.80/lamda-omega*t)
Mzetatheta6=836059.8662*wavep*cos(-306.64/lamda-omega*t)
Mzetatheta7=0*wavep*cos(-217.48/lamda-omega*t)
Mzetatheta8=0*wavep*cos(-128.32/lamda-omega*t)
Mzetatheta9=0
Mzetatheta10=0
Mzetatheta11=0
Mzetatheta12=231728.4746*wavep*cos(228.31/lamda-omega*t)
Mzetatheta13=896171.9847*wavep*cos(317.47/lamda-omega*t)
Mzetatheta14=13340500.91*wavep*cos(406.63/lamda-omega*t)
Mzetatheta15=97828133.41*wavep*cos(495.79/lamda-omega*t)
Mzetatheta16=131343519.5*wavep*cos(584.95/lamda-omega*t)
Mzetatheta17=187450360.9*wavep*cos(674.1/lamda-omega*t)
Mzetatheta18=223627594.8*wavep*cos(763.27/lamda-omega*t)
Mzetatheta19=164798953.3*wavep*cos(852.42/lamda-omega*t)
Mzetatheta20=63471602.8*wavep*cos(941.58/lamda-omega*t)

Zphiphizeta0=-2652282.373*wavep*cos(-841.6/lamda-omega*t)
Zphiphizeta1=-481874.8298*wavep*cos(-752.4/lamda-omega*t)
Zphiphizeta2=-230856.4361*wavep*cos(-663.3/lamda-omega*t)
Zphiphizeta3=-224954.0632*wavep*cos(-574.11/lamda-omega*t)
Zphiphizeta4=-214240.654*wavep*cos(-484.96/lamda-omega*t)
Zphiphizeta5=-213691.2078*wavep*cos(-395.80/lamda-omega*t)
Zphiphizeta6=-214038.9675*wavep*cos(-306.64/lamda-omega*t)
Zphiphizeta7=-213993.601*wavep*cos(-217.48/lamda-omega*t)
Zphiphizeta8=-214206.7217*wavep*cos(-128.32/lamda-omega*t)
Zphiphizeta9=-214579.035*wavep*cos(-39.16/lamda-omega*t)
Zphiphizeta10=-215031.5213*wavep*cos(50/lamda-omega*t)
Zphiphizeta11=-215031.5213*wavep*cos(139.15/lamda-omega*t)
Zphiphizeta12=-215031.5213*wavep*cos(228.31/lamda-omega*t)
Zphiphizeta13=--215031.5213*wavep*cos(317.47/lamda-omega*t)
Zphiphizeta14=-214780.14*wavep*cos(406.63/lamda-omega*t)
Zphiphizeta15=-389673.2383*wavep*cos(495.79/lamda-omega*t)
Zphiphizeta16=-292917.2385*wavep*cos(584.95/lamda-omega*t)
Zphiphizeta17=-232427.14*wavep*cos(674.1/lamda-omega*t)
Zphiphizeta18=-146673.368*wavep*cos(763.27/lamda-omega*t)
Zphiphizeta19=-54201.0619*wavep*cos(852.42/lamda-omega*t)
Zphiphizeta20=-1045.246709*wavep*cos(941.58/lamda-omega*t)

Kzetazetaphi0=-2652282.373*(wavep*cos(-841.6/lamda-omega*t))^2
Kzetazetaphi1=-481874.8298*(wavep*cos(-752.4/lamda-omega*t))^2
Kzetazetaphi2=-230856.4361*(wavep*cos(-663.3/lamda-omega*t))^2
Kzetazetaphi3=-224954.0632*(wavep*cos(-574.11/lamda-omega*t))^2
Kzetazetaphi4=-214240.654*(wavep*cos(-484.96/lamda-omega*t))^2
Kzetazetaphi5=-214903.2626*(wavep*cos(-395.80/lamda-omega*t))^2
Kzetazetaphi6=-214903.2626*(wavep*cos(-306.64/lamda-omega*t))^2

Kzetazetaphi7=--213903.2626*(wavep*cos(-217.48/lamda-omega*t))^2
Kzetazetaphi8=-214206.7217*(wavep*cos(-128.32/lamda-omega*t))^2
Kzetazetaphi9=-214579.035*(wavep*cos(-39.16/lamda-omega*t))^2
Kzetazetaphi10=-215031.5213*(wavep*cos(50/lamda-omega*t))^2
Kzetazetaphi11=-215031.5213*(wavep*cos(139.15/lamda-omega*t))^2
Kzetazetaphi12=-215031.5213*(wavep*cos(228.31/lamda-omega*t))^2
Kzetazetaphi13=--215031.5213*(wavep*cos(317.47/lamda-omega*t))^2
Kzetazetaphi14=-214780.14*(wavep*cos(406.63/lamda-omega*t))^2
Kzetazetaphi15=-389673.2383*(wavep*cos(495.79/lamda-omega*t))^2
Kzetazetaphi16=-292917.2385*(wavep*cos(584.95/lamda-omega*t))^2
Kzetazetaphi17=-232427.14*(wavep*cos(674.1/lamda-omega*t))^2
Kzetazetaphi18=-146673.368*(wavep*cos(763.27/lamda-omega*t))^2
Kzetazetaphi19=-54201.06198*(wavep*cos(852.42/lamda-omega*t))^2
Kzetazetaphi20=-1045.246709*(wavep*cos(941.58/lamda-omega*t))^2

Kzetazphi0=-5304564.7*wavep*(cos(-841.6/lamda-omega*t))
Kzetazphi1=-963749.66*wavep*(cos(-752.4/lamda-omega*t))
Kzetazphi2=-461712.87*wavep*(cos(-663.3/lamda-omega*t))
Kzetazphi3=-449908.13*wavep*(cos(-574.11/lamda-omega*t))
Kzetazphi4=-428481.31*wavep*(cos(-484.96/lamda-omega*t))
Kzetazphi5=-429806.5252*wavep*(cos(-395.80/lamda-omega*t))
Kzetazphi6=-428077.935*wavep*(cos(-306.64/lamda-omega*t))
Kzetazphi7=-427987.202*wavep*(cos(-217.48/lamda-omega*t))
Kzetazphi8=-428413*wavep*(cos(-128.32/lamda-omega*t))
Kzetazphi9=-429158*wavep*(cos(-39.16/lamda-omega*t))
Kzetazphi10=-430063*wavep*(cos(50/lamda-omega*t))
Kzetazphi11=-430364*wavep*(cos(139.15/lamda-omega*t))
Kzetazphi12=-430364.7*wavep*(cos(228.31/lamda-omega*t))
Kzetazphi13=-430364.7*wavep*(cos(317.47/lamda-omega*t))
Kzetazphi14=-430364.7*wavep*(cos(406.63/lamda-omega*t))
Kzetazphi15=-779346.48*wavep*(cos(495.79/lamda-omega*t))
Kzetazphi16=-585834.48*wavep*(cos(584.95/lamda-omega*t))
Kzetazphi17=-464854.28*wavep*(cos(674.1/lamda-omega*t))
Kzetazphi18=-293346.74*wavep*(cos(763.27/lamda-omega*t))
Kzetazphi19=-108402.12*wavep*(cos(852.42/lamda-omega*t))
Kzetazphi20=-2090.4934*wavep*(cos(941.58/lamda-omega*t))

Kzetaphitheta0=-710509315.8*wavep*(cos(-841.6/lamda-omega*t))
Kzetaphitheta1=-115411913.0*wavep*(cos(-752.4/lamda-omega*t))
Kzetaphitheta2=-48739795.9*wavep*(cos(-663.3/lamda-omega*t))
Kzetaphitheta3=-41109455.2*wavep*(cos(-574.11/lamda-omega*t))
Kzetaphitheta4=-33071472.8*wavep*(cos(-484.96/lamda-omega*t))
Kzetaphitheta5=-26922100.5*wavep*(cos(-395.80/lamda-omega*t))
Kzetaphitheta6=-20917681.8*wavep*(cos(-306.64/lamda-omega*t))
Kzetaphitheta7=-14896213.4*wavep*(cos(-217.48/lamda-omega*t))
Kzetaphitheta8=-8789338.3*wavep*(cos(-128.32/lamda-omega*t))
Kzetaphitheta9=-2682463.2*wavep*(cos(-39.16/lamda-omega*t))
Kzetaphitheta10=3424411.9*wavep*(cos(50/lamda-omega*t))
Kzetaphitheta11=9509017.6*wavep*(cos(139.15/lamda-omega*t))
Kzetaphitheta12=15589383.4*wavep*(cos(228.31/lamda-omega*t))

Kzetaphitheta13=21554939.2*wavep*(cos(317.47/lamda-omega*t))
Kzetaphitheta14=27814149.8*wavep*(cos(406.63/lamda-omega*t))
Kzetaphitheta15=61495892.4*wavep*(cos(495.79/lamda-omega*t))
Kzetaphitheta16=54539432.3*wavep*(cos(584.95/lamda-omega*t))
Kzetaphitheta17=49872821.1*wavep*(cos(674.1/lamda-omega*t))
Kzetaphitheta18=35634881.4*wavep*(cos(763.27/lamda-omega*t))
Kzetaphitheta19=14706591.0*wavep*(cos(852.42/lamda-omega*t))
Kzetaphitheta20=313275.1*wavep*(cos(941.58/lamda-omega*t))

Mphiphizeta0=-355254657.9*wavep*(cos(-841.6/lamda-omega*t))
Mphiphizeta1=-57705956.49*wavep*(cos(-752.4/lamda-omega*t))
Mphiphizeta2=-24369897.96*wavep*(cos(-663.3/lamda-omega*t))
Mphiphizeta3=-20554727.61*wavep*(cos(-574.11/lamda-omega*t))
Mphiphizeta4=-16535736.4*wavep*(cos(-484.96/lamda-omega*t))
Mphiphizeta5=-13461050.25*wavep*(cos(-395.80/lamda-omega*t))
Mphiphizeta6=-10458840.89*wavep*(cos(-306.64/lamda-omega*t))
Mphiphizeta7=-7448106.681*wavep*(cos(-217.48/lamda-omega*t))
Mphiphizeta8=-4394669.134*wavep*(cos(-128.32/lamda-omega*t))
Mphiphizeta9=-1341231.588*wavep*(cos(-39.16/lamda-omega*t))
Mphiphizeta10=1712205.959*wavep*(cos(50/lamda-omega*t))
Mphiphizeta11=4754508.824*wavep*(cos(139.15/lamda-omega*t))
Mphiphizeta12=7794691.698*wavep*(cos(228.31/lamda-omega*t))
Mphiphizeta13=10777469.62*wavep*(cos(317.47/lamda-omega*t))
Mphiphizeta14=13907074.88*wavep*(cos(406.63/lamda-omega*t))
Mphiphizeta15=30747946.22*wavep*(cos(495.79/lamda-omega*t))
Mphiphizeta16=27269716.15*wavep*(cos(584.95/lamda-omega*t))
Mphiphizeta17=24936410.57*wavep*(cos(674.1/lamda-omega*t))
Mphiphizeta18=17817440.72*wavep*(cos(763.27/lamda-omega*t))
Mphiphizeta19=7353295.476*wavep*(cos(852.42/lamda-omega*t))
Mphiphizeta20=156637.5361*wavep*(cos(941.58/lamda-omega*t))

Z=36198080*cos(omega*t+0.16)*wavep-Zzdot*w-Zthetadot*q-Zz*z-Ztheta*theta-0.5*Zzz*z^2-0.5*Zphiphi*phi^2-0.5*Zthetatheta*theta^2-Zztheta*z*theta-0.5*Zphiphiz*phi^2*z-0.5*Zphiphitheta*phi^2*theta-(1/6)*Zthetathetatheta*theta^3-14.19*(Zzetaz0+Zzetaz1+Zzetaz2+Zzetaz3+Zzetaz4+Zzetaz5+Zzetaz6+Zzetaz7+Zzetaz8+Zzetaz9+Zzetaz10+Zzetaz11+Zzetaz12+Zzetaz13+Zzetaz14+Zzetaz15+Zzetaz16+Zzetaz17+Zzetaz18+Zzetaz19+Zzetaz20)*z-14.19*(Zzetatheta0+Zzetatheta1+Zzetatheta2+Zzetatheta3+Zzetatheta4+Zzetatheta5+Zzetatheta6+Zzetatheta7+Zzetatheta8+Zzetatheta9+Zzetatheta10+Zzetatheta11+Zzetatheta12+Zzetatheta13+Zzetatheta14+Zzetatheta15+Zzetatheta16+Zzetatheta17+Zzetatheta18+Zzetatheta19+Zzetatheta20)*theta-14.19*(Zphiphizeta0+Zphiphizeta1+Zphiphizeta2+Zphiphizeta3+Zphiphizeta4+Zphiphizeta5+Zphiphizeta6+Zphiphizeta7+Zphiphizeta8+Zphiphizeta9+Zphiphizeta10+Zphiphizeta11+Zphiphizeta12+Zphiphizeta13+Zphiphizeta14+Zphiphizeta15+Zphiphizeta16+Zphiphizeta17+Zphiphizeta18+Zphiphizeta19+Zphiphizeta20)*phi^2*froude1

K=-Kphidot*p-Kphi*phi-Kzphi*z*phi-Kphitheta*phi*theta-0.5*Kzzphi*z^2*phi-(1/6)*Kphiphiphi*(phi^3)-0.5*Kthetathetaphi*(theta^2)*phi-Kzphitheta*z*phi*theta-

14.19*(Kzetaphi0+Kzetaphi1+Kzetaphi2+Kzetaphi3+Kzetaphi4+Kzetaphi5+Kzetaphi6+Kzetaphi7+Kzetaphi8+Kzetaphi9+Kzetaphi10+Kzetaphi11+Kzetaphi12+Kzetaphi13+Kzetaphi14+Kzetaphi15+Kzetaphi16+Kzetaphi17+Kzetaphi18+Kzetaphi19+Kzetaphi20)*phi-
14.19*(Kzetazetaphi0+Kzetazetaphi1+Kzetazetaphi2+Kzetazetaphi3+Kzetazetaphi4+Kzetazetaphi5+Kzetazetaphi6+Kzetazetaphi7+Kzetazetaphi8+Kzetazetaphi9+Kzetazetaphi10+Kzetazetaphi11+Kzetazetaphi12+Kzetazetaphi13+Kzetazetaphi14+Kzetazetaphi15+Kzetazetaphi16+Kzetazetaphi17+Kzetazetaphi18+Kzetazetaphi19+Kzetazetaphi20)*phi*froude2-
14.19*(Kzetazphi0+Kzetazphi1+Kzetazphi2+Kzetazphi3+Kzetazphi4+Kzetazphi5+Kzetazphi6+Kzetazphi7+Kzetazphi8+Kzetazphi9+Kzetazphi10+Kzetazphi11+Kzetazphi12+Kzetazphi13+Kzetazphi14+Kzetazphi15+Kzetazphi16+Kzetazphi17+Kzetazphi18+Kzetazphi19+Kzetazphi20)*z*phi*froude3-
14.19*(Kzetaphitheta0+Kzetaphitheta1+Kzetaphitheta2+Kzetaphitheta3+Kzetaphitheta4+Kzetaphitheta5+Kzetaphitheta6+Kzetaphitheta7+Kzetaphitheta8+Kzetaphitheta9+Kzetaphitheta10+Kzetaphitheta11+Kzetaphitheta12+Kzetaphitheta13+Kzetaphitheta14+Kzetaphitheta15+Kzetaphitheta16+Kzetaphitheta17+Kzetaphitheta18+Kzetaphitheta19+Kzetaphitheta20)*phi*theta*froude4

M=3814299800*cos(omega*t-1.27)*wavep-Mthetadot*q-Mzdot*w-Mz*z-Mtheta*theta-0.5*Mzz*z^2-0.5*Mphiphi*phi^2-0.5*Mthetatheta*theta^2-Mztheta*z*theta-0.5*Mphiphiz*z*phi^2-0.5*Mphiphitheta*phi^2*theta-(1/6)*Mthetathetatheta*theta^3-
14.19*(Mzetaz0+Mzetaz1+Mzetaz2+Mzetaz3+Mzetaz4+Mzetaz5+Mzetaz6+Mzetaz7+Mzetaz8+Mzetaz9+Mzetaz10+Mzetaz11+Mzetaz12+Mzetaz13+Mzetaz14+Mzetaz15+Mzetaz16+Mzetaz17+Mzetaz18+Mzetaz19+Mzetaz20)*z-
14.19*(Mzetatheta0+Mzetatheta1+Mzetatheta2+Mzetatheta3+Mzetatheta4+Mzetatheta5+Mzetatheta6+Mzetatheta7+Mzetatheta8+Mzetatheta9+Mzetatheta10+Mzetatheta11+Mzetatheta12+Mzetatheta13+Mzetatheta14+Mzetatheta15+Mzetatheta16+Mzetatheta17+Mzetatheta18+Mzetatheta19+Mzetatheta20)*theta-
14.19*(Mphiphizeta0+Mphiphizeta1+Mphiphizeta2+Mphiphizeta3+Mphiphizeta4+Mphiphizeta5+Mphiphizeta6+Mphiphizeta7+Mphiphizeta8+Mphiphizeta9+Mphiphizeta10+Mphiphizeta11+Mphiphizeta12+Mphiphizeta13+Mphiphizeta14+Mphiphizeta15+Mphiphizeta16+Mphiphizeta17+Mphiphizeta18+Mphiphizeta19+Mphiphizeta20)*phi^2*froude5

w'=-((JpsipsisinMthetadot2)*Z-M*Zthetadot2)/(Mzdot2*Zthetadot2-(JpsipsisinMthetadot2)*(msinZzdot2))
q'=-(M*(msinZzdot2)-Mzdot2*Z)/(-m*(JpsipsisinMthetadot2)+Mzdot2*Zthetadot2-Zzdot2*(JpsipsisinMthetadot2))
p'=K/(JxxsinKphidot2)
z'=w
theta'=q
phi'=p

Appendix II

The full series of graphs is presented below showing all the runs of the program that were made for the completion of the thesis

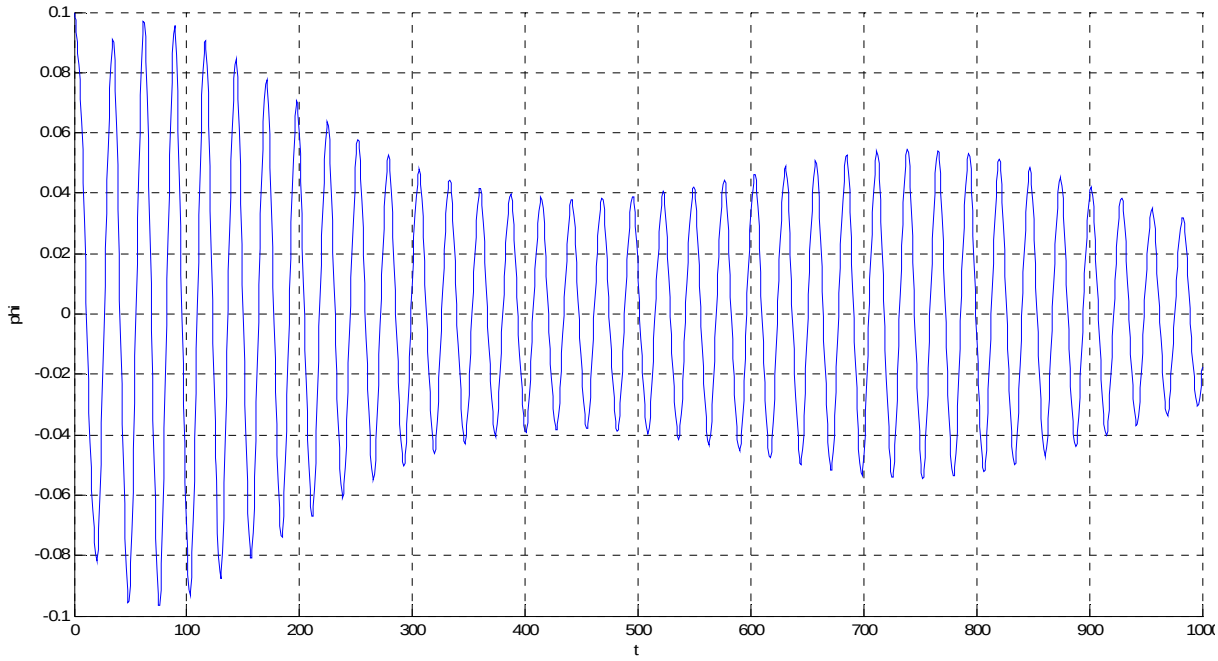

Roll only a=0.8 H=7.8m

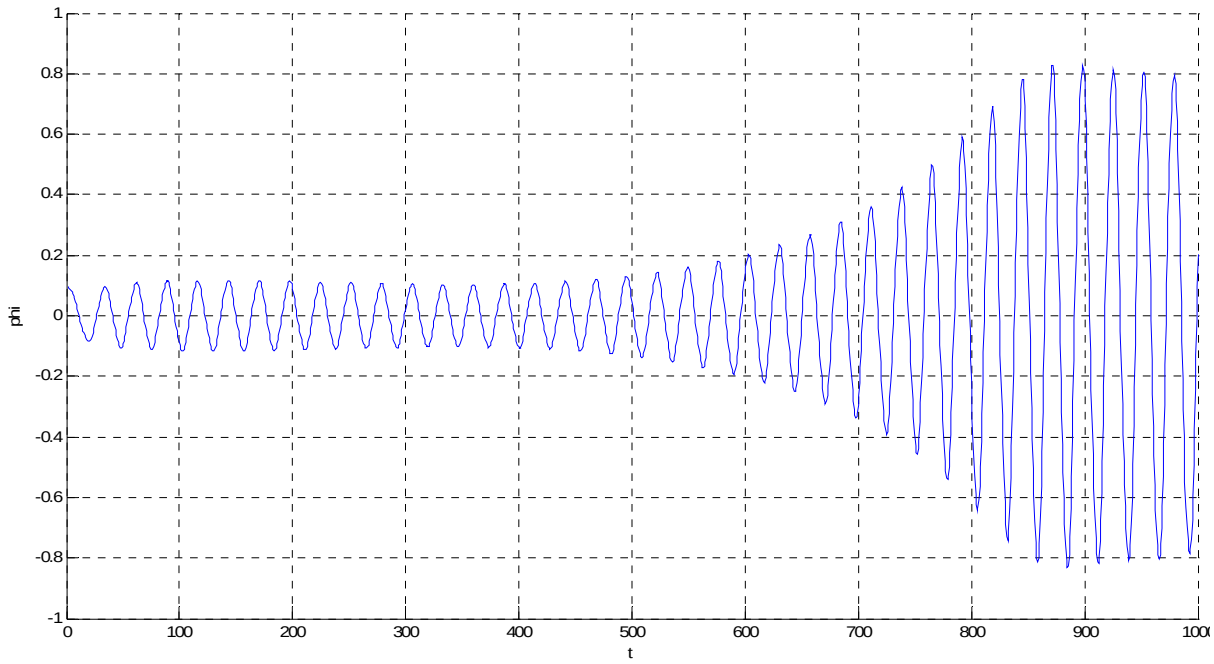

Roll only a=0.8 H=8.2m

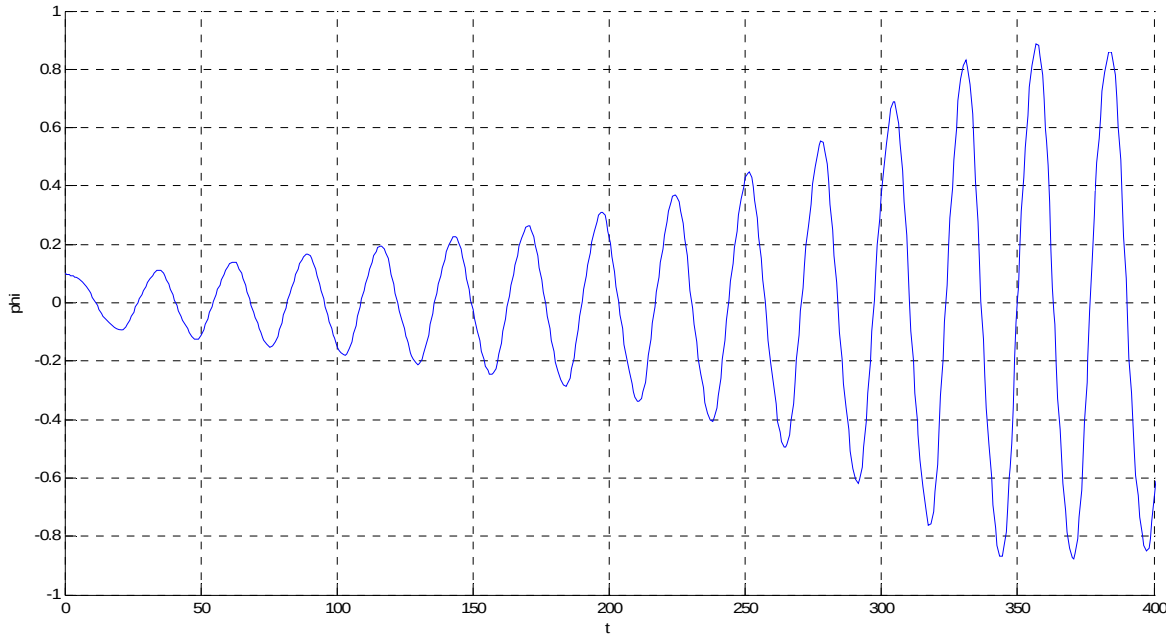

Roll only a=0.8 H=9m

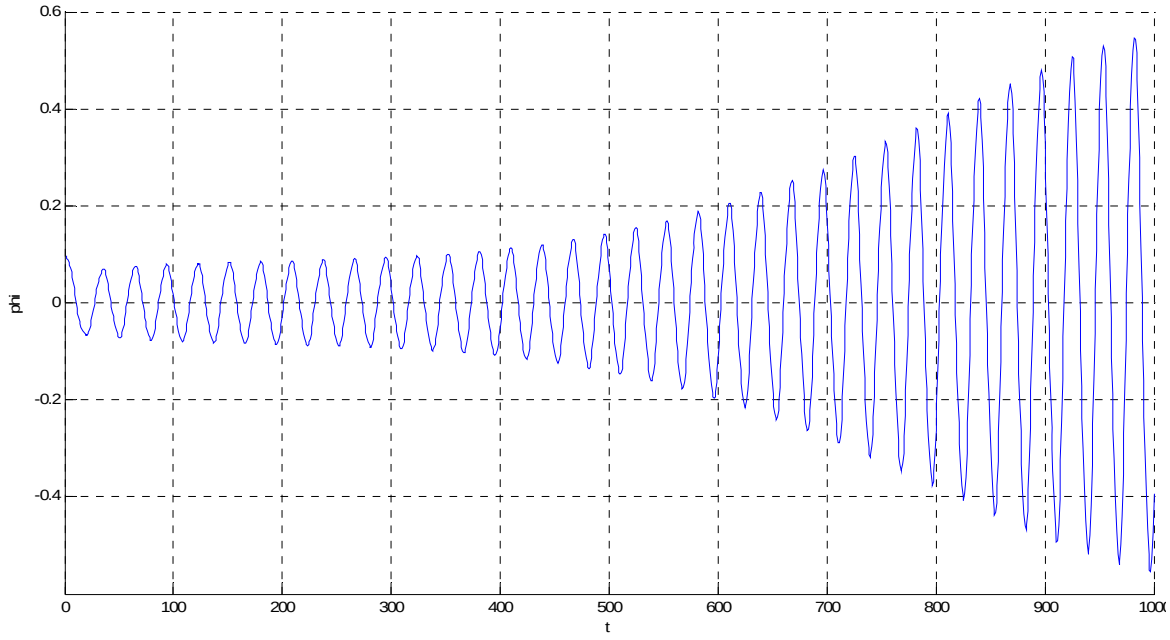

Roll only a=0.9 H=6.6m

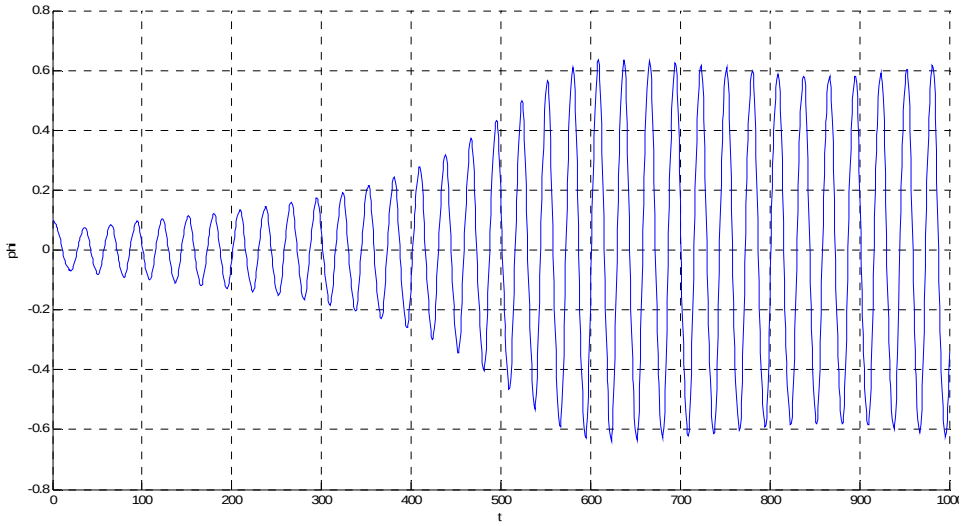

Roll only a=0.9 H=7m

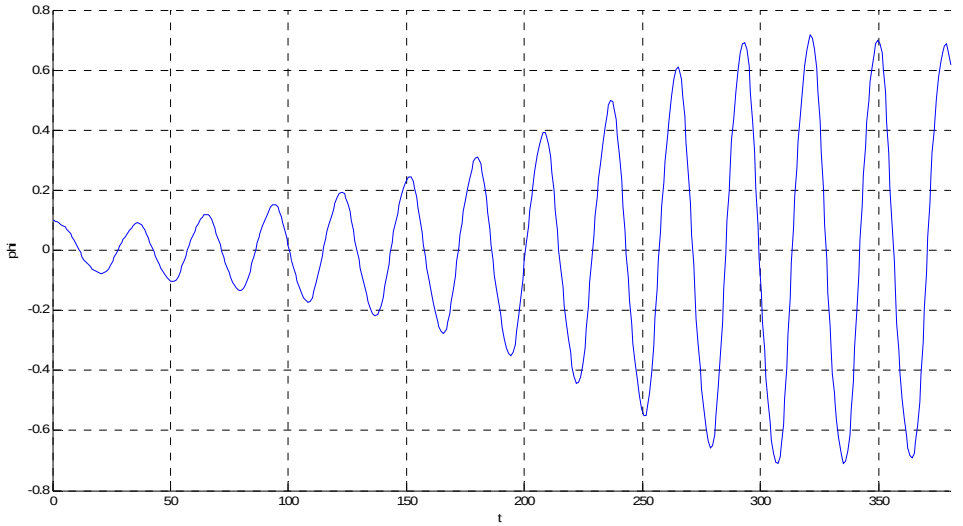

Roll only a=0.9 H=8m

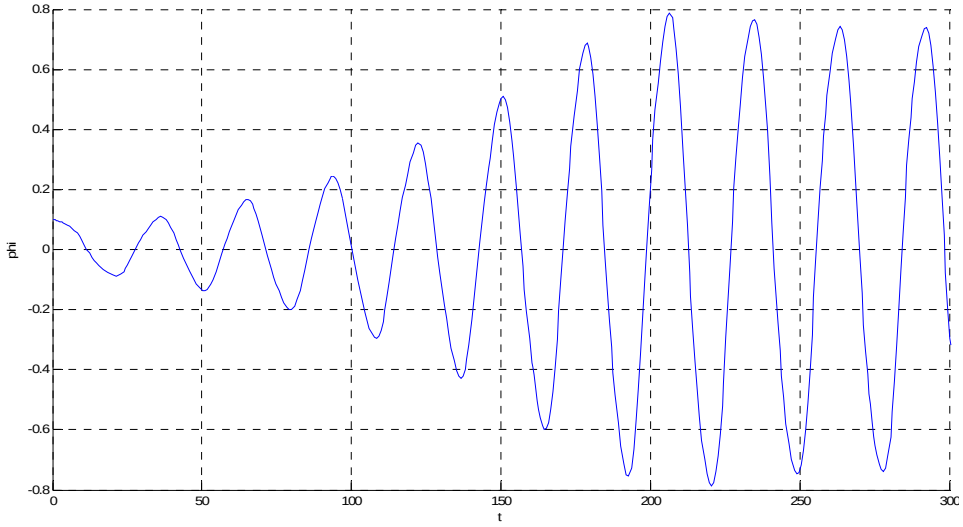

Roll only a=0.9 H=9m

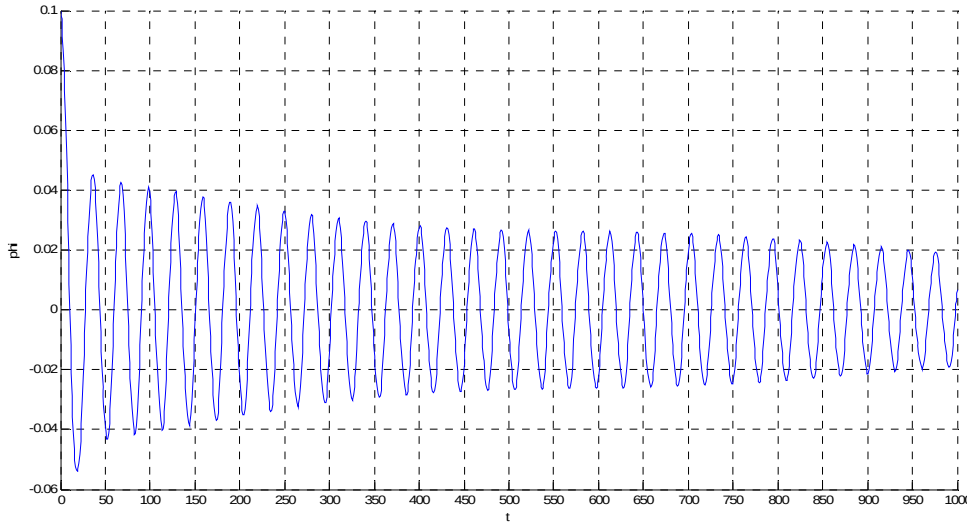

Roll only a=1 H=5.4m

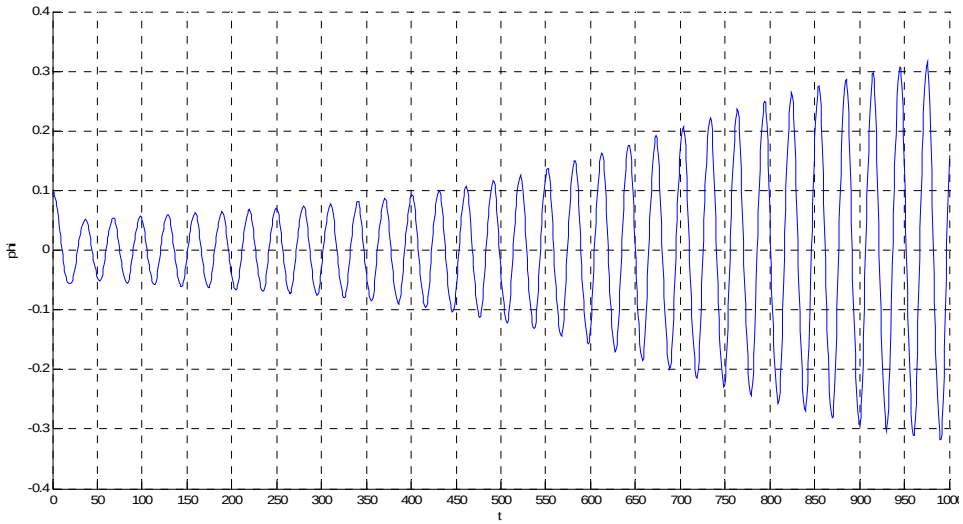

Roll only a=1 H=6m

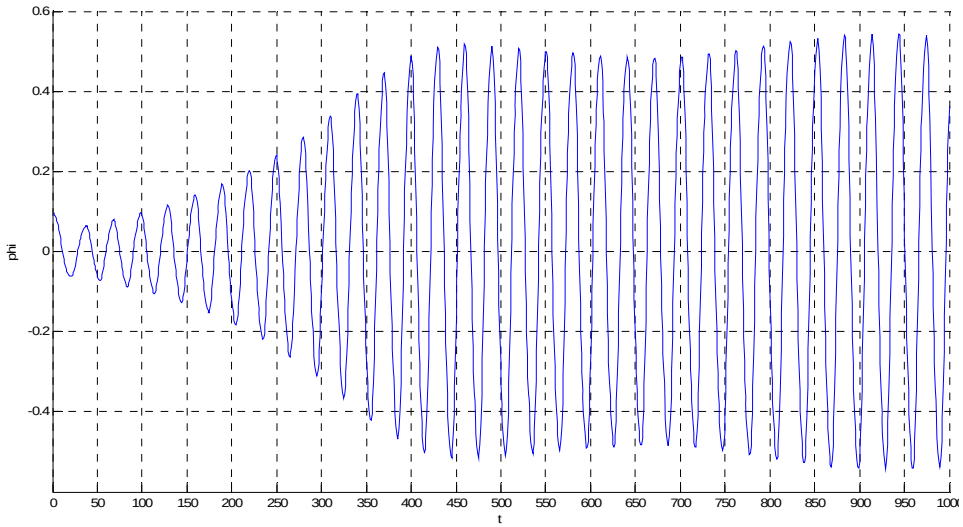

Roll only a=1 H=7m

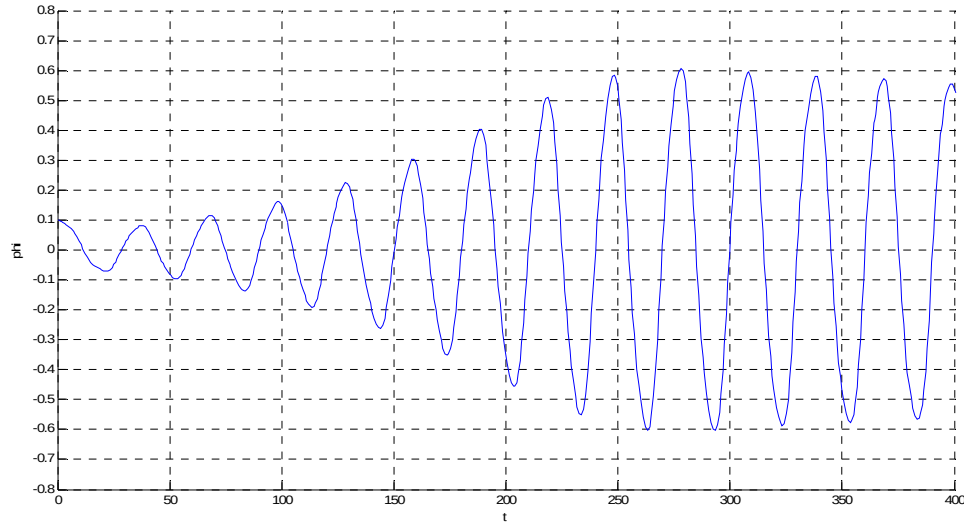

Roll only a=1 H=8m

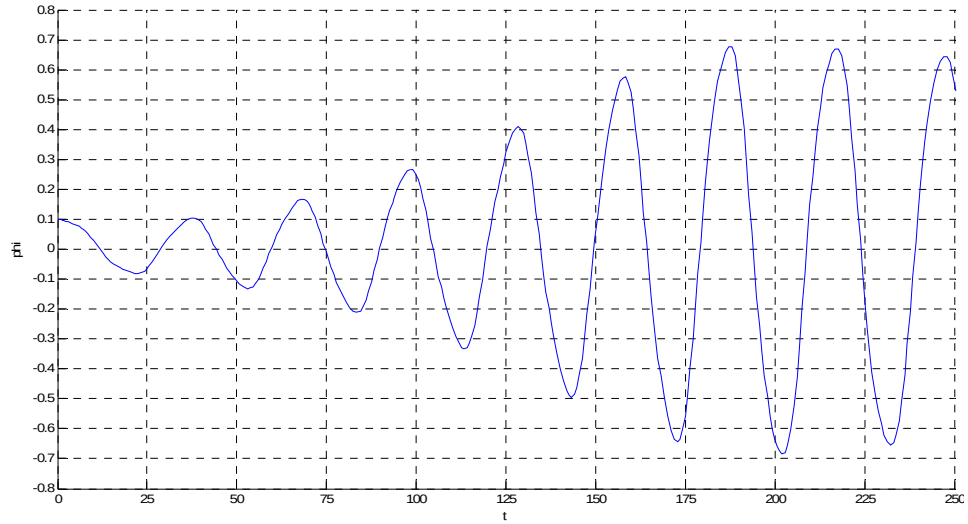

Roll only a=1 H=9m

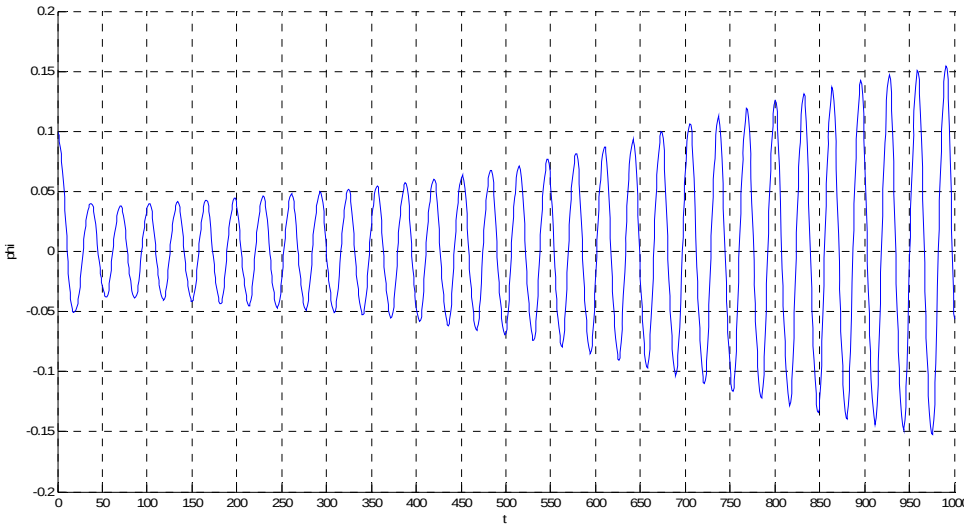

Roll only a=1.1 H=6m

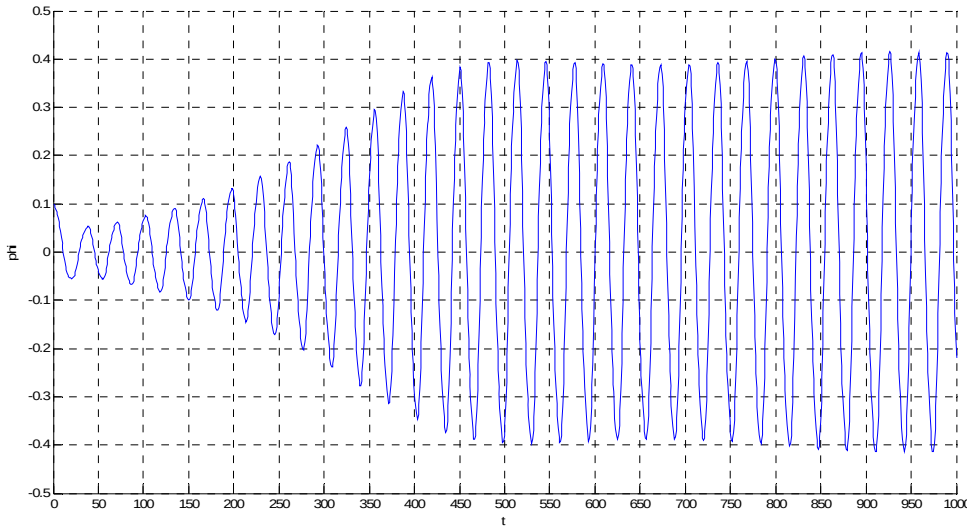

Roll only a=1.1 H=7m

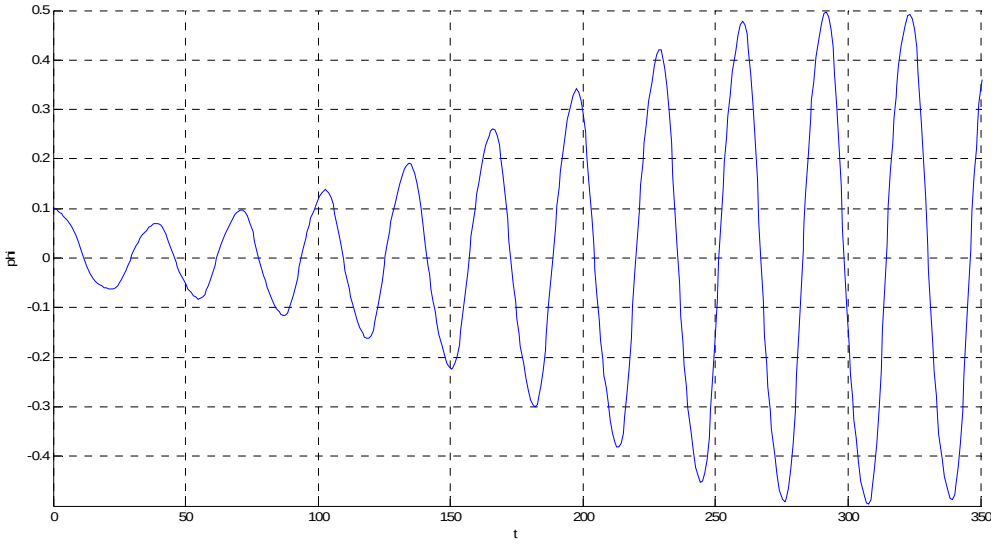

Roll only a=1.1 H=8m

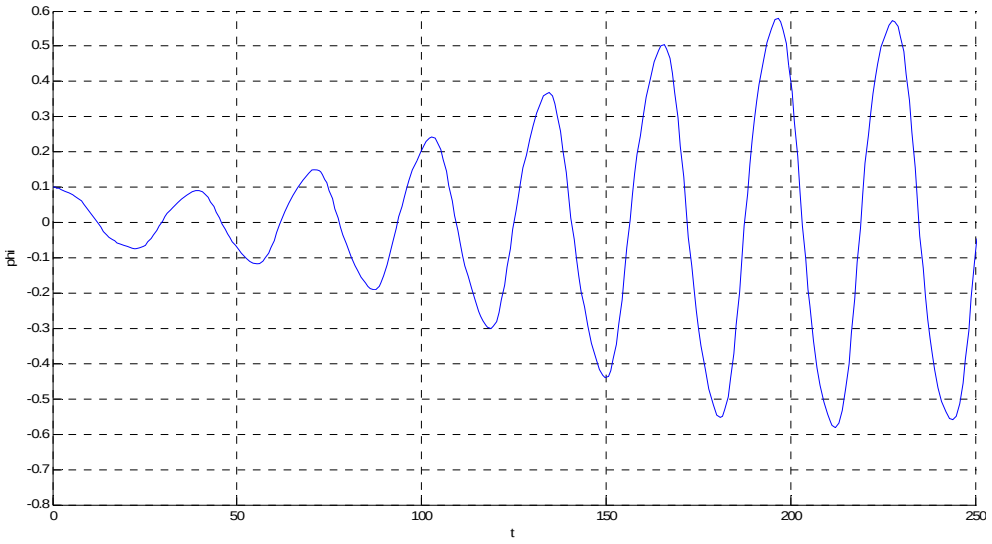

Roll only a=1.1 H=9m

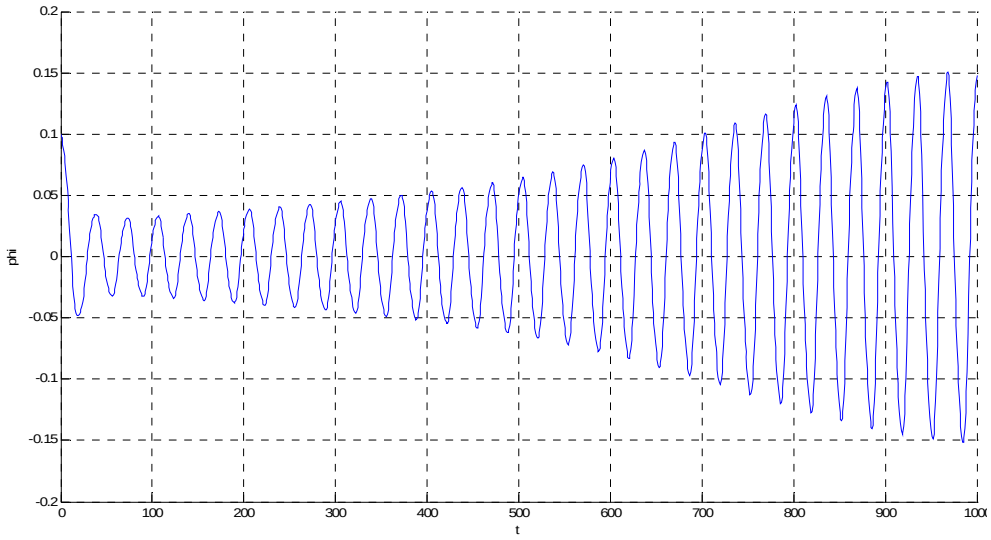

Roll only a=1.2 H=6.6m

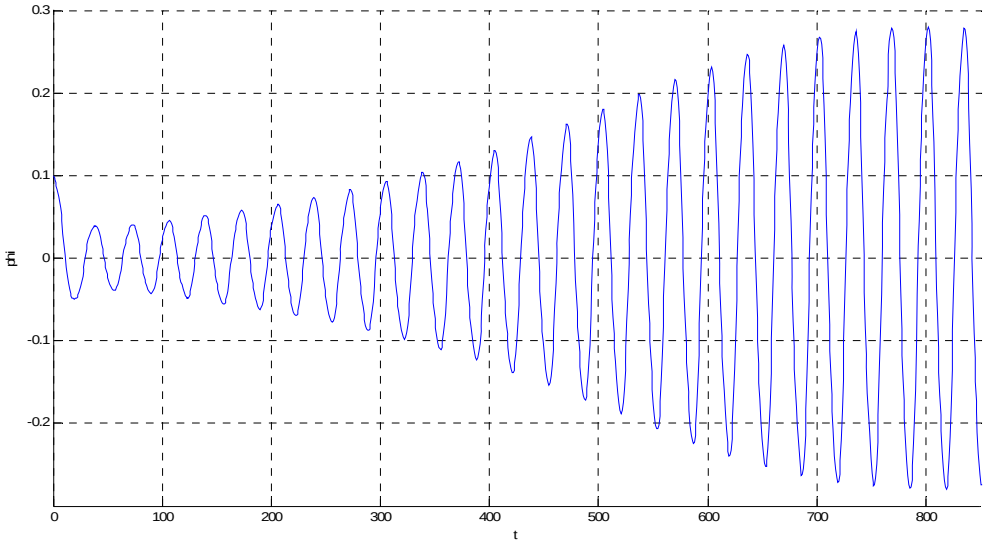

Roll only a=1.2 H=7m

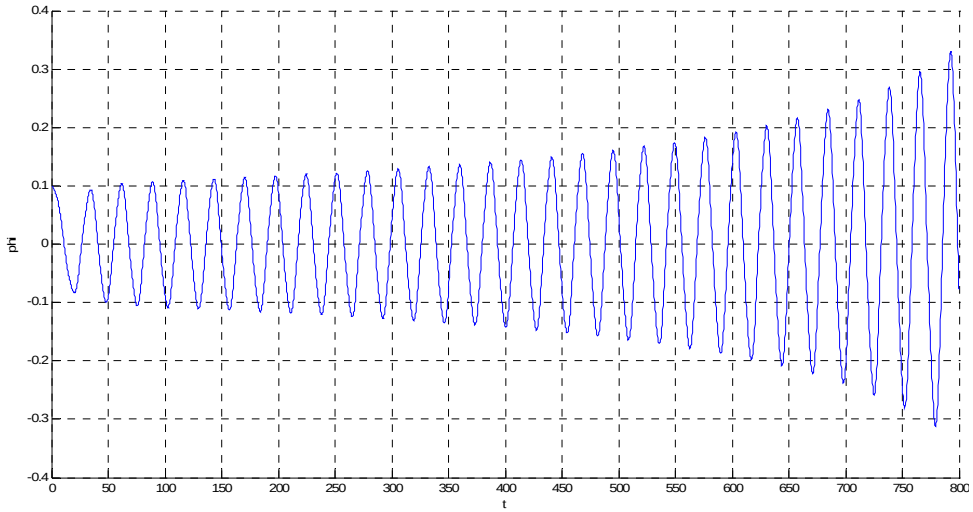

Linear Coupled a=0.8 H=8m Roll

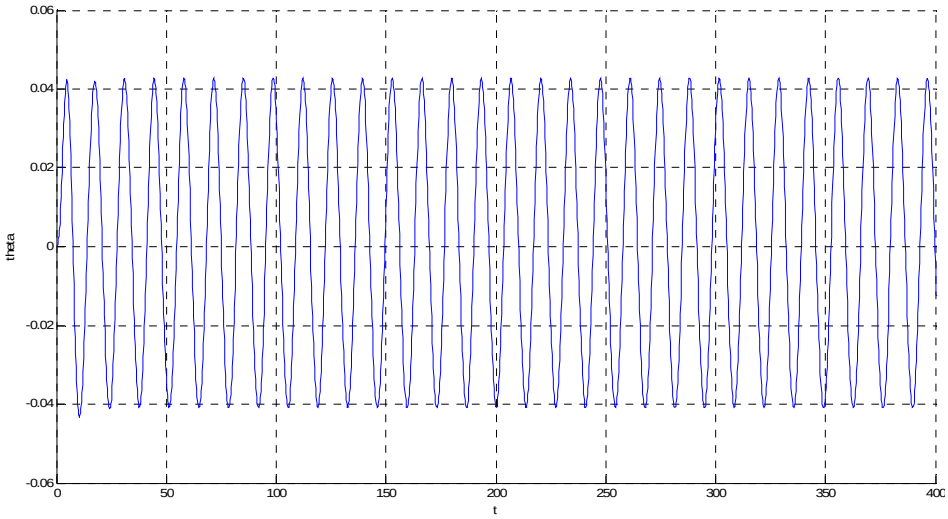

Linear Coupled a=0.8 H=8m Pitch

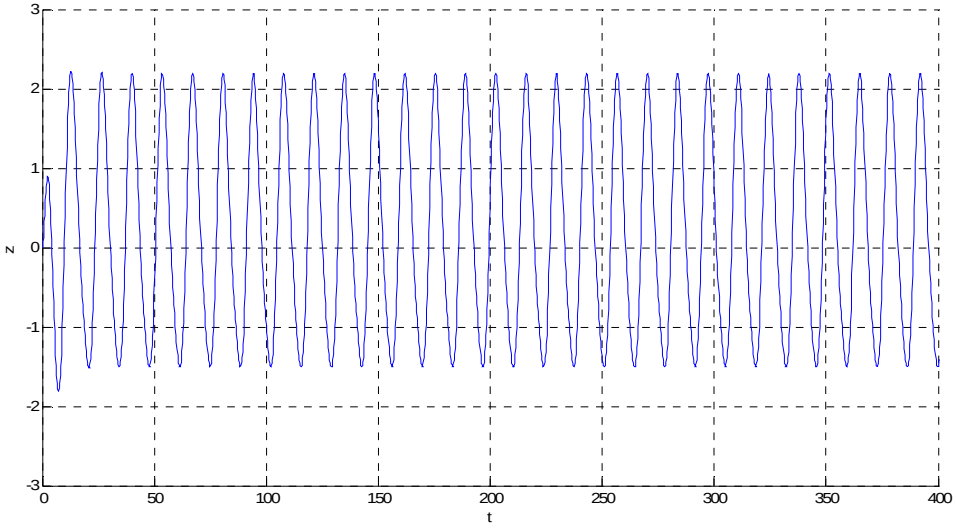

Linear Coupled a=0.8 H=8m Heave

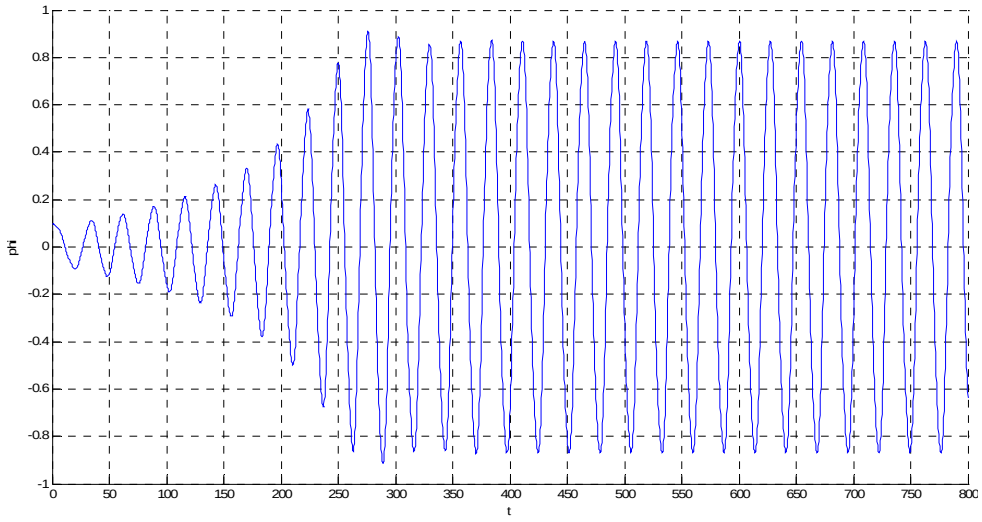

Linear Coupled a=0.8 H=9m Roll

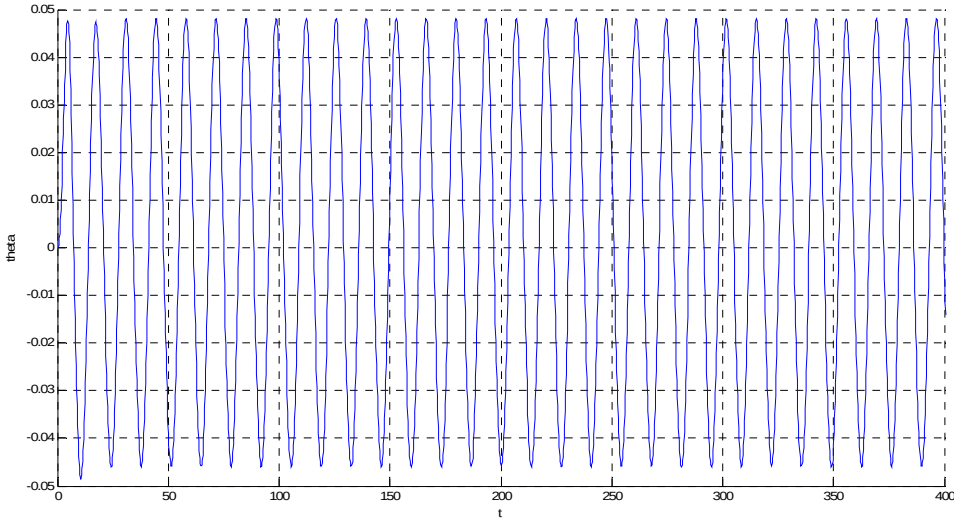

Linear Coupled a=0.8 H=9m Pitch

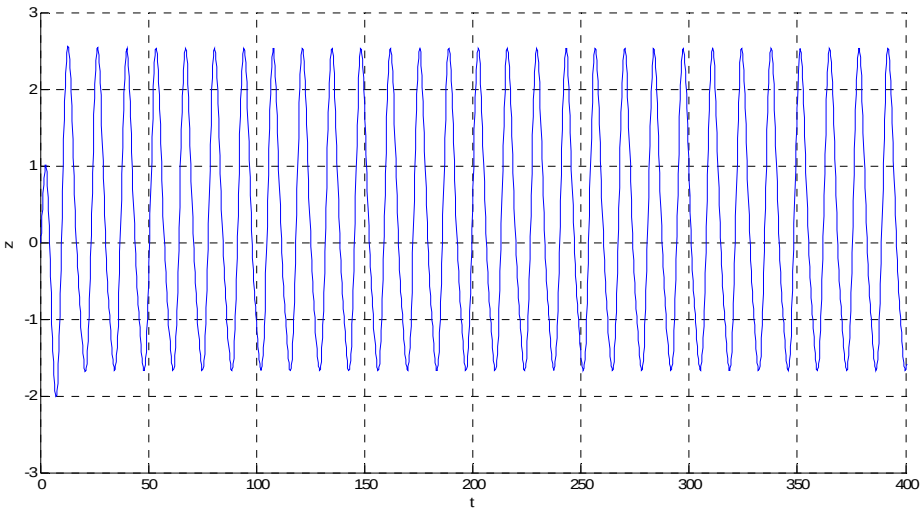

Linear Coupled a=0.8 H=9m Heave

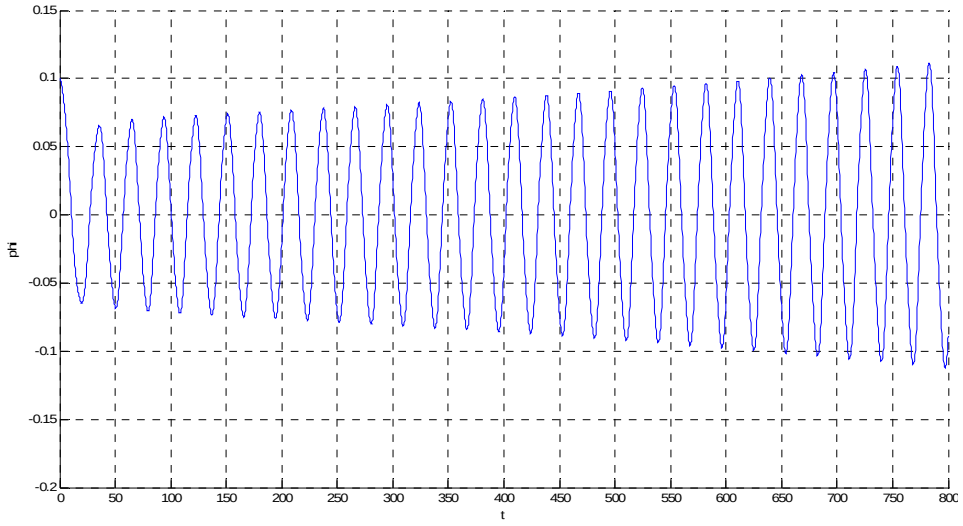

Linear Coupled a=0.9 H=6.4m Roll

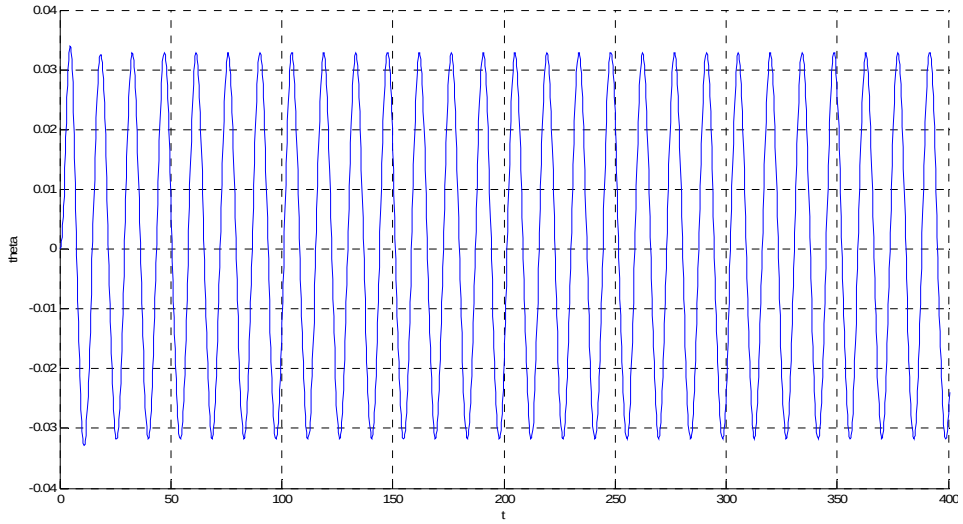

Linear Coupled a=0.9 H=6.4m Pitch

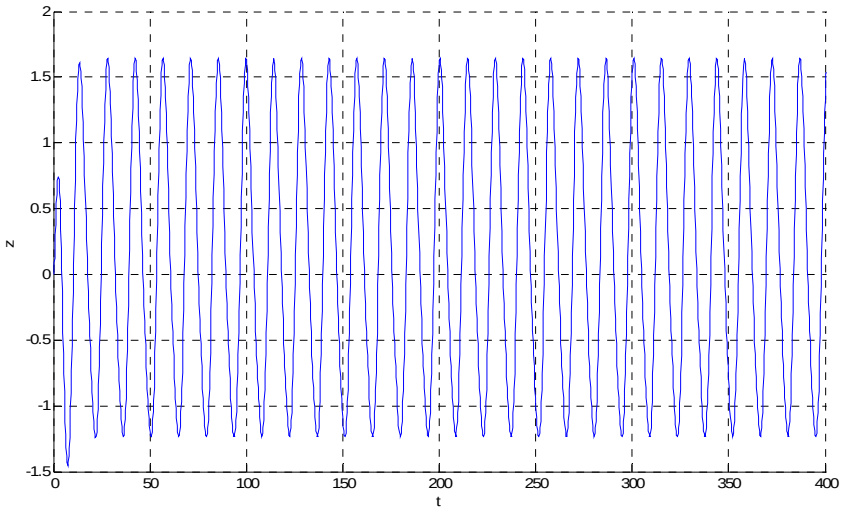

Linear Coupled a=0.9 H=6.4m Heave

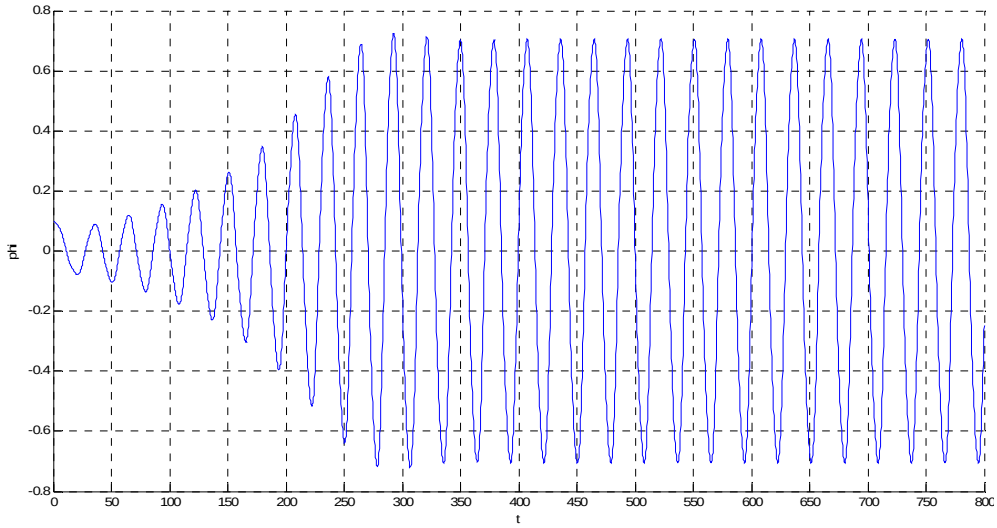

Linear Coupled a=0.9 H=8m Roll

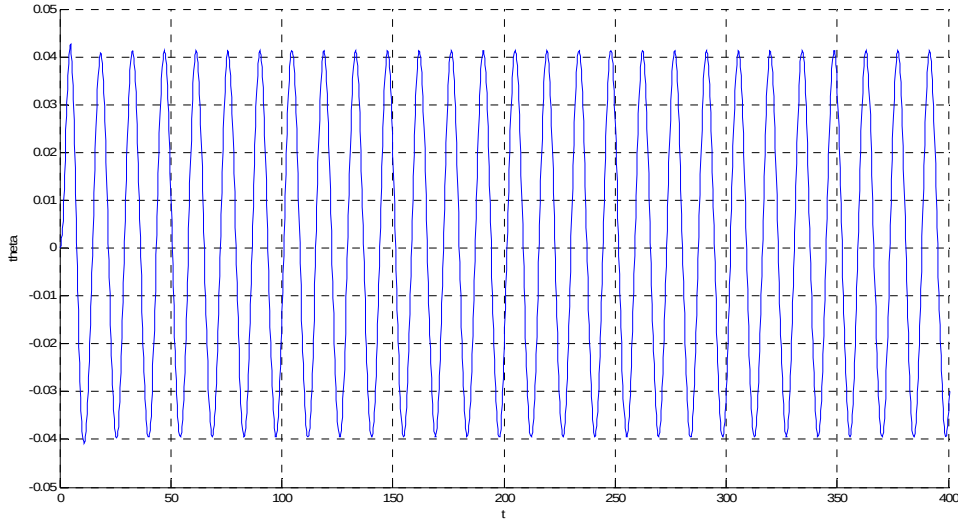

Linear Coupled a=0.9 H=8m Pitch

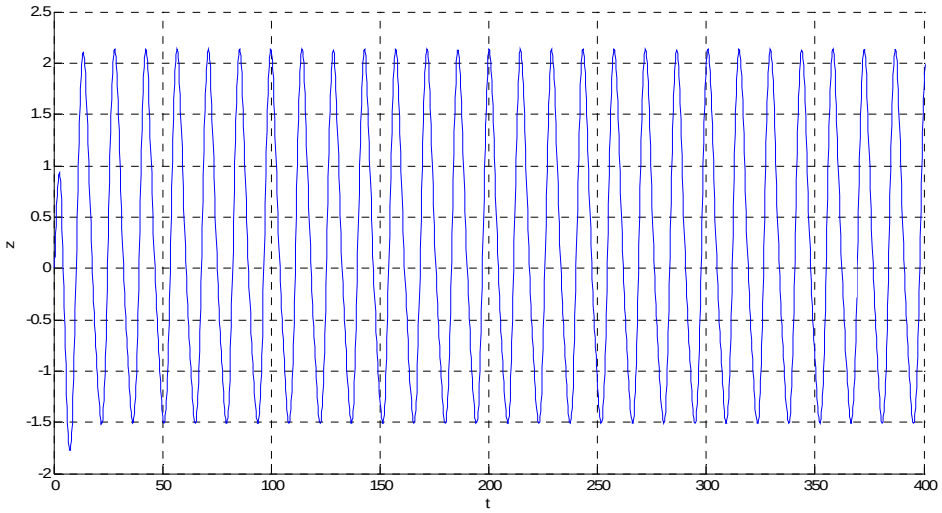

Linear Coupled a=0.9 H=8m Heave

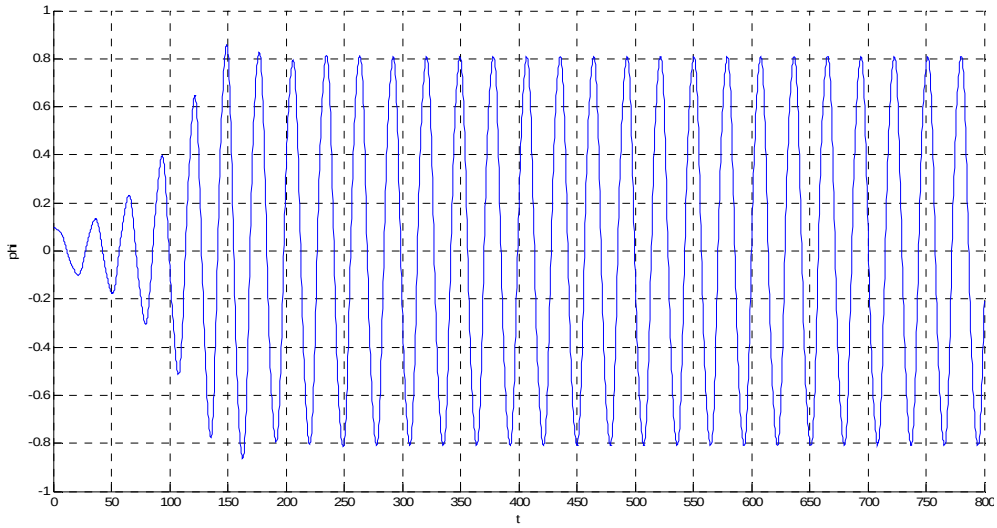

Linear Coupled a=0.9 H=10m Roll

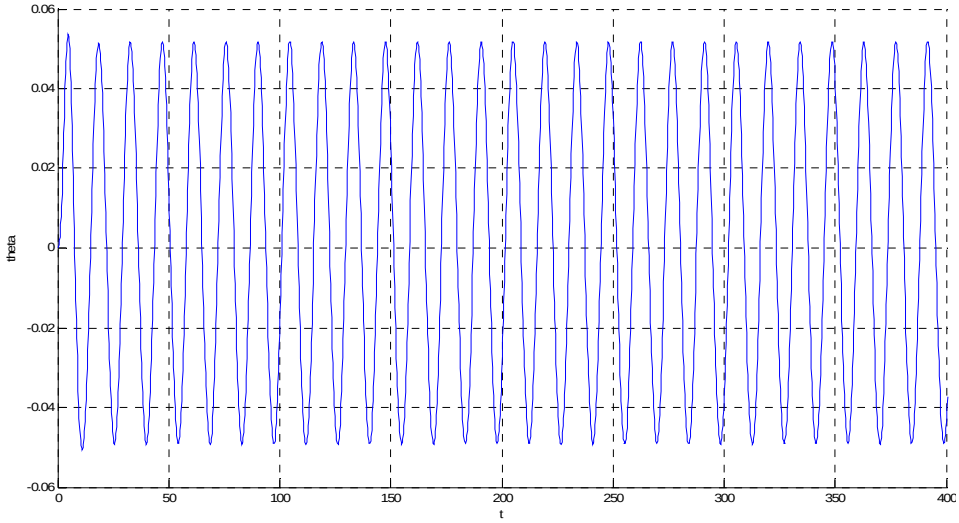

Linear Coupled a=0.9 H=10m Pitch

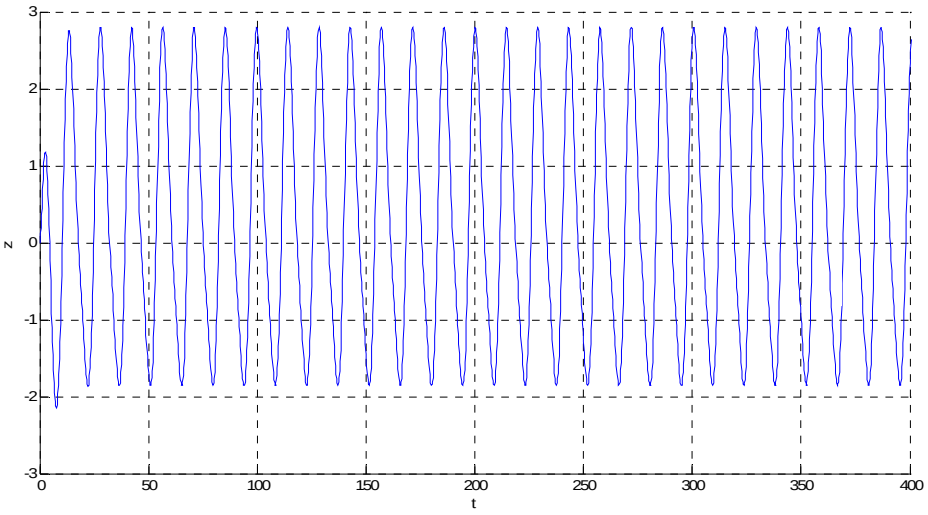

Linear Coupled a=0.9 H=10m Heave

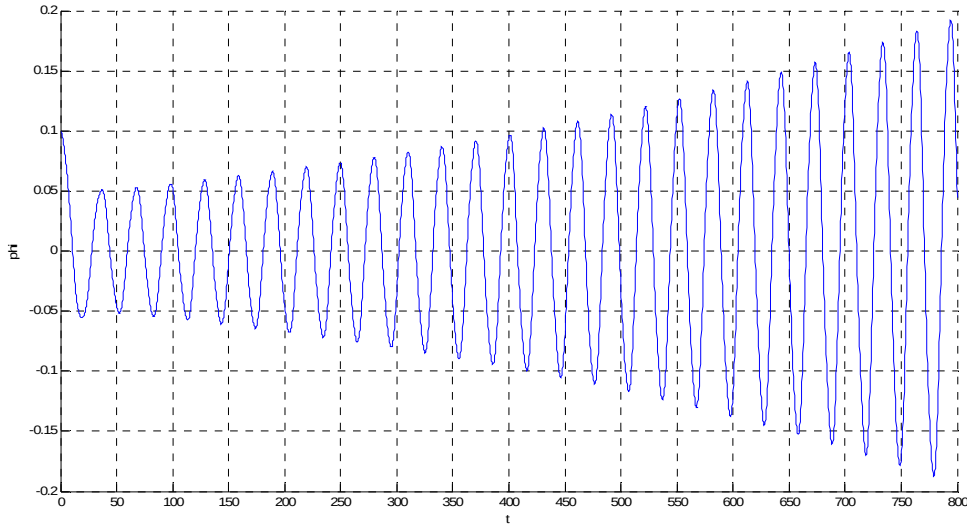

Linear Coupled a=1 H=6m Roll

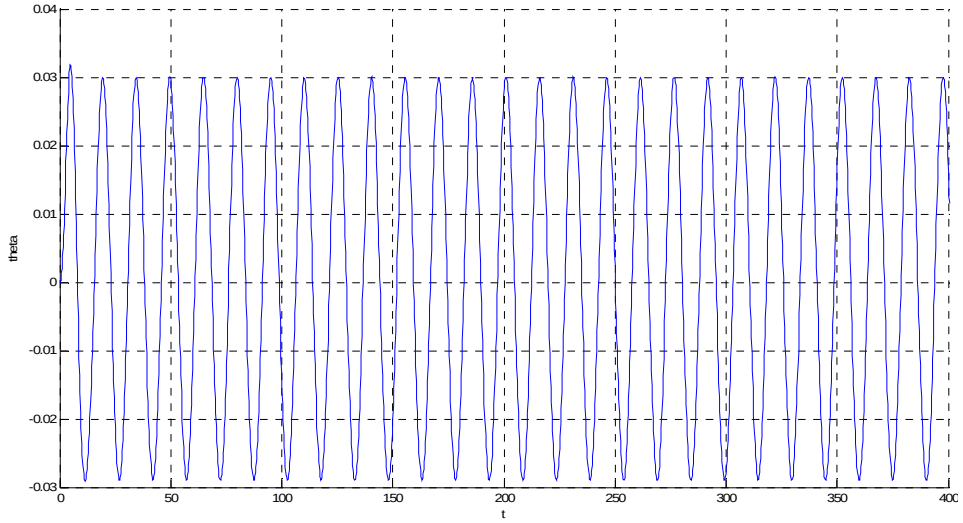

Linear Coupled a=1 H=6m Pitch

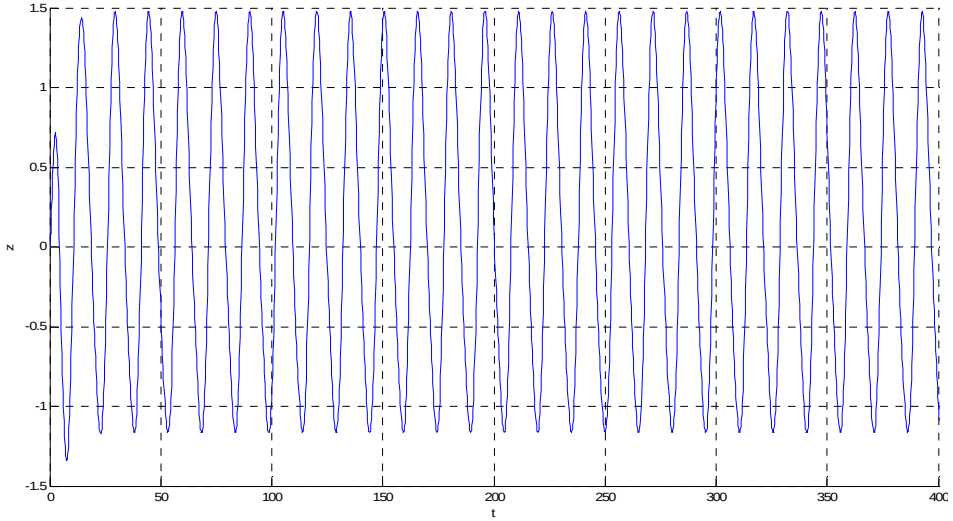

Linear Coupled a=1 H=6m Heave

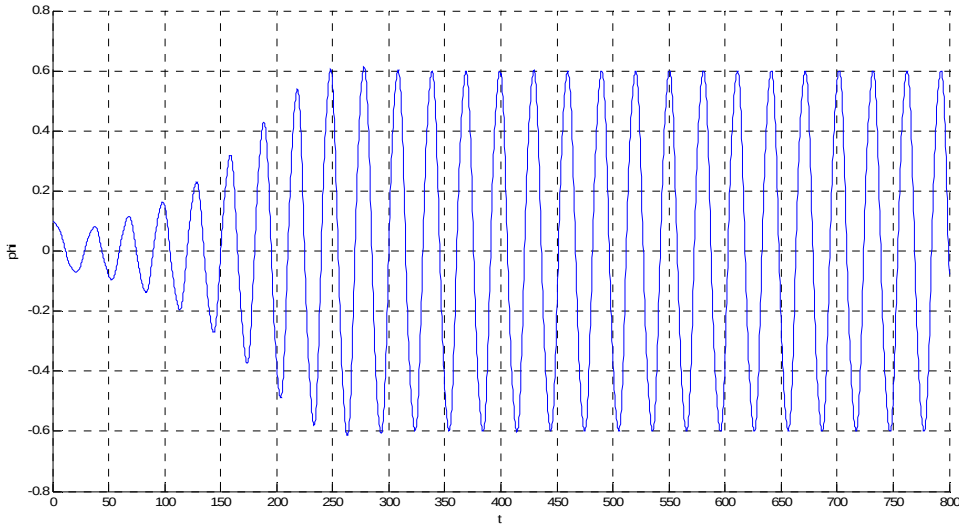

Linear Coupled a=1 H=8m Roll

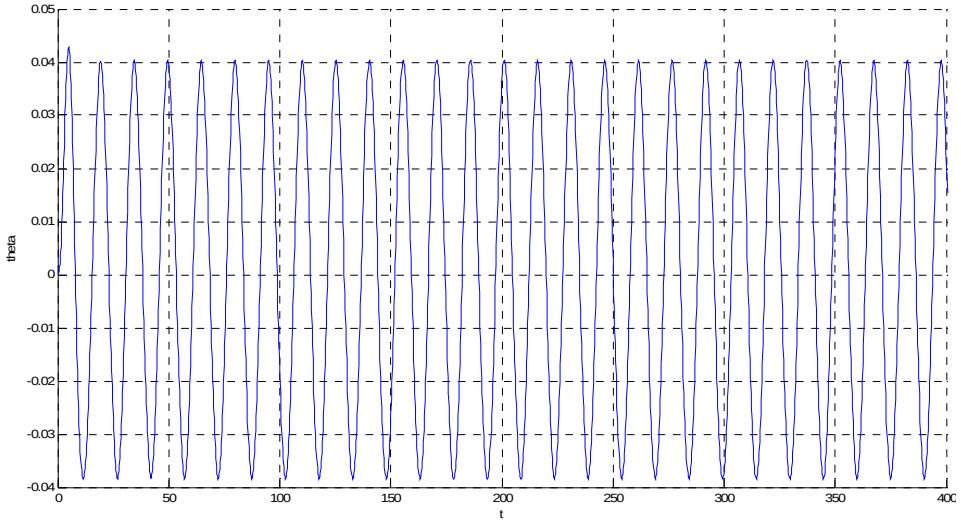

Linear Coupled a=1 H=8m Pitch

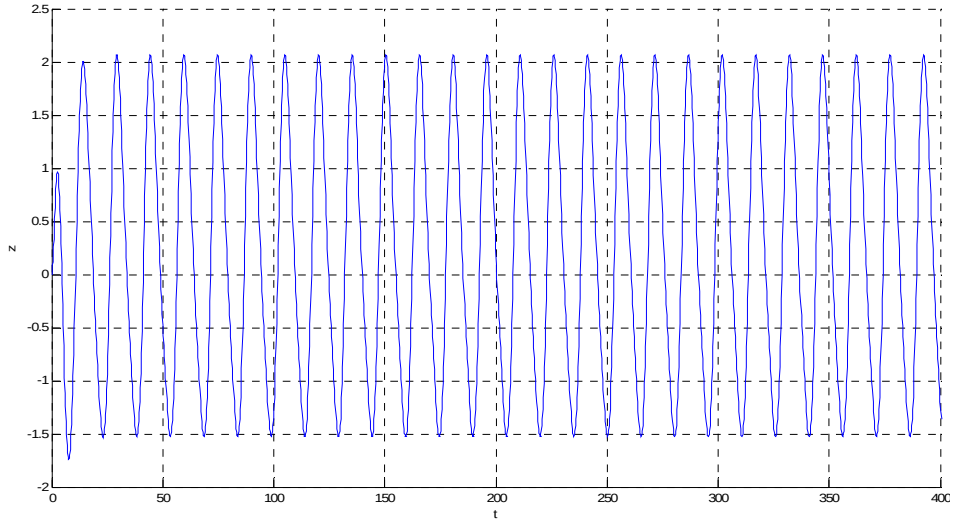

Linear Coupled a=1 H=8m Heave

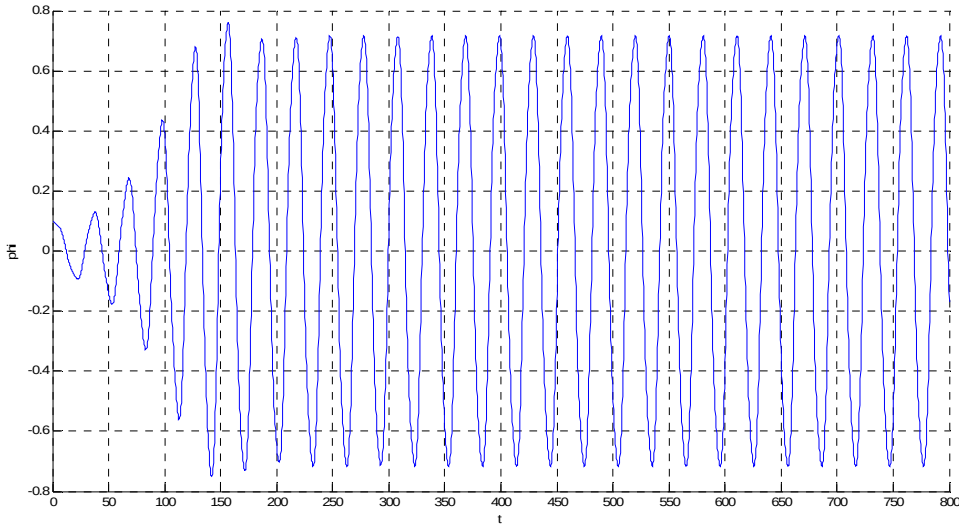

Linear Coupled a=1 H=10m Roll

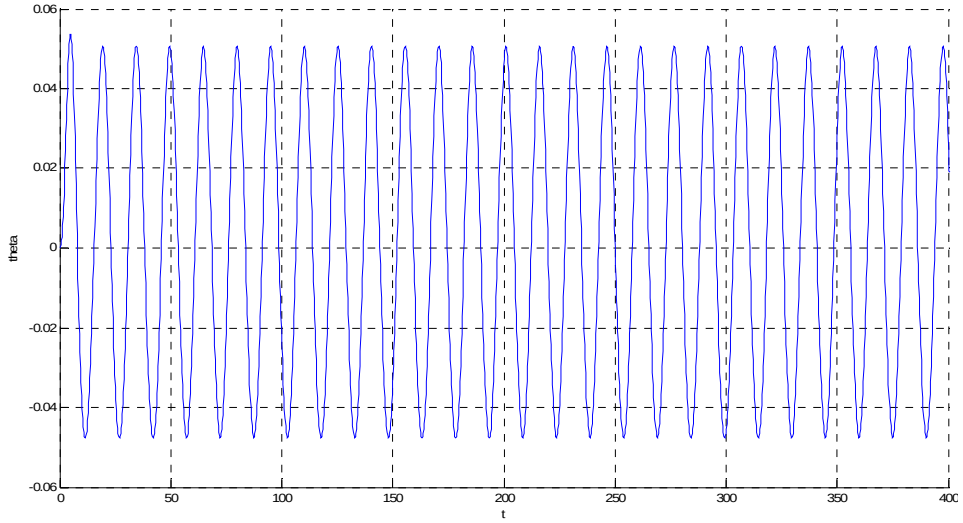

Linear Coupled a=1 H=10m Pitch

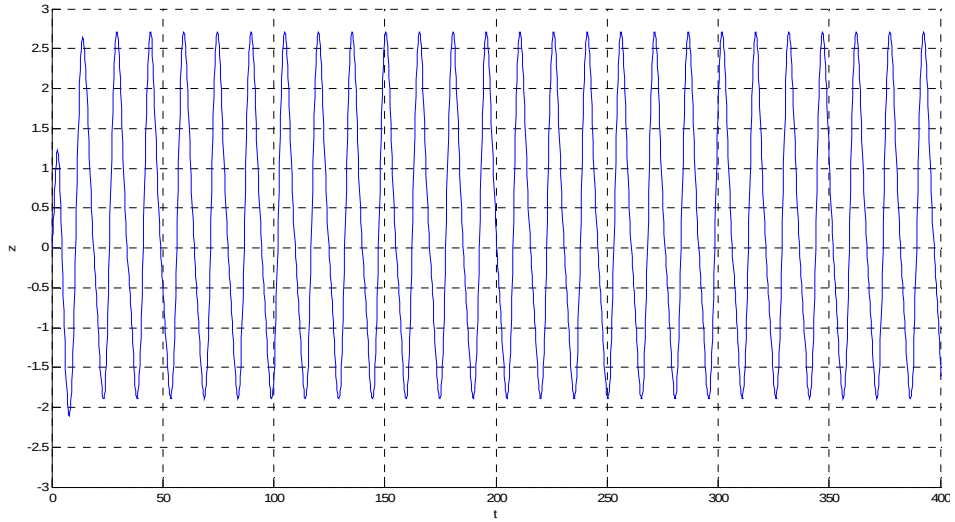

Linear Coupled a=1 H=10m Heave

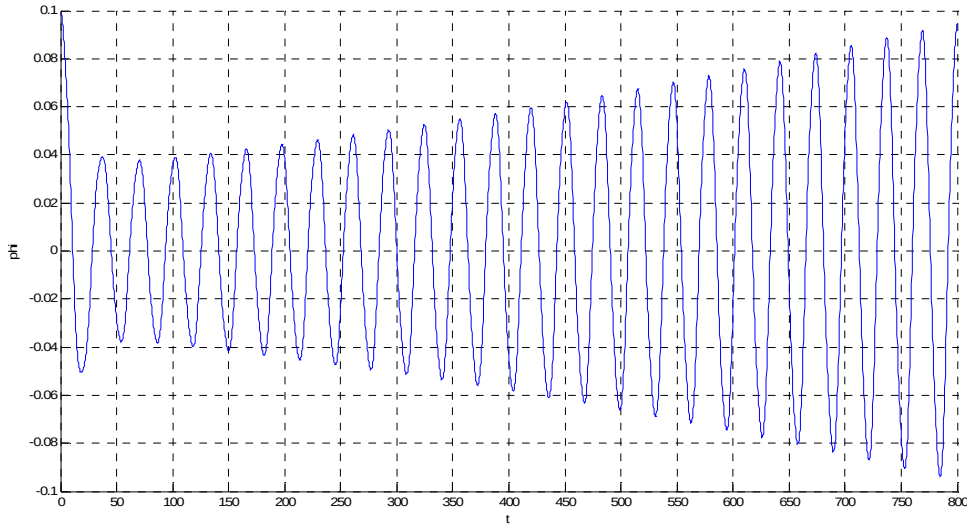

Linear Coupled a=1.1 H=6m Roll

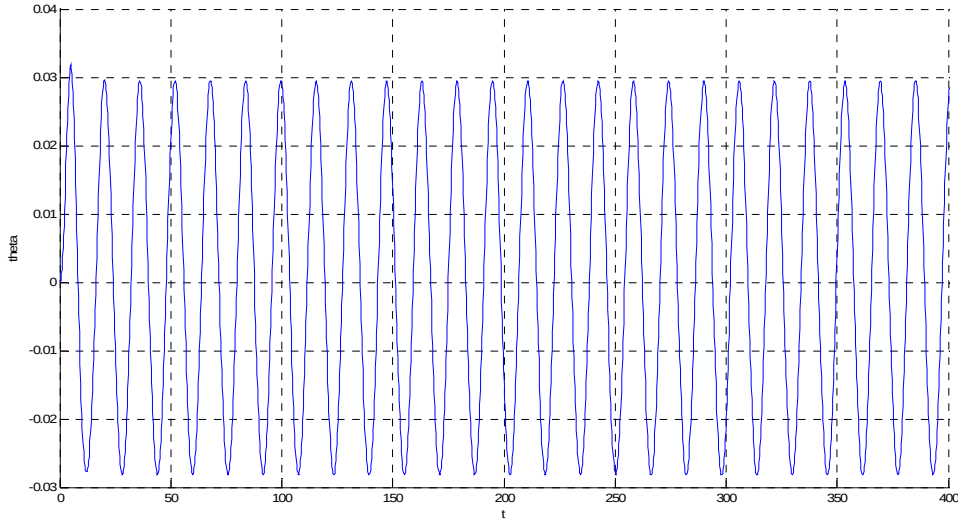

Linear Coupled a=1.1 H=6m Pitch

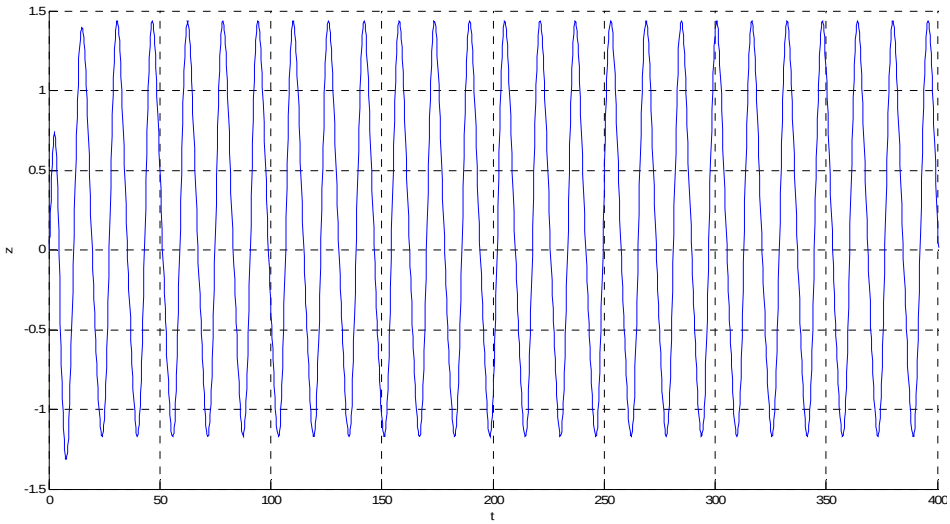

Linear Coupled a=1.1 H=6m Heave

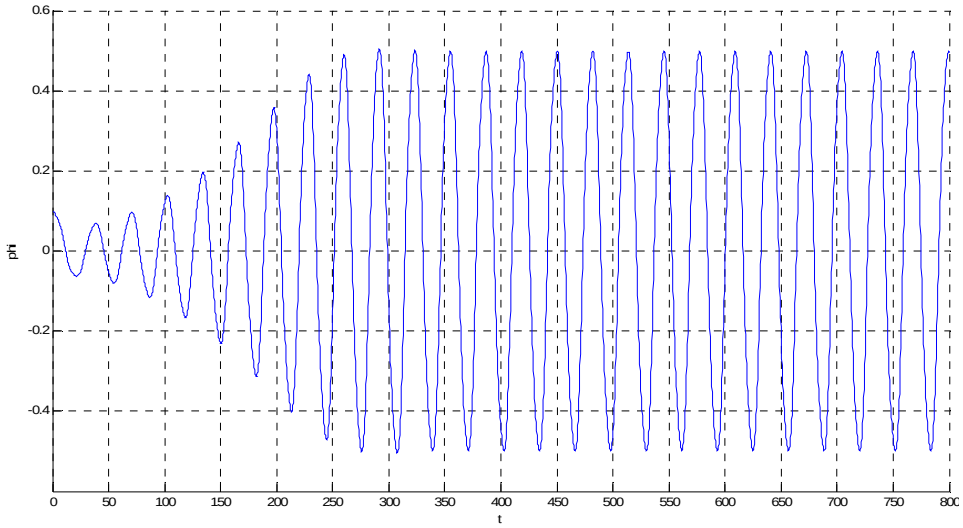

Linear Coupled a=1.1 H=8m Roll

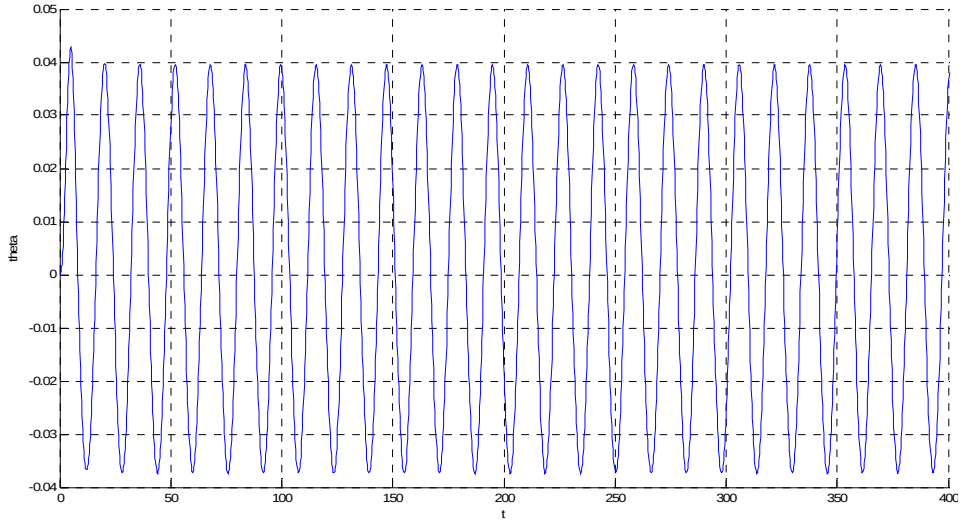

Linear Coupled a=1.1 H=8m Pitch

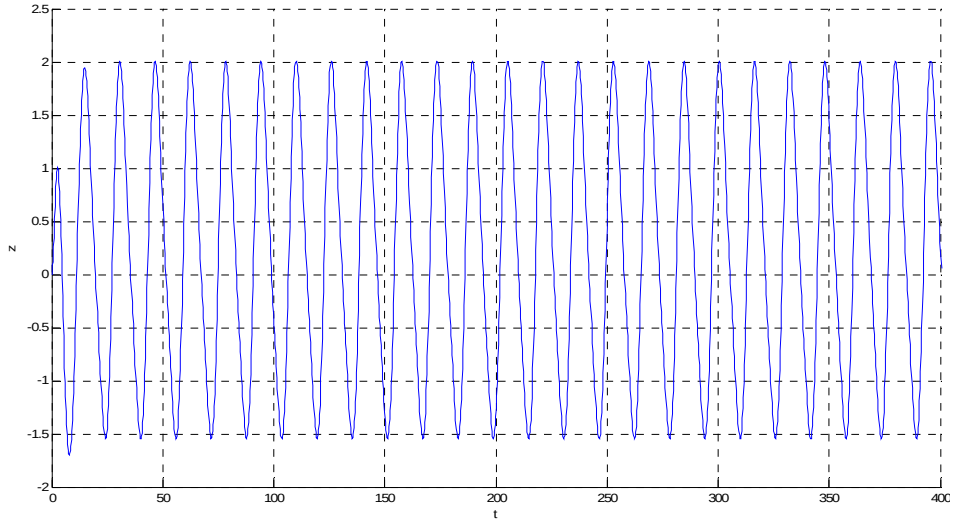

Linear Coupled a=1.1 H=8m Heave

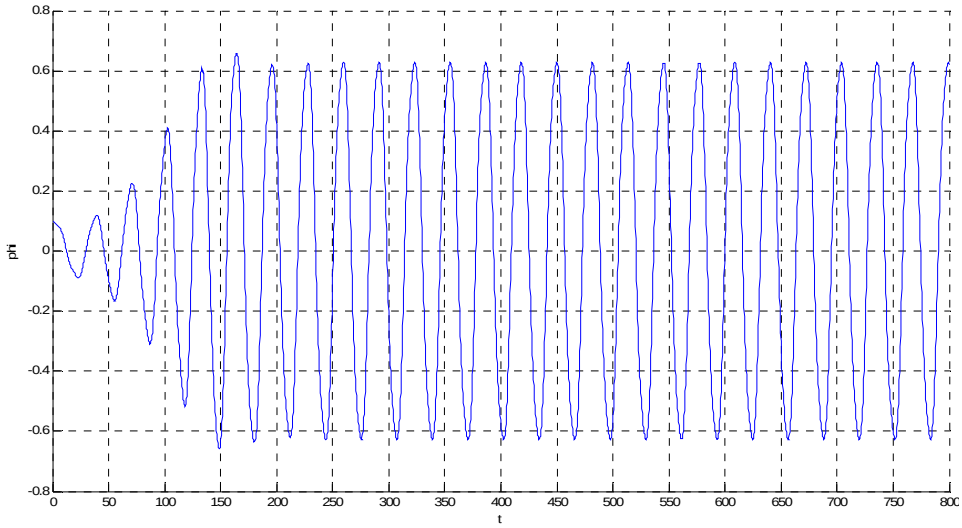

Linear Coupled a=1.1 H=10m Roll

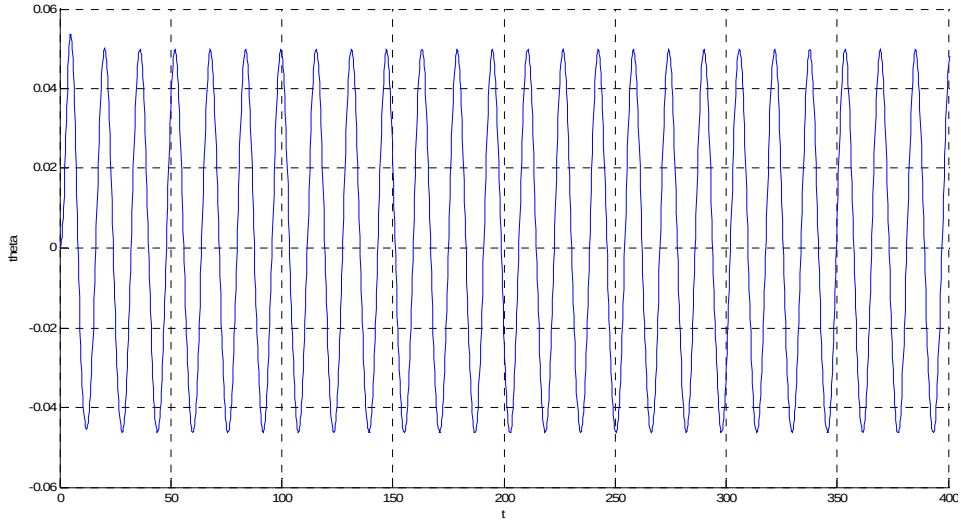

Linear Coupled a=1.1 H=10m Pitch

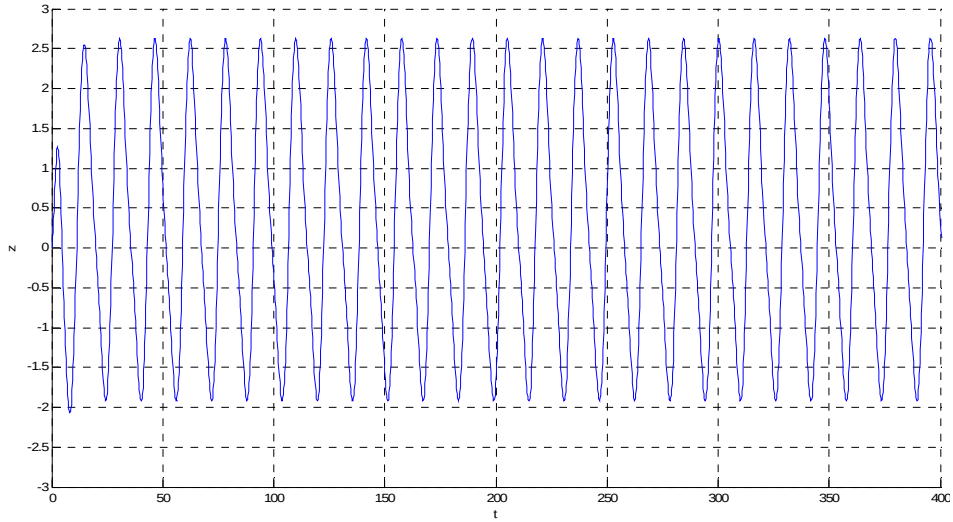

Linear Coupled a=1.1 H=10m Heave

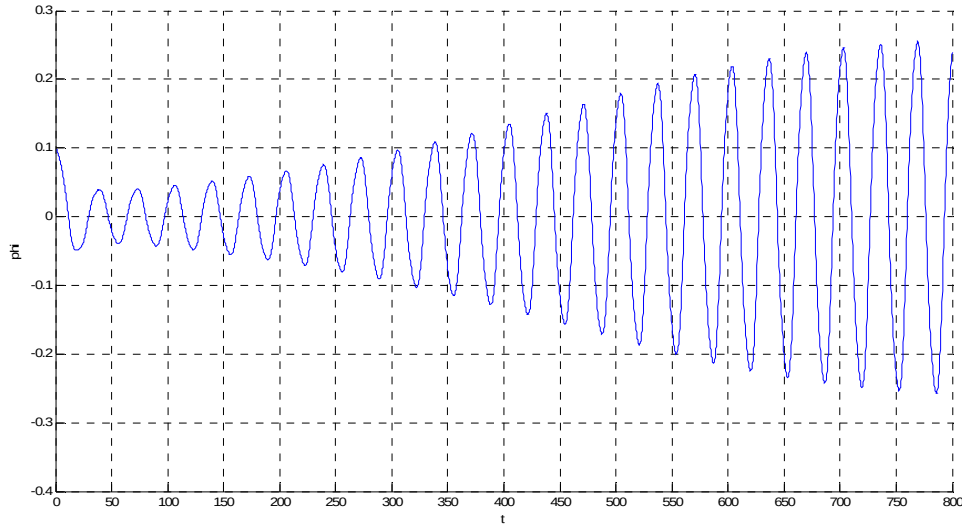

Linear Coupled a=1.2 H=7m Roll

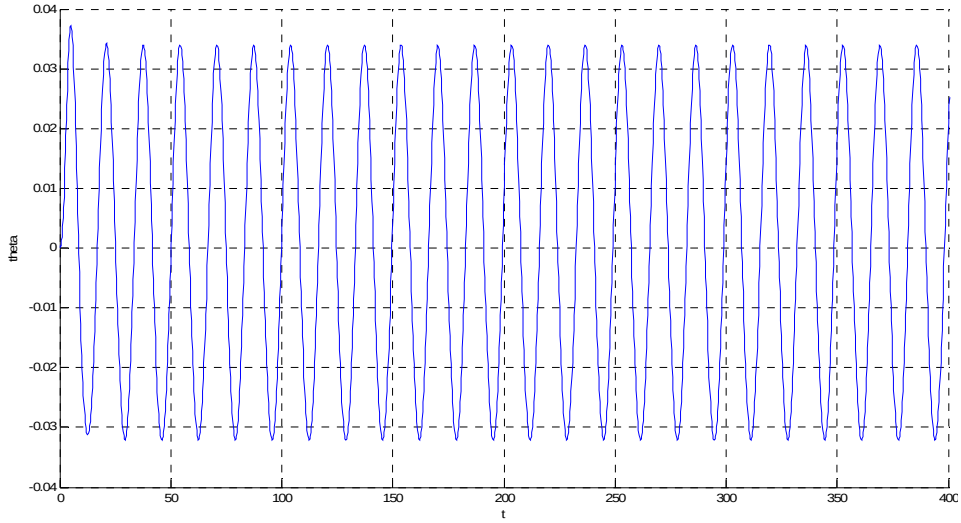

Linear Coupled a=1.2 H=7m Pitch

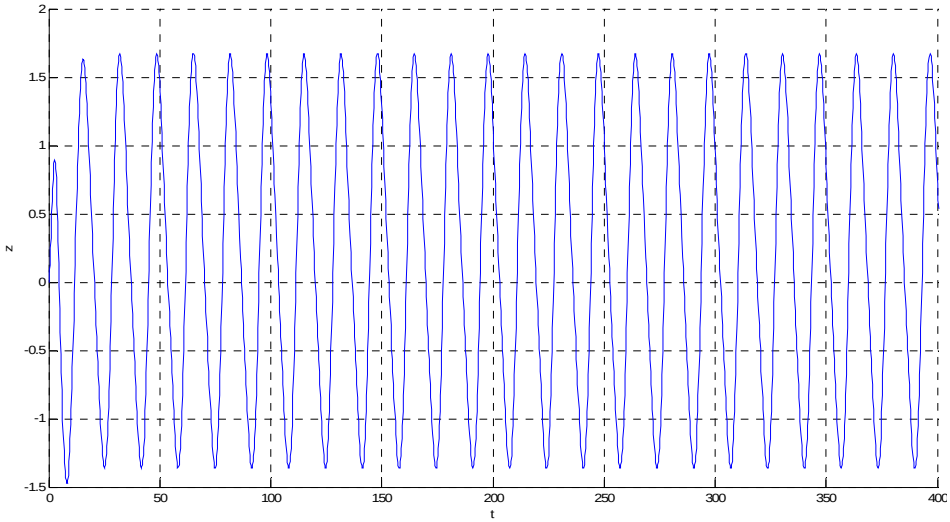

Linear Coupled a=1.2 H=7m Heave

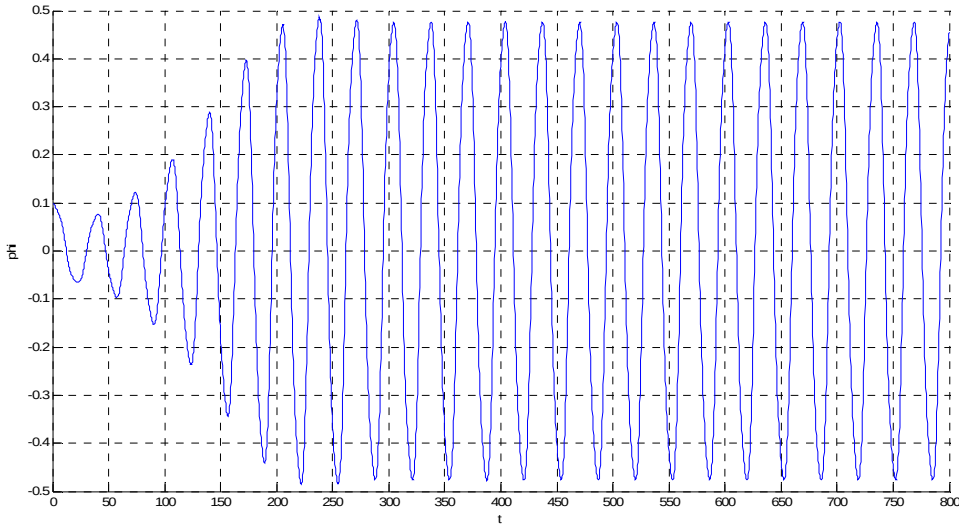

Linear Coupled a=1.2 H=9m Roll

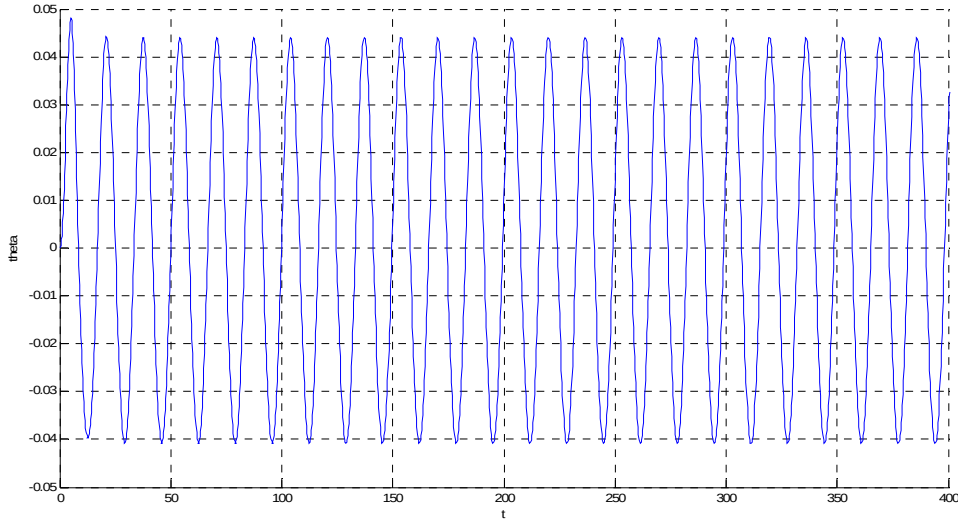

Linear Coupled a=1.2 H=9m Pitch

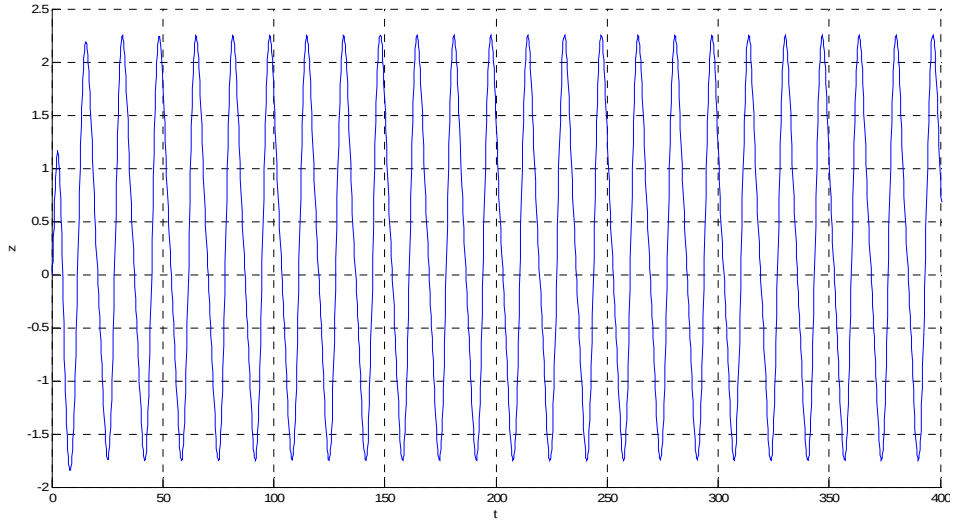

Linear Coupled a=1.2 H=9m Heave

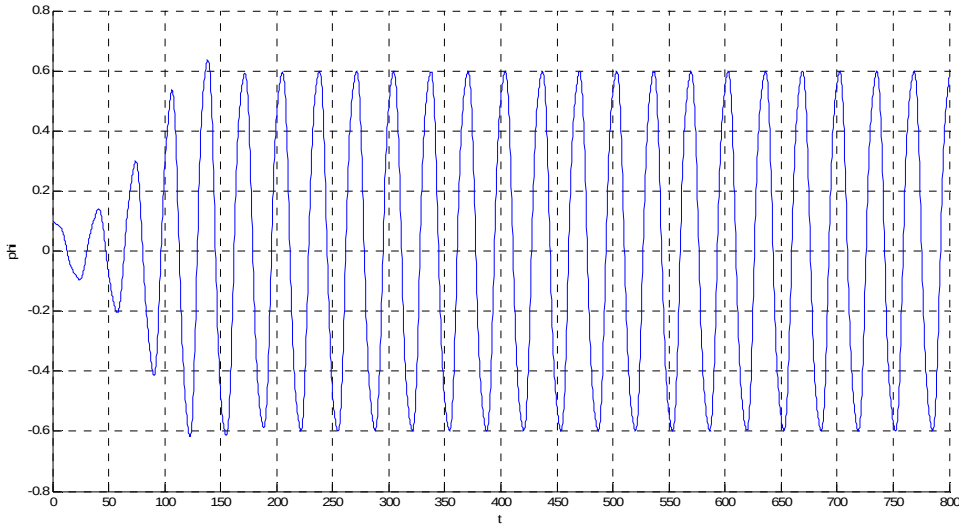

Linear Coupled a=1.2 H=11m Roll

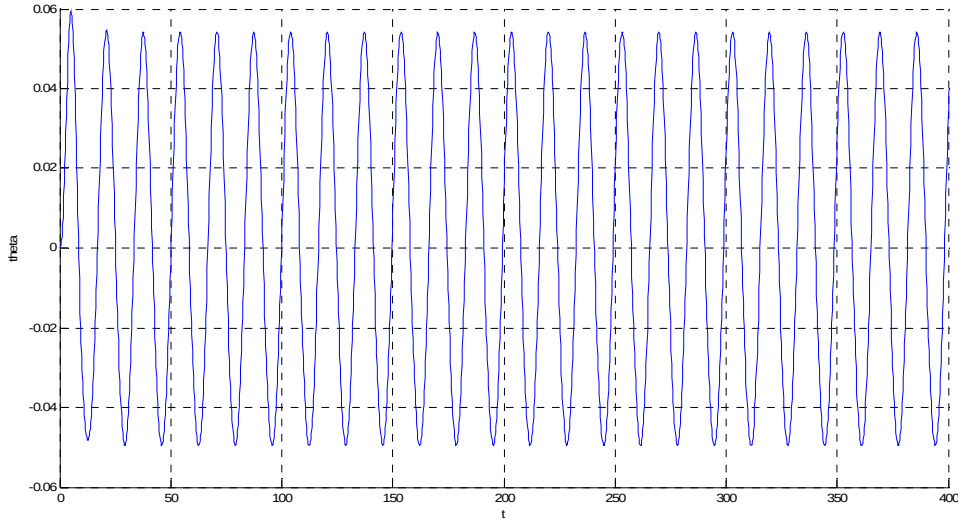

Linear Coupled a=1.2 H=11m Pitch

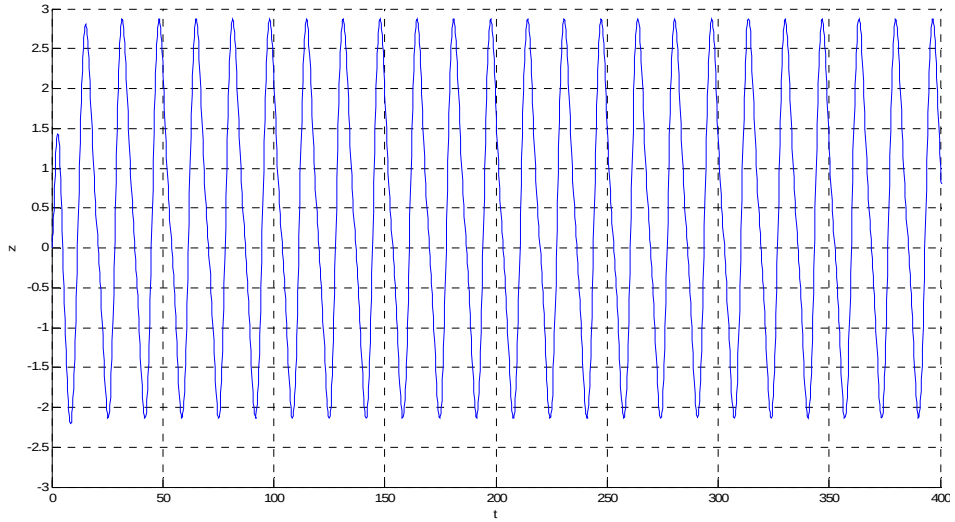

Linear Coupled a=1.2 H=11m Heave

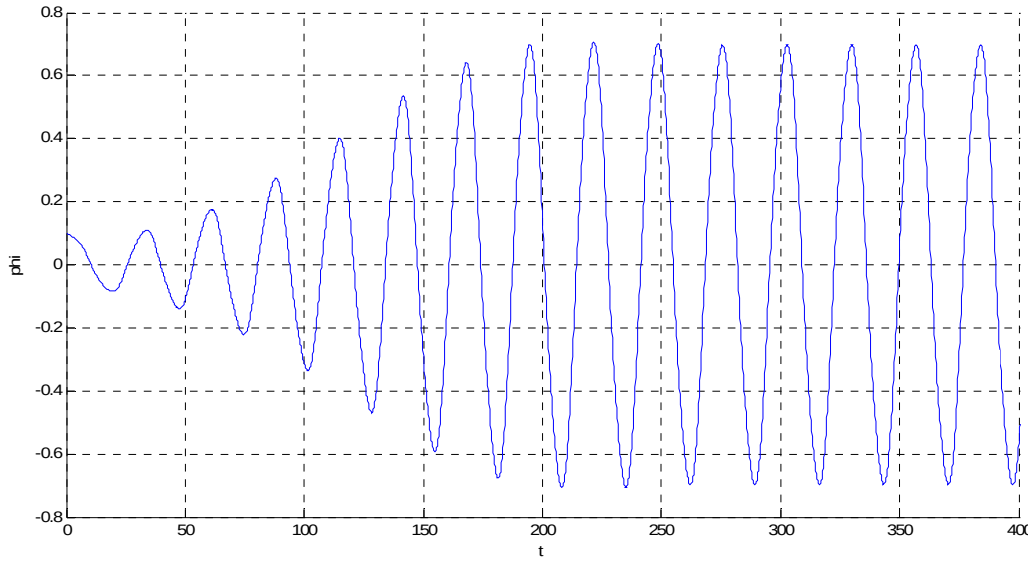

Full Coupled a=0.8 H=4m Roll

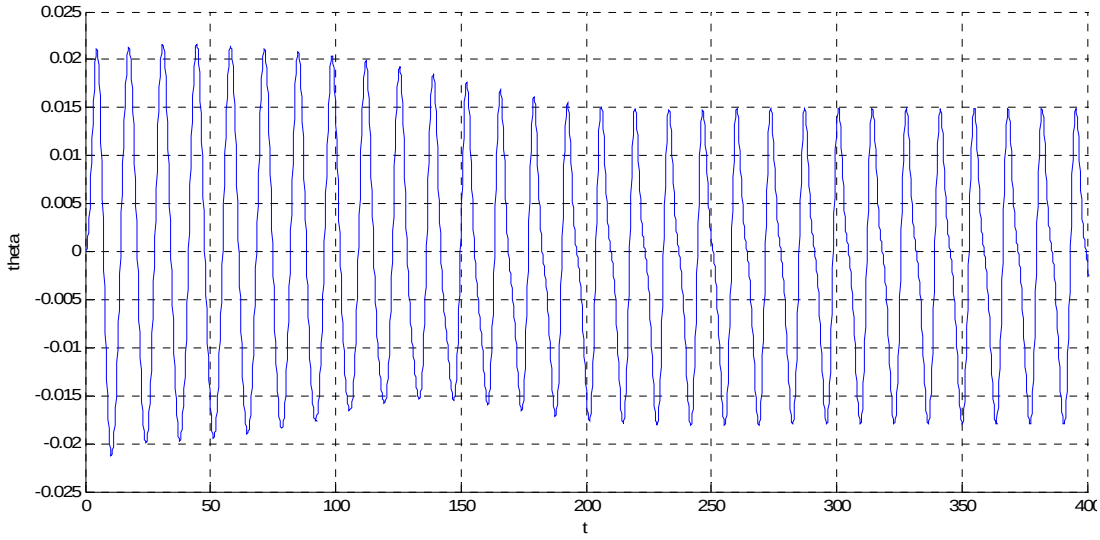

Full Coupled a=0.8 H=4m Pitch

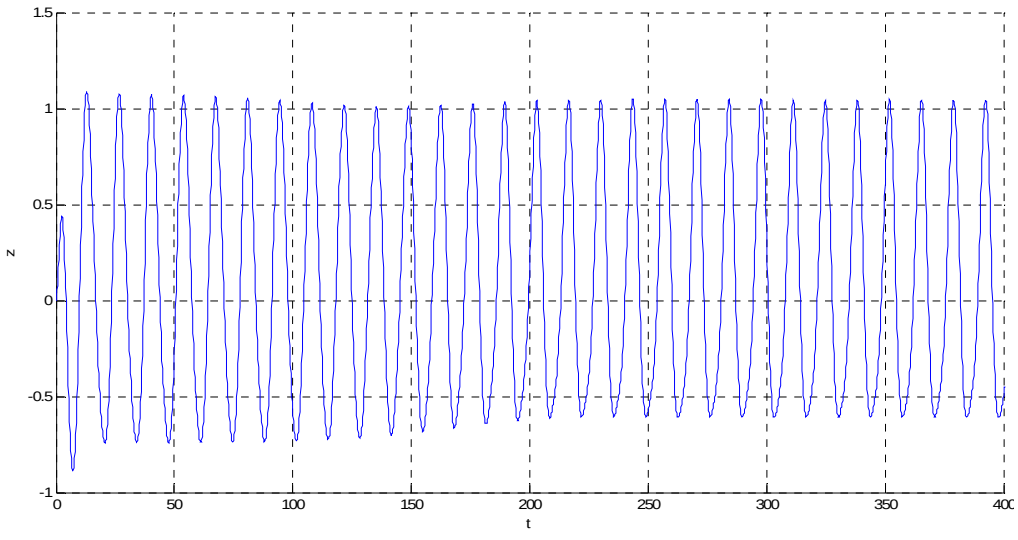

Full Coupled a=0.8 H=4m Heave

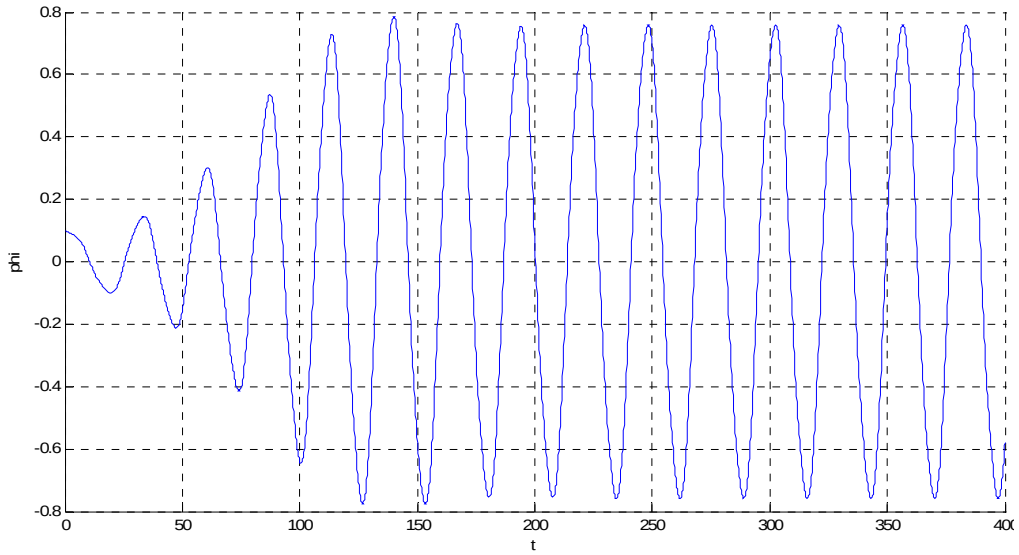

Full Coupled a=0.8 H=5m Roll

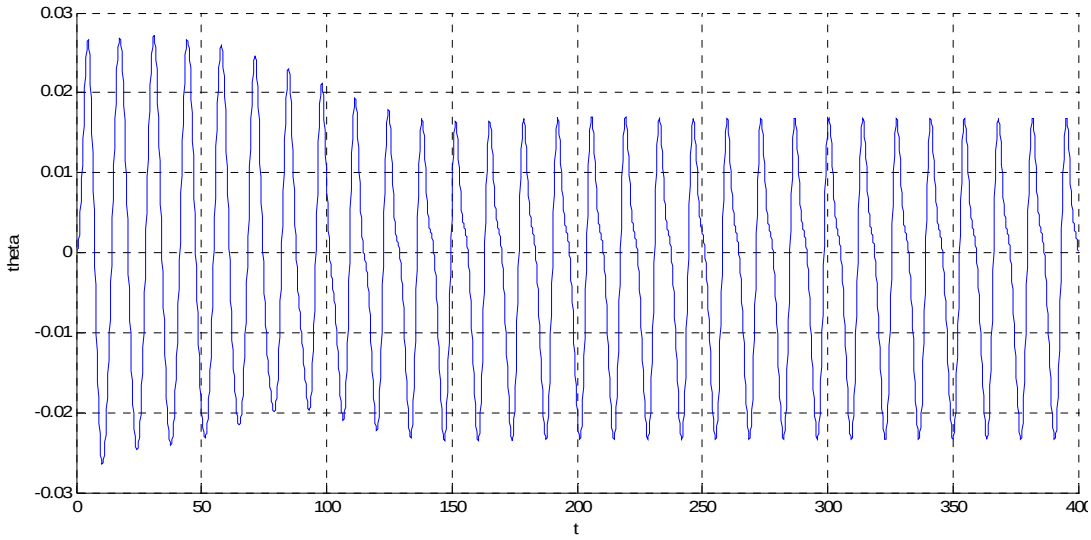

Full Coupled a=0.8 H=5m Pitch

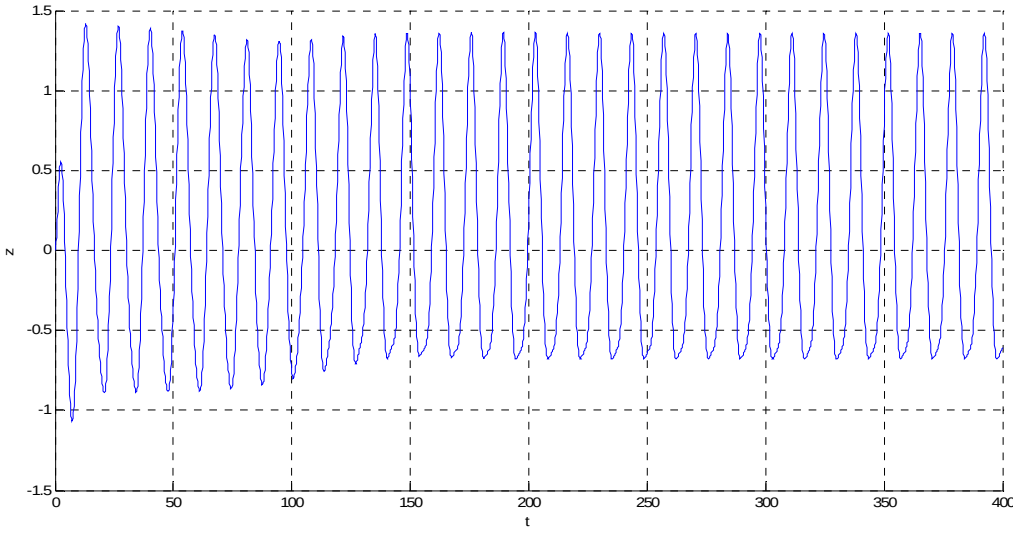

Full Coupled a=0.8 H=5m Heave

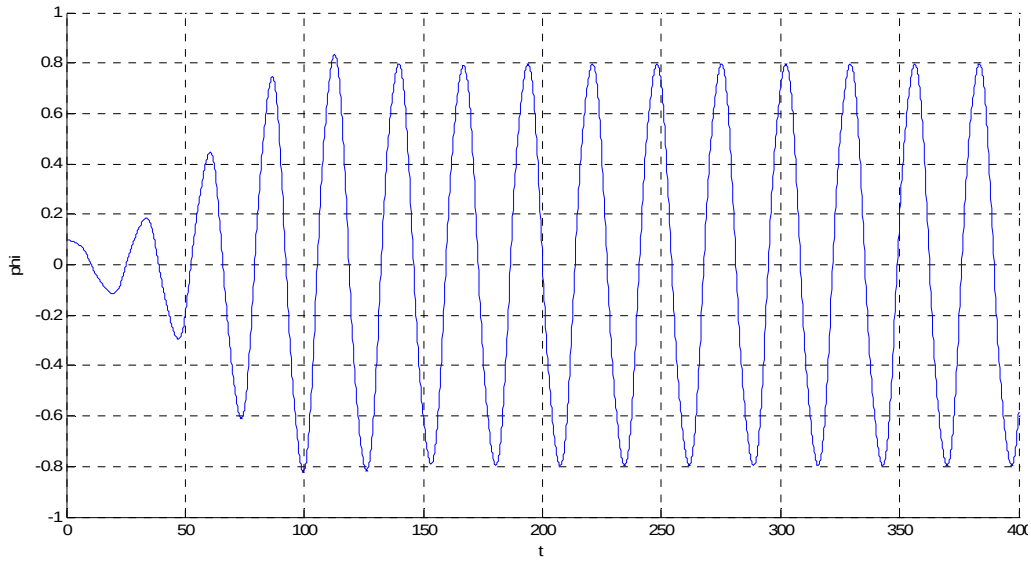

Full Coupled a=0.8 H=6m Roll

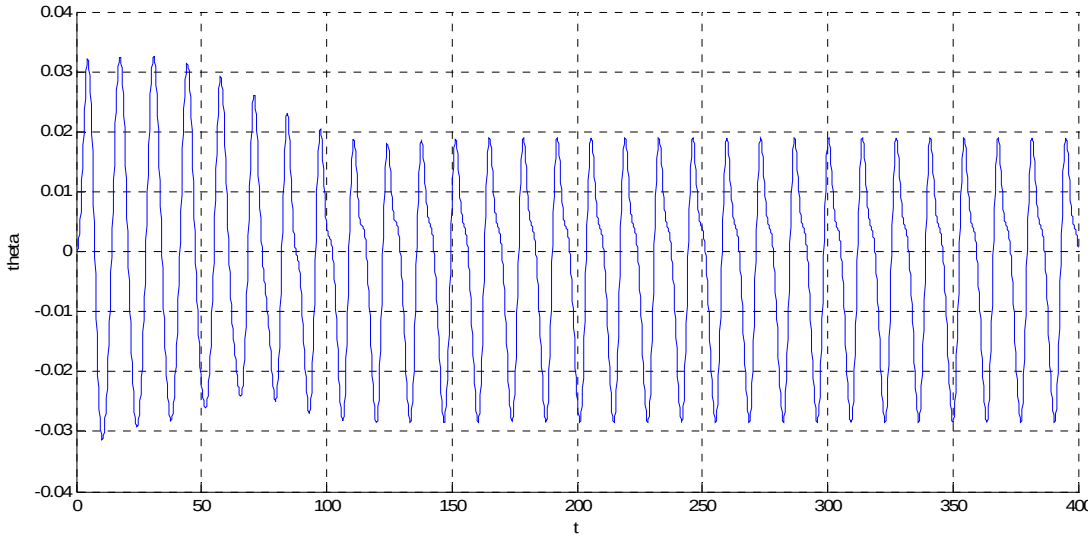

Full Coupled a=0.8 H=6m Pitch

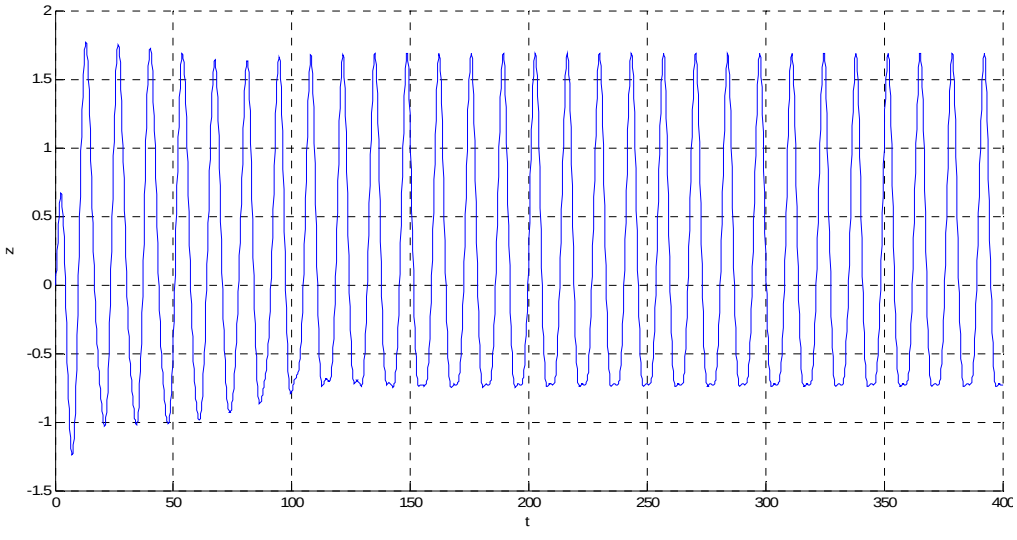

Full Coupled a=0.8 H=6m Heave

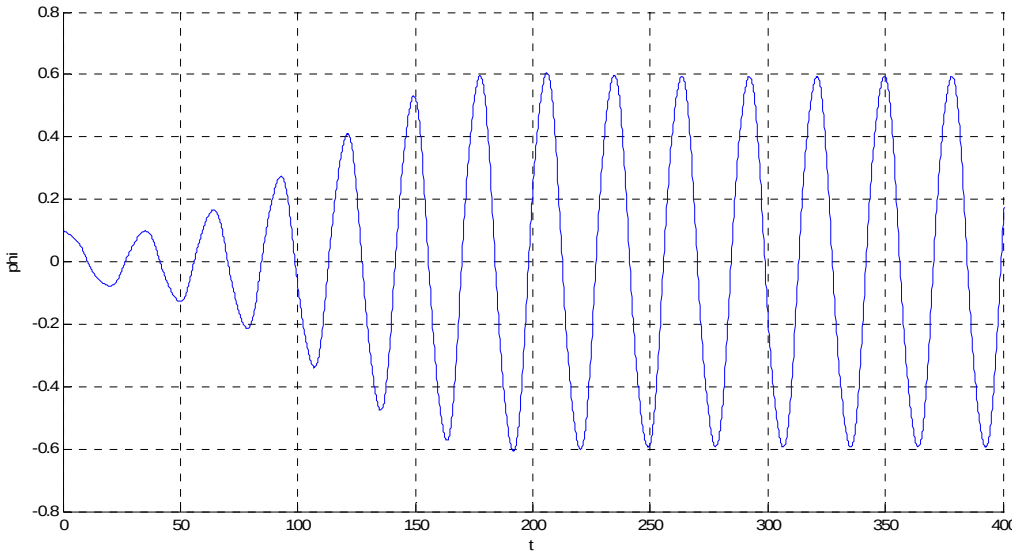

Full Coupled a=0.9 H=4m Roll

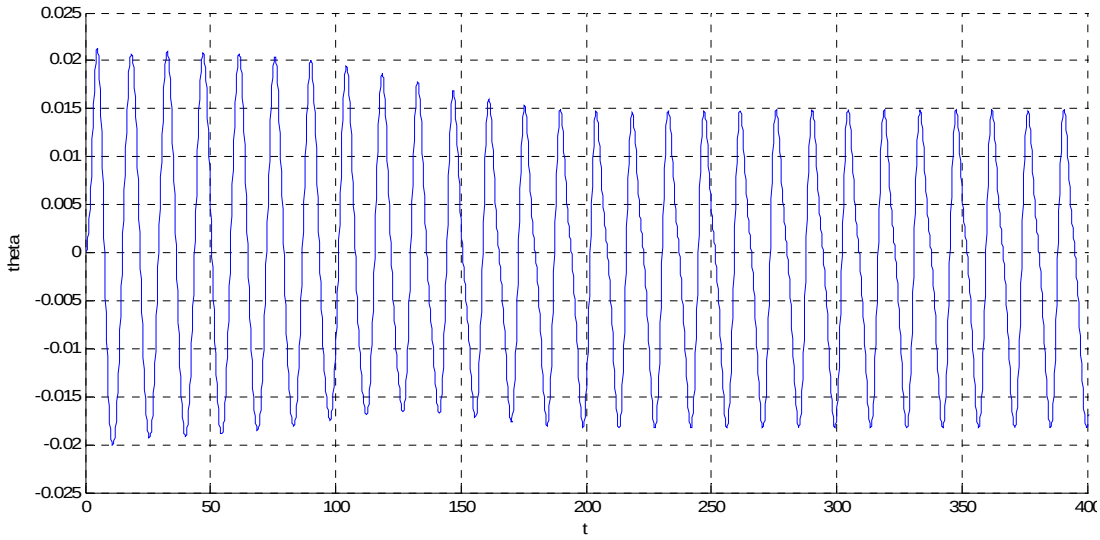

Full Coupled a=0.9 H=4m Pitch

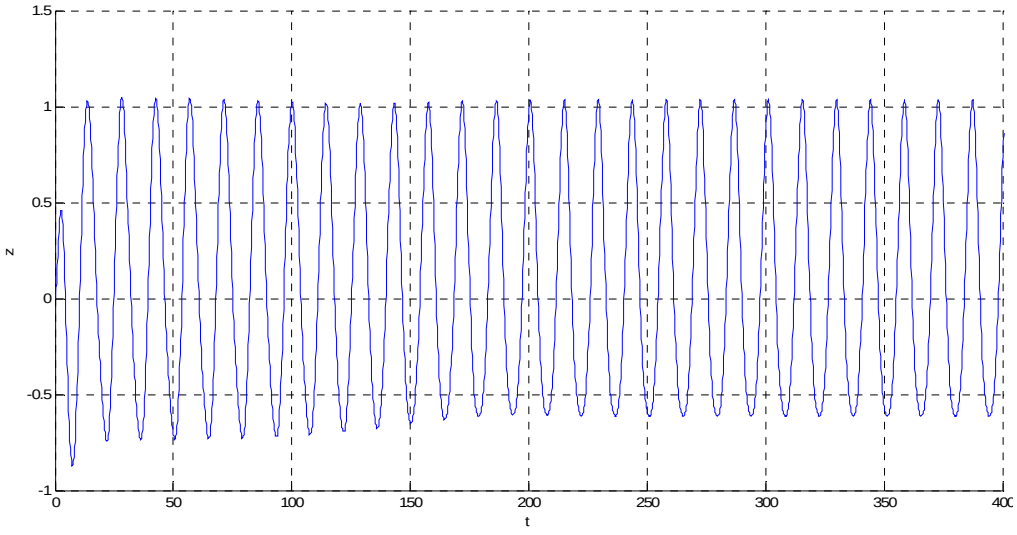

Full Coupled a=0.9 H=4m Heave

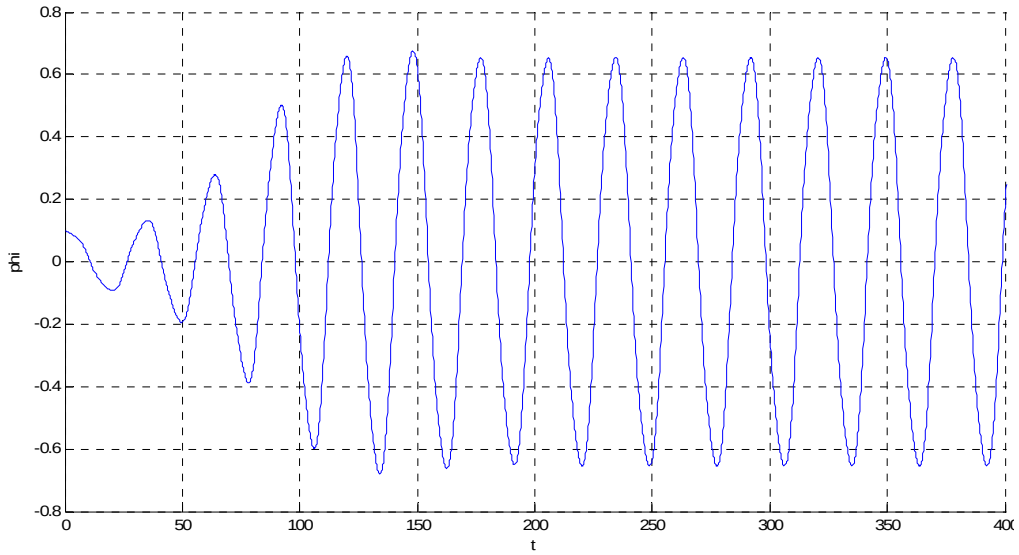

Full Coupled a=0.9 H=5m Roll

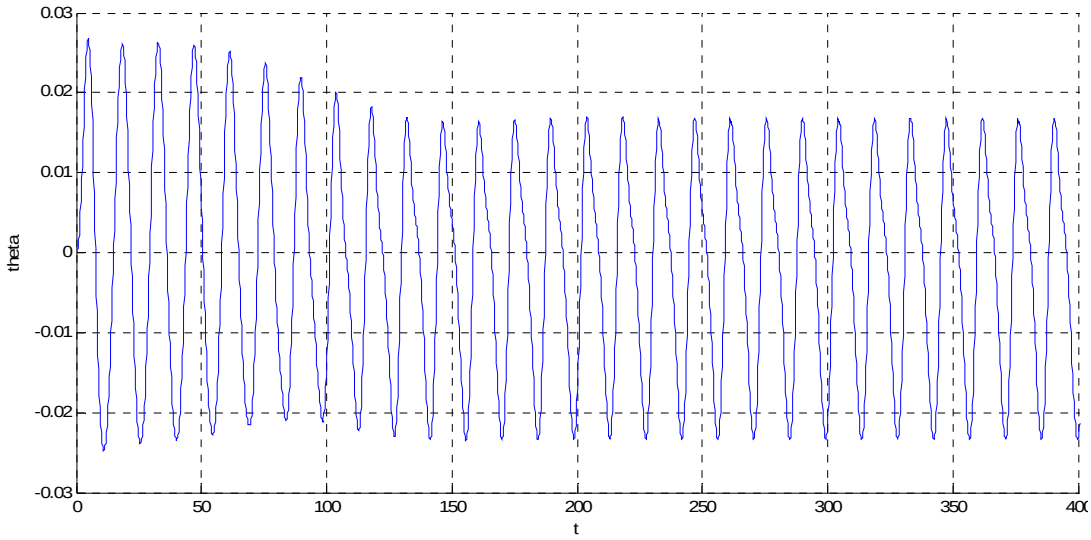

Full Coupled a=0.9 H=5m Pitch

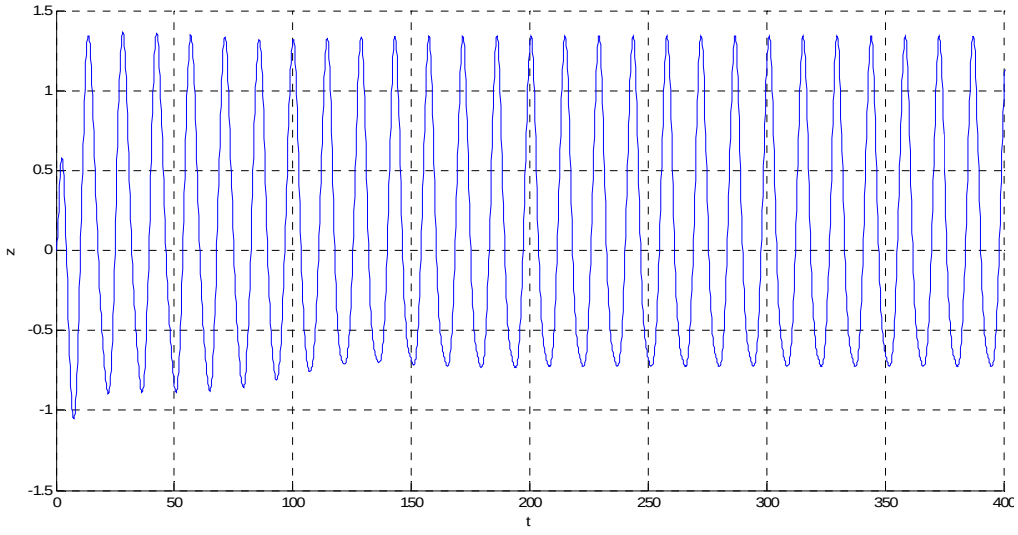

Full Coupled a=0.9 H=5m Heave

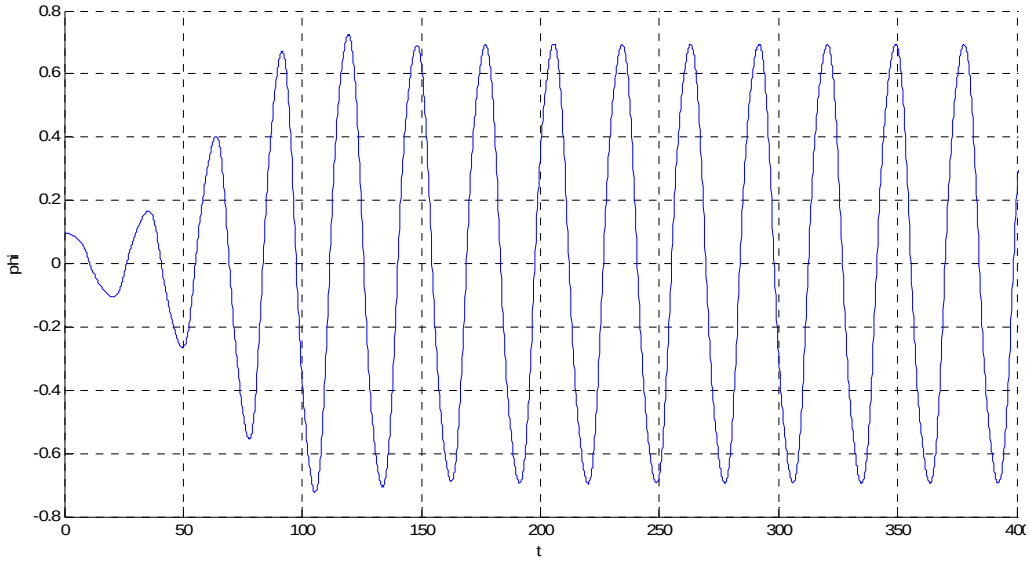

Full Coupled a=0.9 H=6m Roll

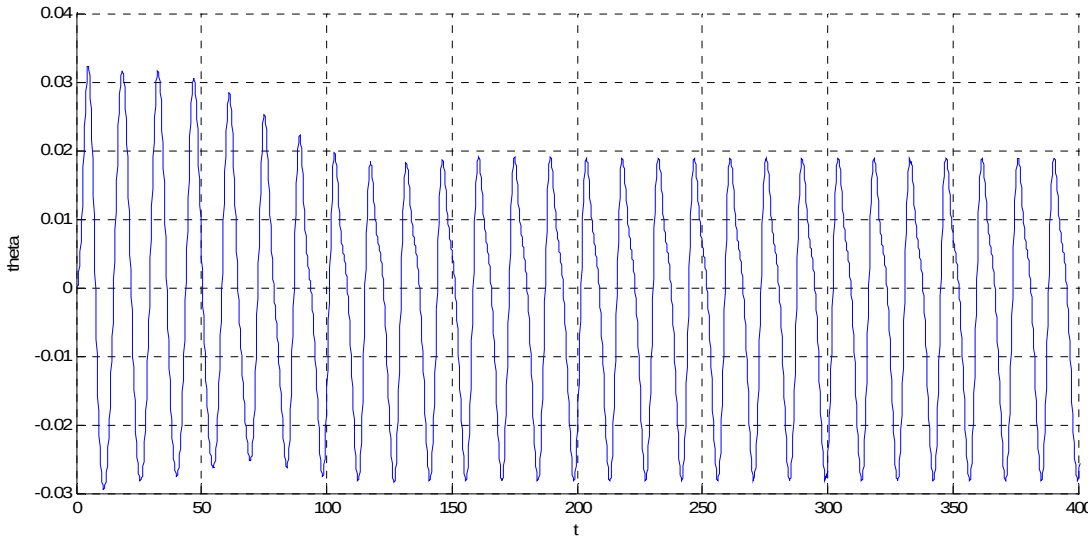

Full Coupled a=0.9 H=6m Pitch

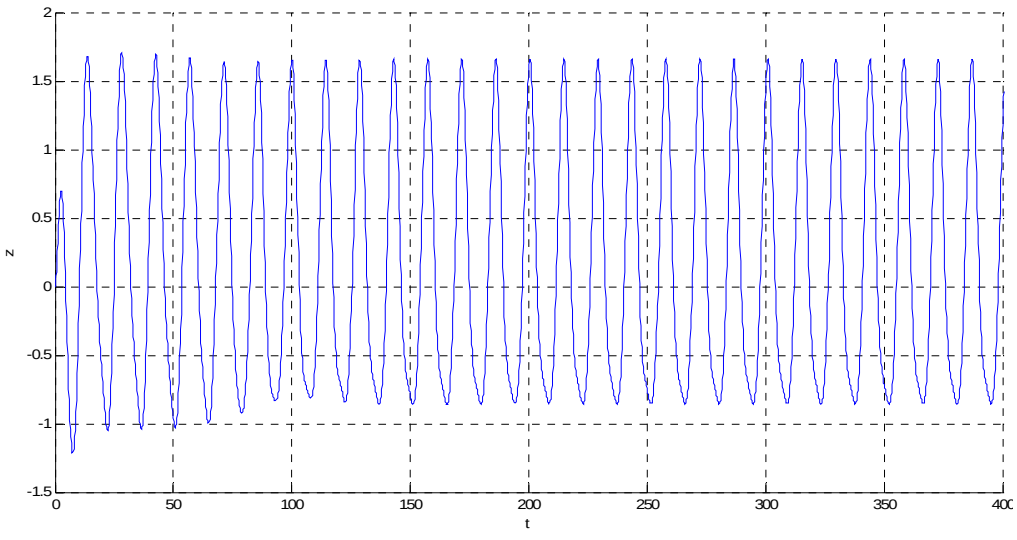

Full Coupled a=0.9 H=6m Heave

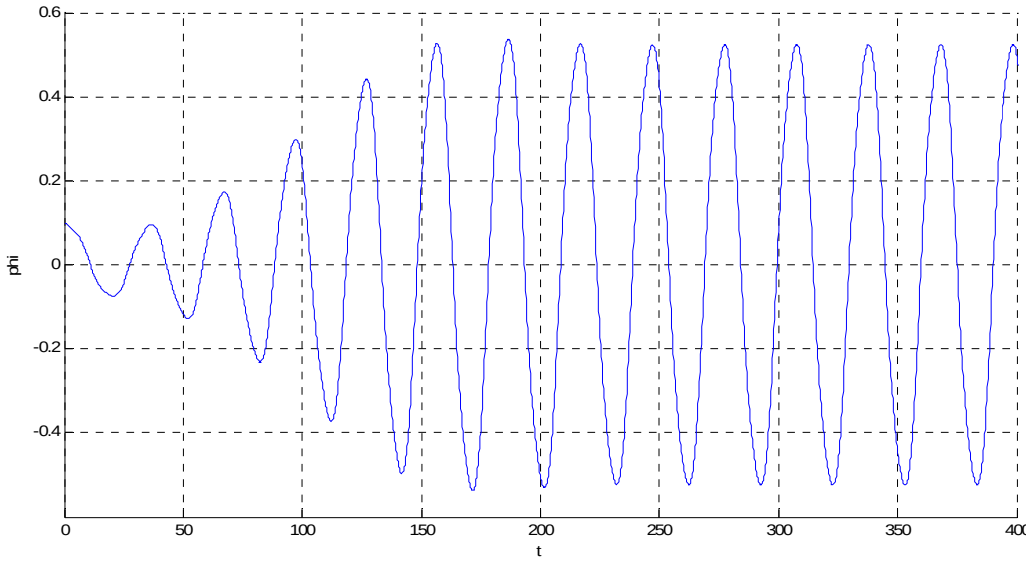

Full Coupled a=1 H=4.4m Roll

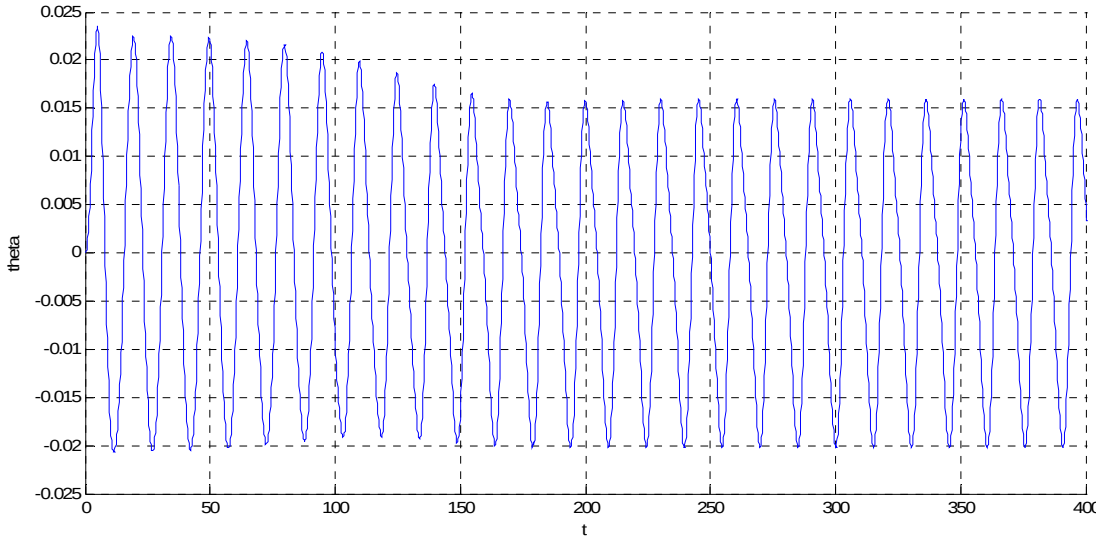

Full Coupled a=1 H=4.4m Pitch

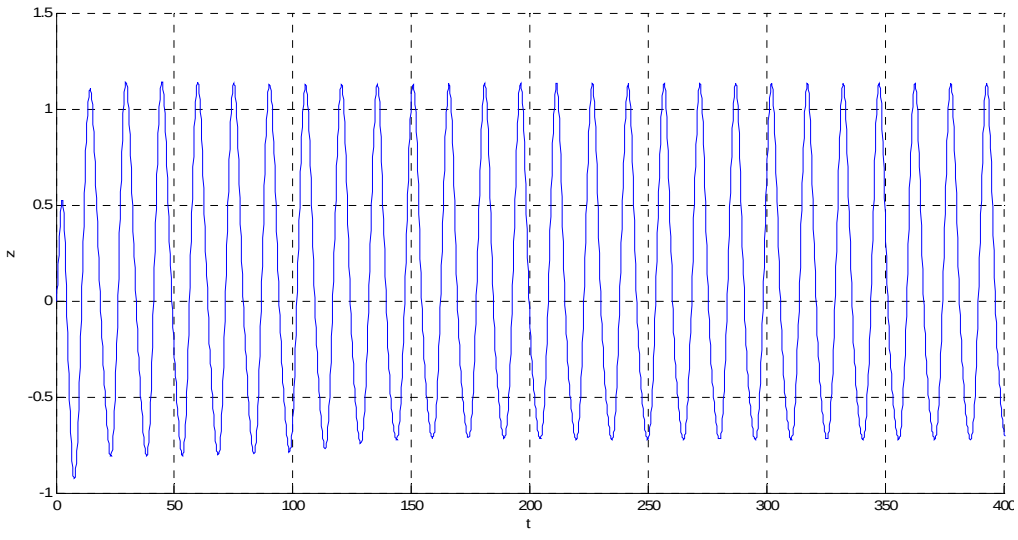

Full Coupled a=1 H=4.4m Heave

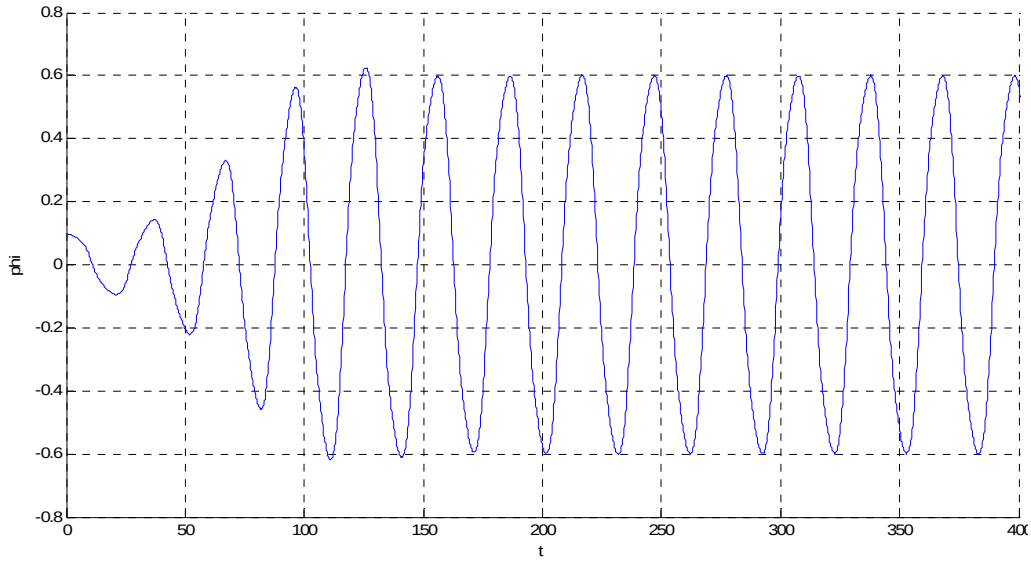

Full Coupled a=1 H=6m Roll

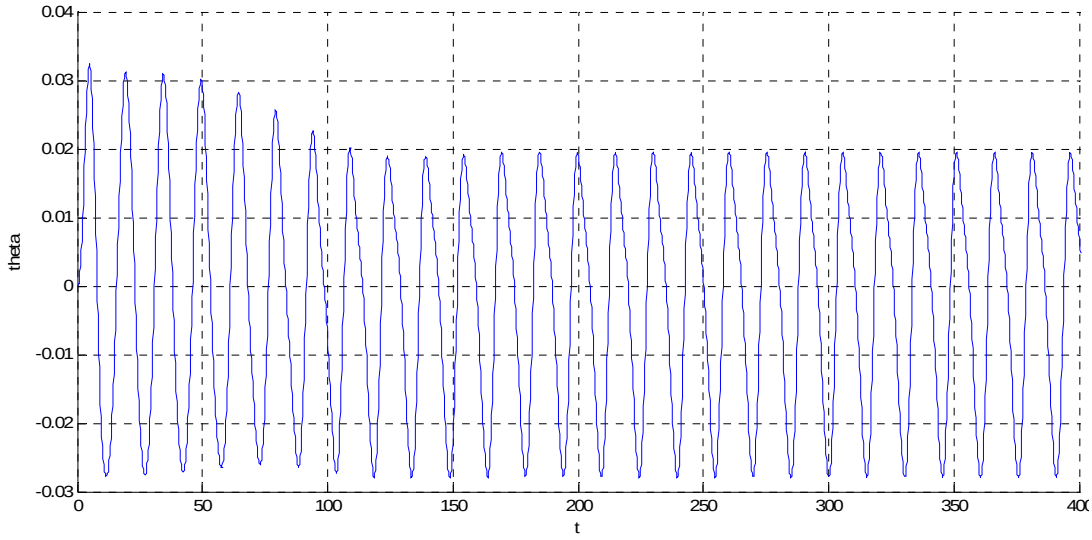

Full Coupled a=1 H=6m Pitch

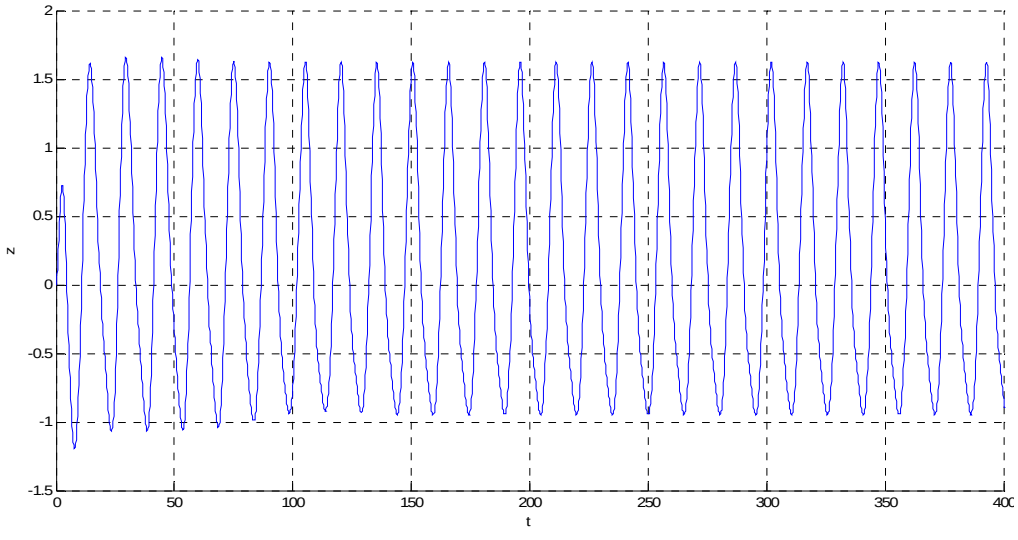

Full Coupled a=1 H=6m Heave

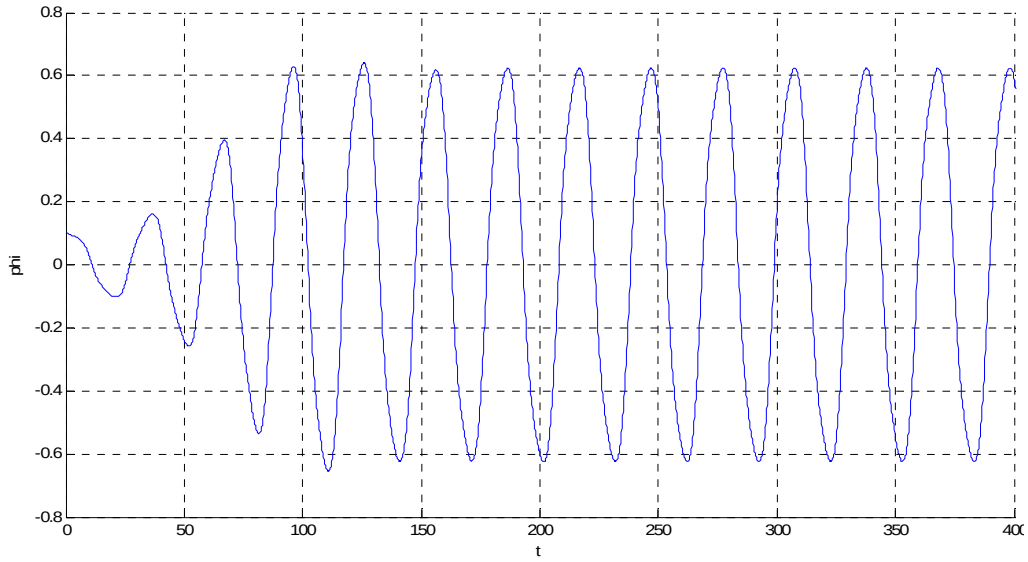

Full Coupled a=1 H=7m Roll

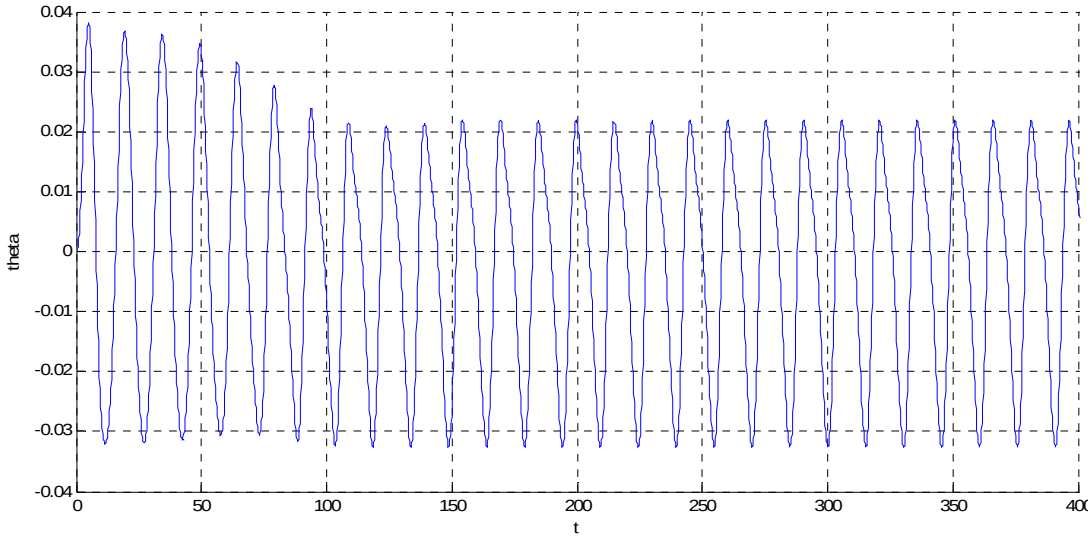

Coupled a=1 H=7m Pitch

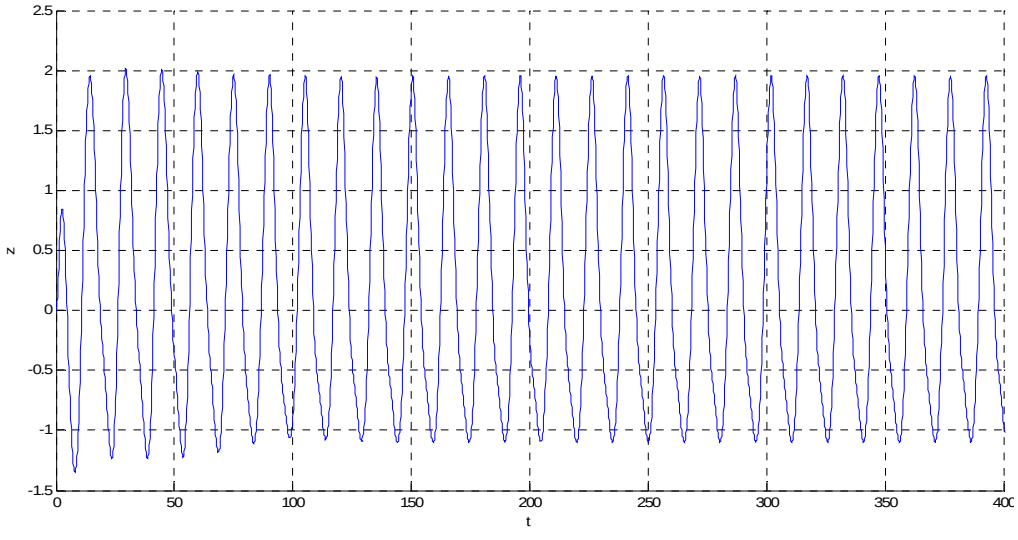

Coupled a=1 H=7m Heave

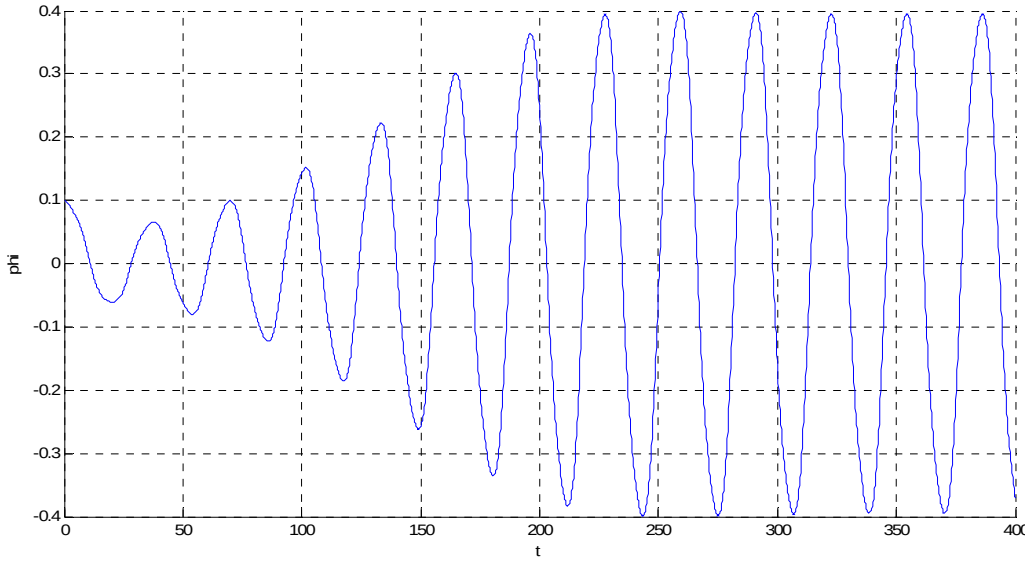

Full Coupled a=1.1 H=4m Roll

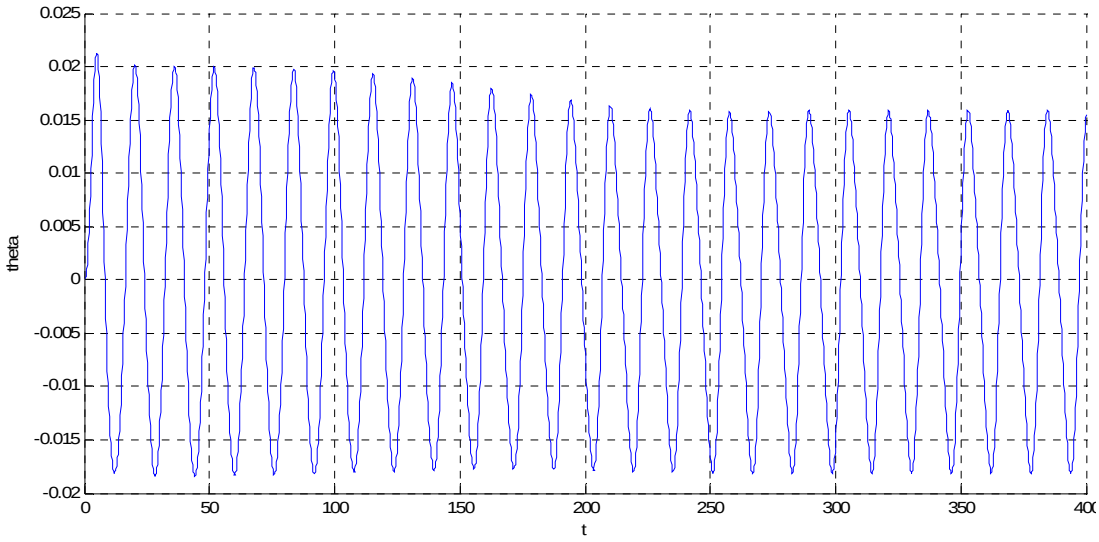

Full Coupled a=1.1 H=4m Pitch

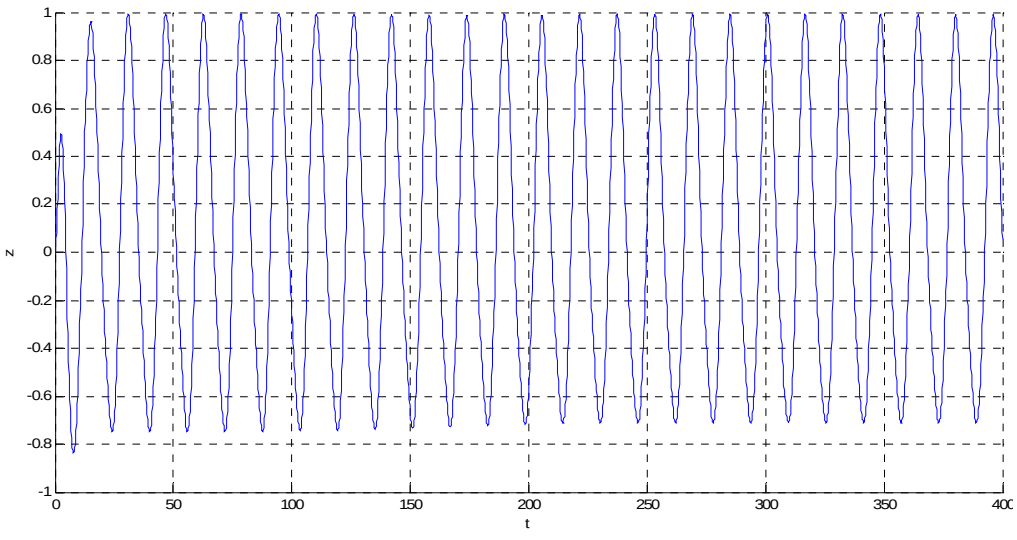

Full Coupled a=1.1 H=4m Heave

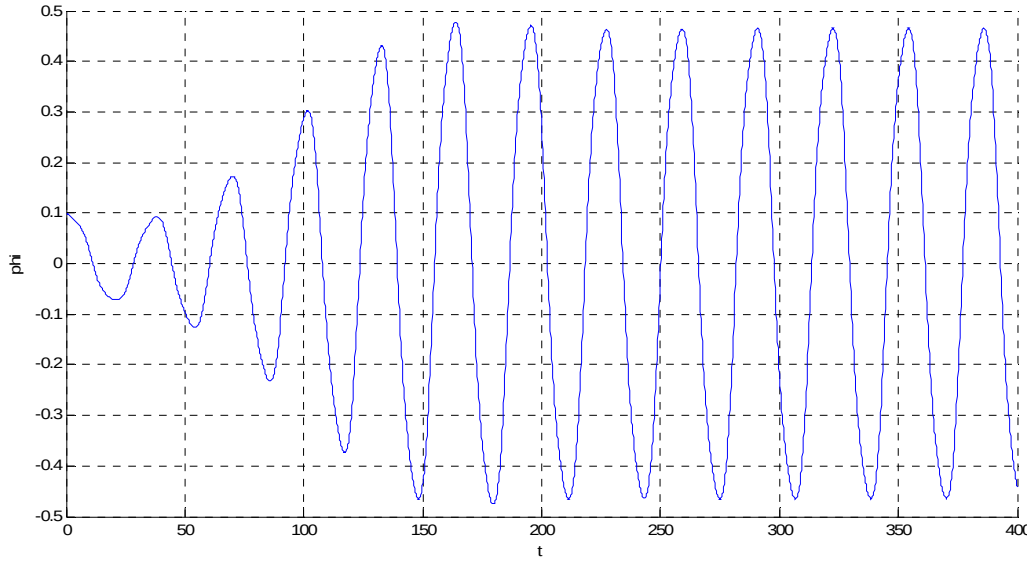

Full Coupled a=1.1 H=5m Roll

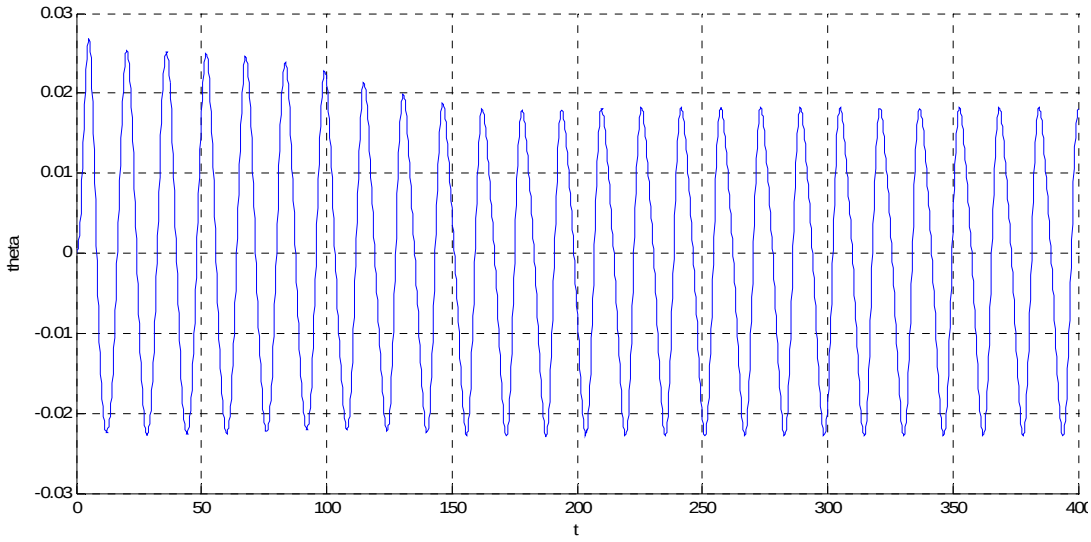

Full Coupled a=1.1 H=5m Pitch

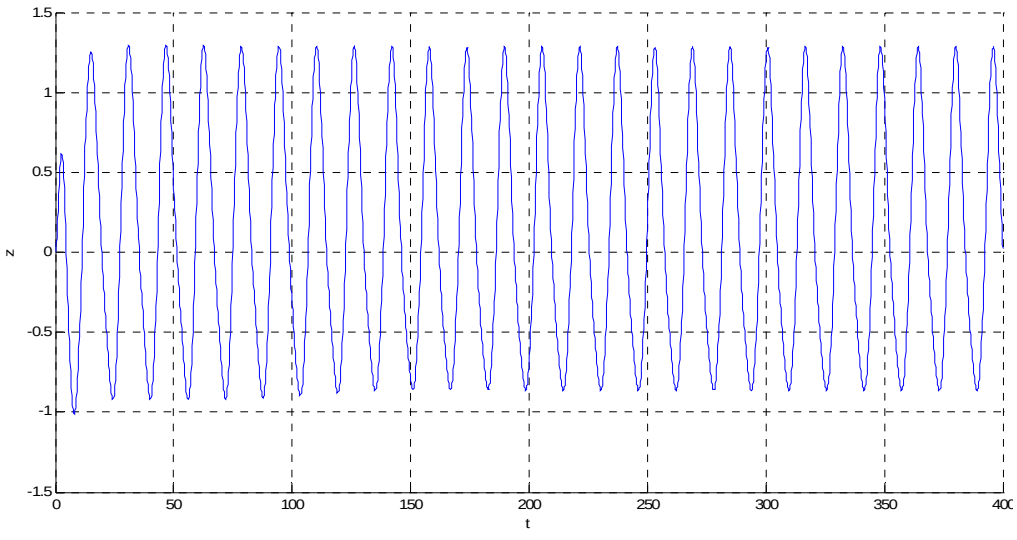

Full Coupled a=1.1 H=5m Heave

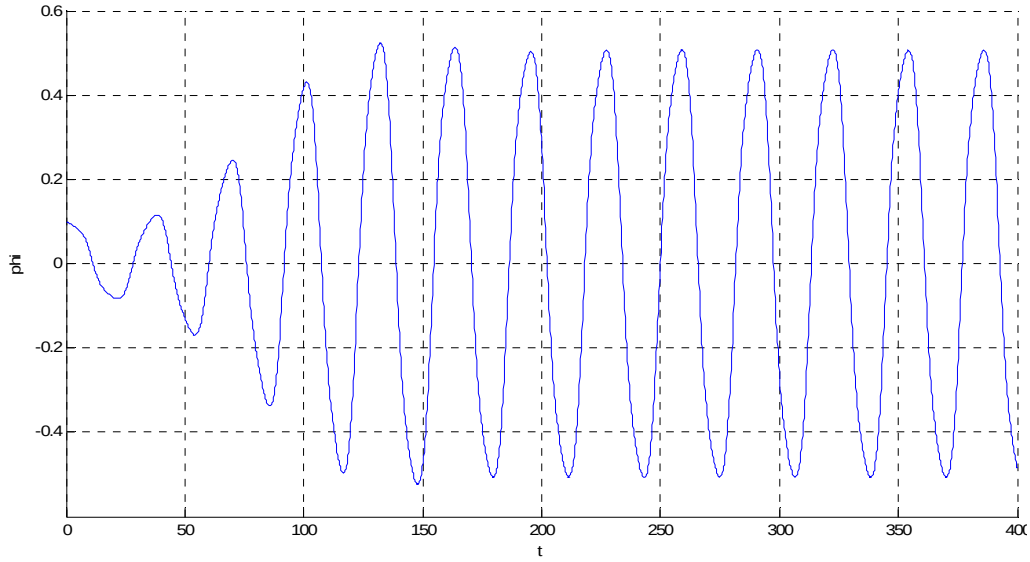

Full Coupled a=1.1 H=6m Roll

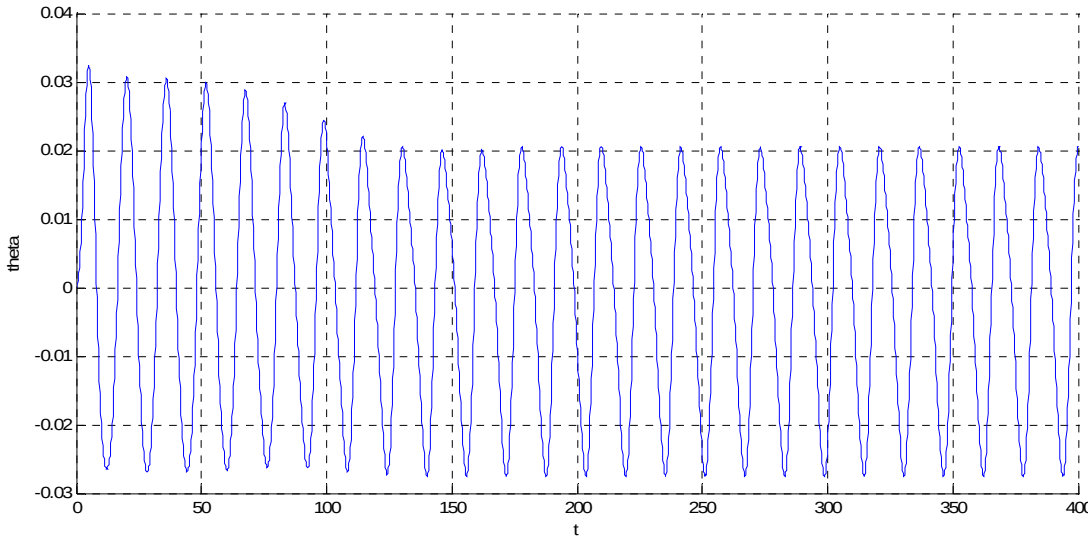

Full Coupled a=1.1 H=6m Pitch

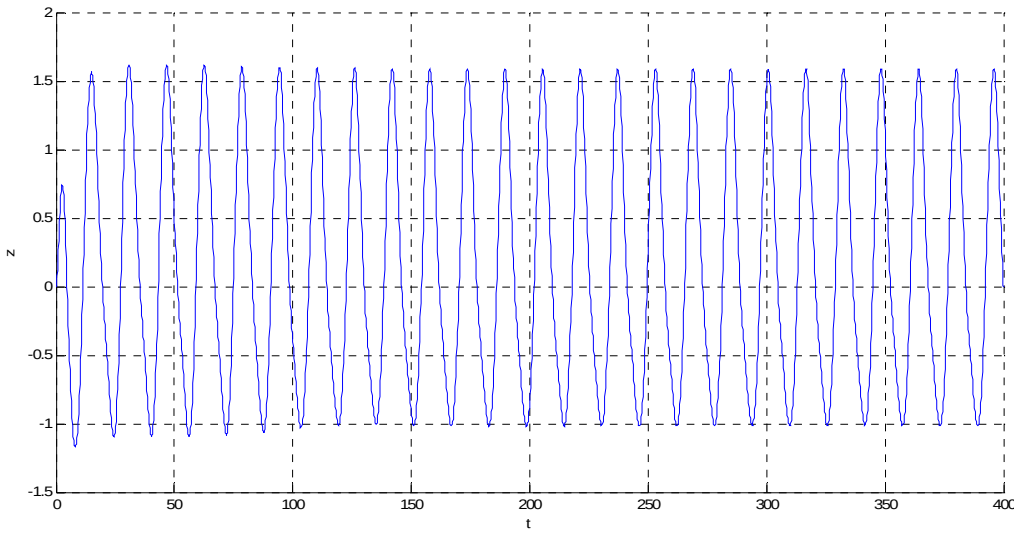

Full Coupled a=1.1 H=6m Heave

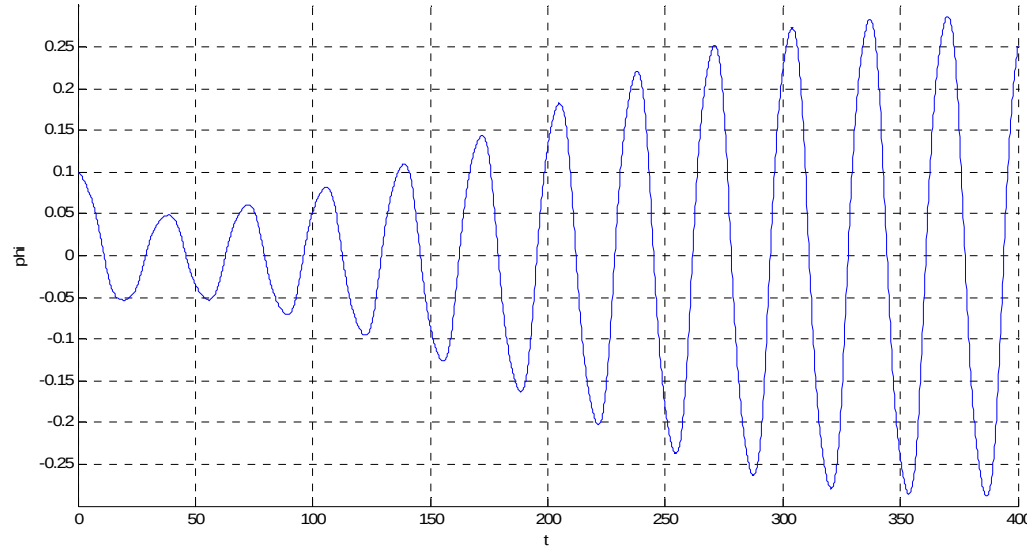

Full Coupled a=1.2 H=4m Roll

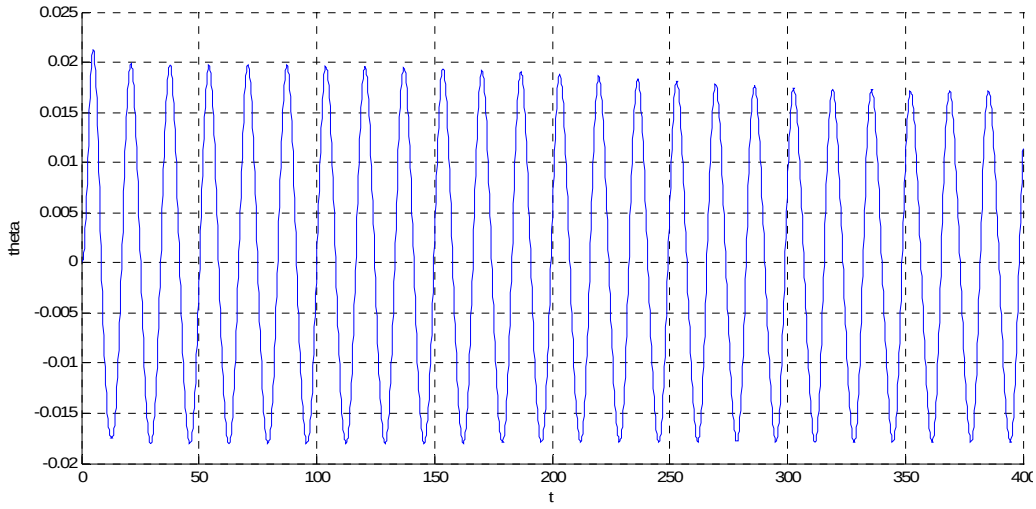

Full Coupled a=1.2 H=4m Pitch

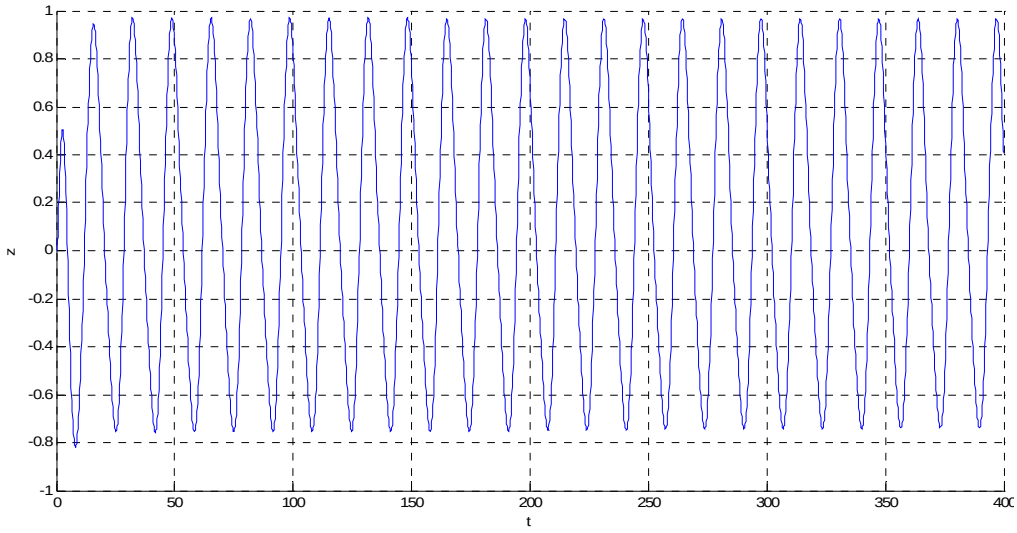

Full Coupled a=1.2 H=4m Heave

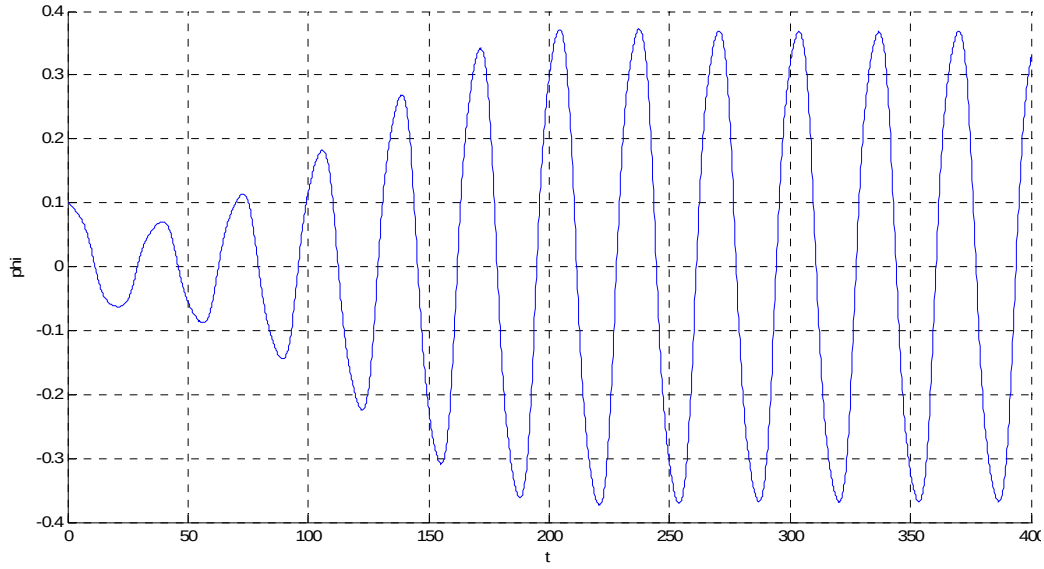

Full Coupled a=1.2 H=5m Roll

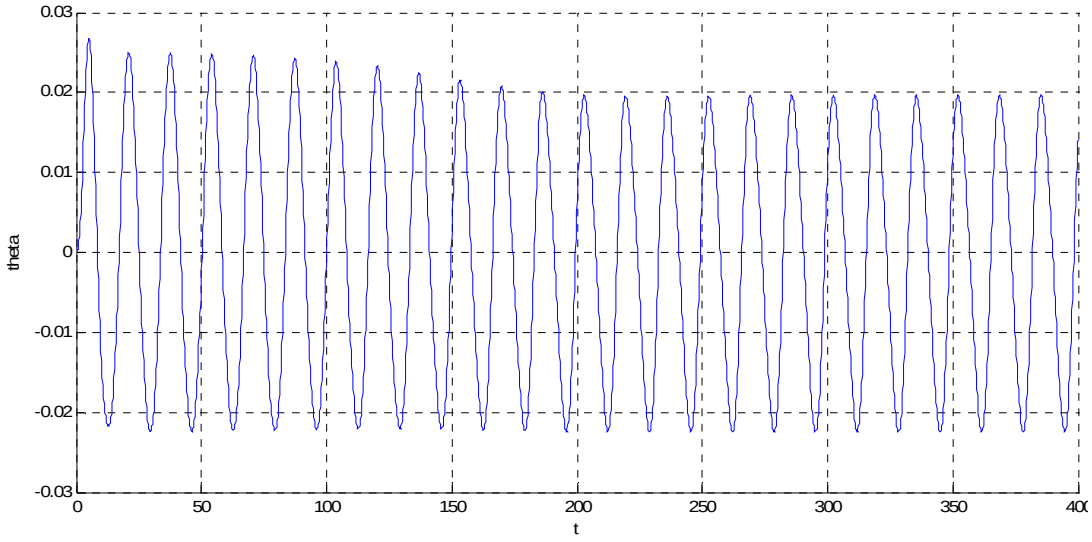

Full Coupled a=1.2 H=5m Pitch

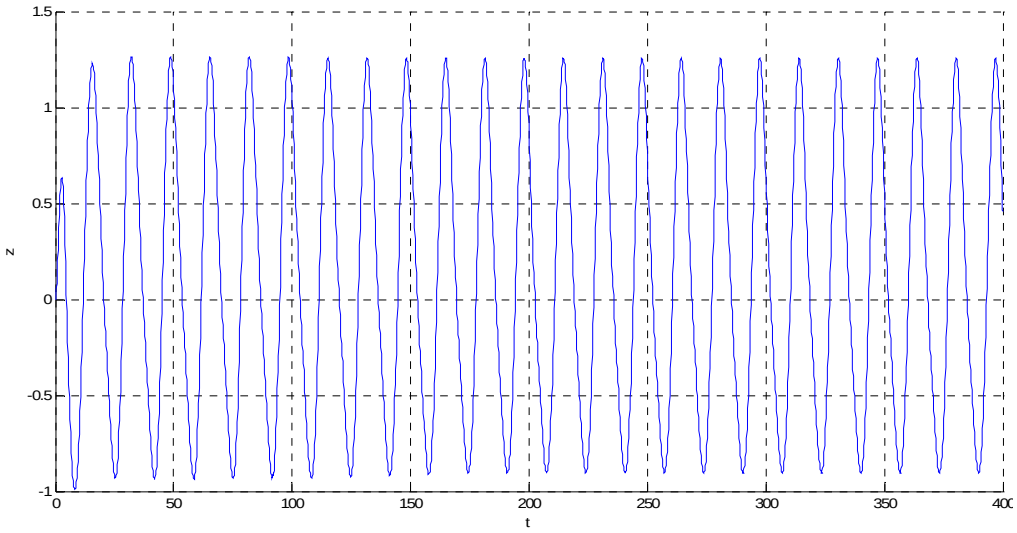

Full Coupled a=1.2 H=5m Heave

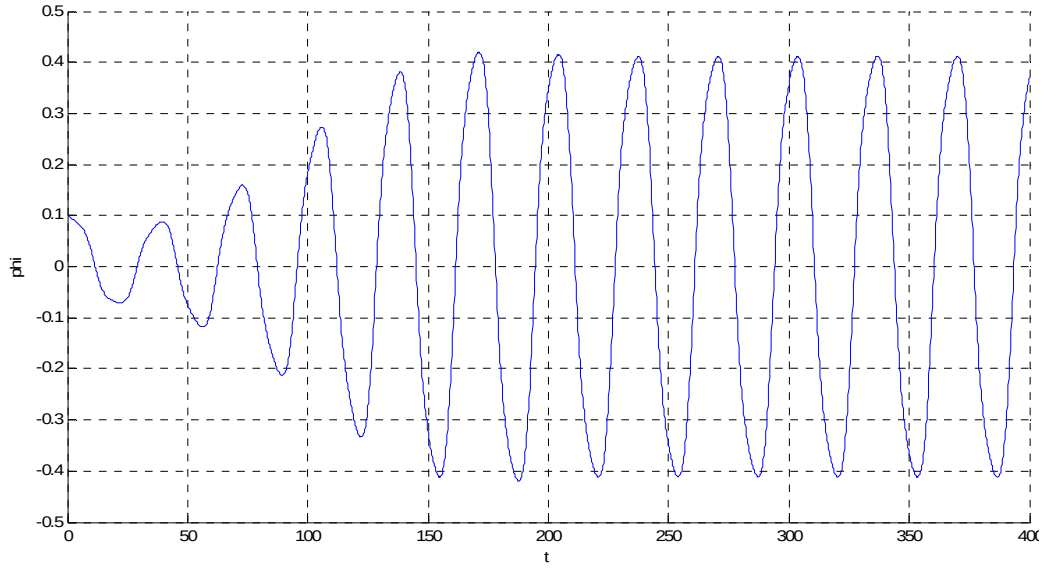

Full Coupled a=1.2 H=6m Roll

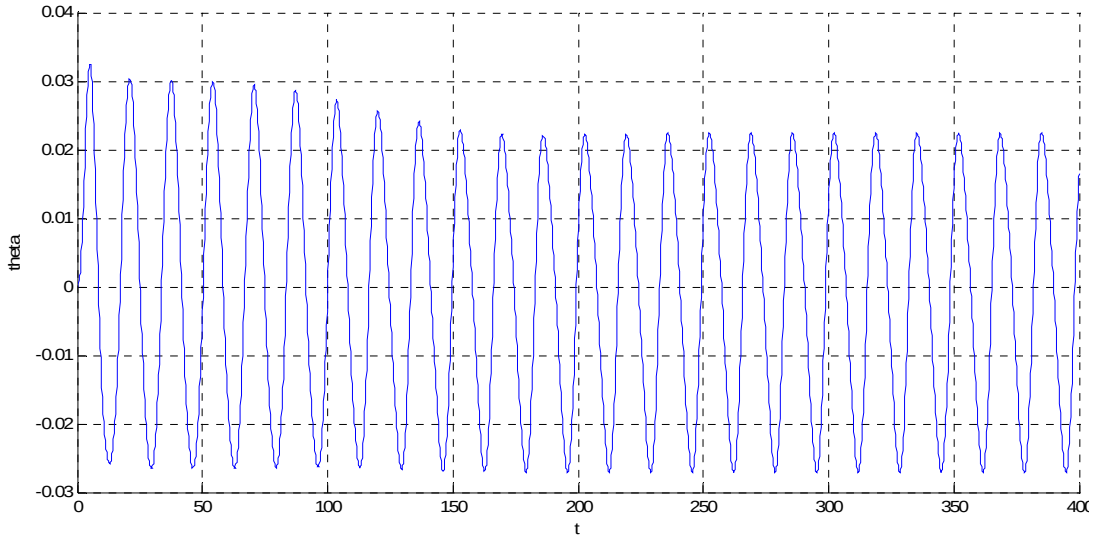

Full Coupled a=1.2 H=6m Pitch

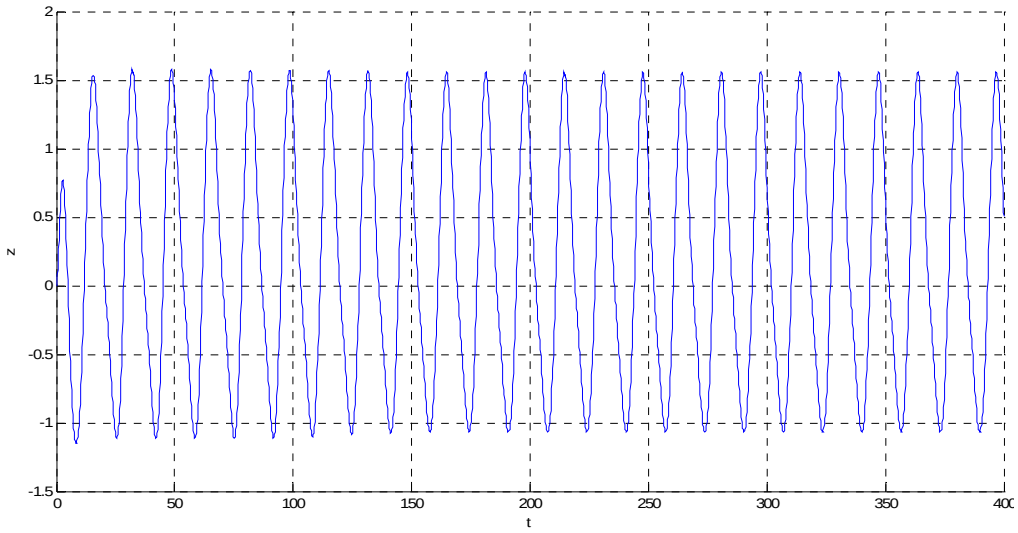

Full Coupled a=1.2 H=6m Heave